

# Evaluation of Metallic Mineral Resources

By Ted G. Theodore

## Introduction

Evaluation of metallic mineral resources primarily addresses known occurrences in the East Mojave National Scenic Area (EMNSA) but also includes some discussion of additional types of metallic-mineral deposits judged to be permissive in the various metallogenic terranes outlined for the EMNSA. Usage of the terms “occurrence” and “deposit” together with some other relevant expressions are defined in this section of the report below. Furthermore, some nonmetallic minerals (for example, fluorite, magnesite, and barite) also have been incorporated into some of the following discussions because of their intimate petrogenetic association with many metal-bearing systems. A total of approximately 15 person-weeks were spent during 1990 in the EMNSA by 10 geologists to gather information first hand for this report. Because of the short timeframe requested to the point of first release of our information concerning the EMNSA (U.S. Geological Survey, 1991) and the accompanying quantitative assessment (Hodges and Ludington, 1991), the conclusions in this report rely heavily on recently completed geologic investigations by others in the region (Miller and others, 1985, 1986; Goldfarb and others, 1988; Wooden and others, 1988; Wooden and Miller, 1990). In addition, studies by the U.S. Bureau of Mines (1990a; see also Schantz and others, 1990) and the California Division of Mines and Geology (for example, see Kohler, 1984) provided the major inventories of metallic minerals available to us for the EMNSA; this inventory was supplemented where appropriate by information contained in records of the Mineral Resources Data System (MRDS) of the U.S. Geological Survey and by data made available from the files of several major mining companies that have been active at various times in the EMNSA during the last 20 years. In addition, the U.S. Bureau of Land Management (1980) analyzed some 29 resource areas that total 7.59 million acres of the entire California Desert Conservation Area (CDCA) (and including all of the EMNSA), and they classified the land with respect to its potential for energy and mineral resources. As classified by them, the Clark Mountain Range, Mescal Range, Ivanpah Mountains, Hackberry Mountain, and Castle Mountains include areas favorable for future discovery of locatable mineral deposits. The New York Mountains, Mid Hills, Providence Mountains, Granite Mountains, and all ranges west of Kelso were classified as areas having unqualified or unknown potential.

Mineral evaluation in this report generally follows a methodology initially developed for the Alaska Mineral Resource Assessment Program (AMRAP) of the U.S. Geological Survey, which in effect is a methodology based on analogy (see Harris, 1984). This methodology in its entirety consists of (1) delineating areas or domains of coherent geology that are consistent with the geology associated with a particular type or types of metalliferous deposits elsewhere, (2) building grade-and-tonnage models that describe the types of deposits recognized, and (3) estimating the numbers of undiscovered deposits (Singer, 1975, 1990, 1993; Singer and Cox, 1988; Menzie and Singer, 1990; see also, Bultman and others, 1993, for an in-depth discussion of the methodology, and Barton and others, 1995, for recommendations on procedures to follow during assessments). The U.S. Geological Survey (1992) recently completed an evaluation of selected metallic and nonmetallic resources in the West Mojave Management Area of the Bureau of Land Management, which is present just to the west of the EMNSA.

Mineral deposits and occurrences listed and described by the U.S. Bureau of Mines (1990a; see also Wetzel and others, 1992) in the EMNSA were classified into about 20 types of metallic-mineral occurrences after first examining a number of these occurrences in the field to (1) confirm their classification(s) and (2) ascertain any mining-district-wide characteristics pertinent to the overall evaluation (table 15). The types of models assigned to the occurrences in the EMNSA generally follow the models for ore deposits in Cox and Singer (1986) and several other deposit-specific supplemental reports (Rytuba and Cox, 1991; Orris and Bliss, 1991, 1992; Bliss, 1992a). The existence of fairly up-to-date compilations of grade-and-tonnage models (see for example, Cox and Singer, 1986; Singer, 1990, 1993; Bliss, 1992a) allows the foregoing of the second part of the evaluation and the comparing instead of the grades and tonnages of the various kinds of deposits in the EMNSA with similar deposits elsewhere. However, throughout the discussions below, the possibility of district-scale, petrogenetic

linkages among many individual types of metallic-mineral occurrences is emphasized (fig. 89). Many of these lithotectonic linkages are well established in a large number of mining districts elsewhere, and they are presented here in graphic form to emphasize that the presence of one type of mineral deposit or occurrence can be used potentially as an indicator of many other types of deposit or occurrence in a surrounding, geologically similar environment. However, the presence of one type of deposit or occurrence does not mean that some other sought-after occurrence will necessarily also be present. In addition, it is not implied that all examples of mineral occurrences from the EMNSA shown on figure 89 are linked temporally and genetically. For example, the Jurassic Vulcan iron-skarn deposit is not linked genetically to the apparently Cretaceous-age Big Hunch stockwork-molybdenum system. Instead, the presence of magnetite skarn in stockwork-molybdenum systems elsewhere suggests that the presence of a stockwork-molybdenum system in the EMNSA demonstrates an environment permissive for iron skarn, and, conversely, the presence of iron skarn in the EMNSA suggests that stockwork systems also are permissive.

Many well-documented genetic linkages exist among metal deposits. One of the best examples of linkages among deposits in a mining district in the North American Cordillera is at Bingham Canyon, Utah (Einaudi, 1982, fig. 7.14A). At Bingham Canyon, igneous rocks and their immediately surrounding sedimentary rocks in the core of the porphyry system contain two zones of disseminated metal, (1) copper plus molybdenum plus gold and (2) copper. In places, this proximal zone is followed outwards by copper plus gold skarn. Distal to these are the lead-zinc-silver ores (polymetallic-replacement deposits), which are as much as 3 km from the outcrops of the central body of middle Tertiary, genetically related monzogranite. By 1976, the Bingham Mining District yielded 1.18 billion tonnes of ore averaging 0.85 weight percent Cu (Einaudi, 1982). The mining district historically also has been a major producer of gold: by 1986, more than 19 million oz Au had been produced from lode and placer deposits, making the Bingham Mining District one of the largest producers of gold in the United States (Tooker, 1990). Most of the gold has been produced as a byproduct from the mining of porphyry-copper ore. Spatial linkages between skarn ores and disseminated, porphyry-hosted ores at Yerington, Nev., Christmas, Ariz., and Ely, Nev., also are depicted graphically by Einaudi (1982), and the zoning relation between precious metals and base metals is discussed by Einaudi (1990). At Ely, over 1 million oz Au have been discovered peripheral to the porphyry-copper ores (Benedetto and others, 1991). In addition, two sediment-hosted or distal disseminated-gold deposits (Mel-Co and Barney's Canyon) have fairly recently been discovered 5 and 8 km, respectively, from the outcrop of the central stock at Bingham Canyon (Sillitoe and Bonham, 1990). These two deposits also are inferred to be related genetically to emplacement of the central copper- and molybdenum-bearing ores in the core of the mining district, although the genetic connection can only be suggested at this time by the symmetry of the gold and arsenic patterns surrounding the porphyry center (Babcock, 1993). Movable-oxide reserves at the Barney's Canyon deposit are 10 million tonnes (t) (at an average grade of 1.44 g Au/t) and, at the Mel-Co deposit, they are 3.1 million tonnes (at an average grade of 2.19 g Au/t) (Gunter and others, 1990). Finally, the characteristics of gold skarn, another type of deposit that may be linked genetically to porphyry-type ores in these types of magmatic-hydrothermal systems is discussed by Theodore and others (1992b). Another example of district-wide linkages is the zonation among various ore bodies and their Ag/Au ratios in the Leadville Mining District, Colo., as discussed in detail by Thompson (1990).

Emplacement of many of the individual epigenetic metallic occurrences and deposits in the EMNSA should not be viewed as isolated events in time and (or) space. The zonal arrangement of silver-copper brecciated dolostone, tungsten, and fluorite veins that surround a centrally located gold-bearing breccia pipe at the Colosseum Mine in the EMNSA provides an excellent example of such a linkage (Sharp, 1984; see section below entitled "Breccia Pipe and Related Deposits"). In addition, several other types of deposits that are not currently (1995) known to be present in the EMNSA may be found there at some time in the future because they are known elsewhere in geologic environments similar to those in the EMNSA. In 1980, new exploration techniques, concepts, and field investigations resulted in the recognition of several mineral environments in the CDCA that before that time were unsuspected of being present there (U.S. Bureau of Land Management, 1980). An attempt to estimate numbers of undiscovered metallic mineral deposits in the EMNSA, as has been done elsewhere (Richter and others, 1975; Singer and others, 1983; Peterson and others, 1983), is included in

the report by Hodges and Ludington (1991). Although model types have been assigned with variable degrees of certainty to 587 of the 701 mineral occurrences identified by the U.S. Bureau of Mines (1990a) in the EMNSA (table 15), only limited first-hand knowledge is known of, for example, (1) the character and intensity of alteration marginal to many of the occurrences, (2) the distribution of deposit-scale anomalous elements and elemental ratios, and (3) the intensity and preferred orientation(s) of fracture patterns that may or may not surround the identified deposits and occurrences. These types of data are critical for understanding the extent of penetration of epigenetic, mineralizing fluids into the rocks that surround any occurrence of metals and, as a corollary, whether or not that particular occurrence of metal is one part of a much larger system as described for the veins that surround the Colosseum Mine in the section below entitled "Breccia Pipe and Related Deposits."

The evaluation in this report assumes that many metalliferous concentrations cannot be treated as isolated occurrences exclusive of other types of deposits, as is presently recognized in much of the economic-geology literature. Indeed, many types of models listed by Cox and Singer (1986), as well as compendia of many others, can be linked genetically into a continuum of deposits whose sites of eventual deposition are controlled both laterally and vertically by various physicochemical processes, including depth below the paleosurface and separation of a vapor phase from the metal-bearing fluids. Furthermore, B.A. Berger (written commun., 1988) emphasized the dynamic nature of the evolution of many epithermal metalliferous systems: "We are using models [currently] as rigid static entities in combination with other geological variables in the assessment process. From my limited perspective, models of epithermal systems are not independent from dynamic geologic processes such as the tectonic evolution of a region, changes in climate through time, and evolving landscape.\*\*\*we must look for ways to portray epithermal systems in a less rigid framework.\*\*\*and to apply them in a more dynamic way." Lastly, we emphasize that (1) exploration methodologies are evolving continually (see for example, Bailly, 1981; Hutchinson and Grauch, 1991) and (2) quantitative, model-based assessments can be made only for those types of mineral deposits that are currently recognized and for which grade-tonnage distributions are available. Any assessment for Proterozoic, carbonatite-related rare earth element (REE) deposits made before the discovery of the deposits at Mountain Pass (just outside the EMNSA) would not have resulted in an accurate characterization of the geology of the EMNSA for these types of deposits. Such model-based, rather than target-based, numerical assessments of many geologic terranes that show signs of widespread mineralization and which are likely to be explored further at some future time would most likely yield estimates of metal endowment that would be lower than future actual endowment measured by physical exploration.

Several examples from north-central Nevada dramatically emphasize this potential for inadequate assessment. Before the discovery and recognition in the early 1960s of the sedimentary-rock-hosted gold-silver deposits near Carlin, Nev., no one could have properly assessed the surrounding geologic terranes as favorable or even permissive for the presence of large gold-silver deposits. Many of these sedimentary-rock-hosted gold-silver deposits are now known to be world class in size and grade (Bagby and Berger, 1985; Bagby and others, 1986; Berger, 1986b). The sedimentary-rock-hosted gold deposits at Getchell, Nev., were discovered in the 1940s (Joralemon, 1951), but the true nature of the deposits was not recognized until much later (see for example, Bagby and Cline, 1991). As pointed out by Roberts (1986), Roberts (1960) defined in one of his previous papers some mineral belts in north-central Nevada and noted that many of the then-known, apparently small mineral deposits, including gold in placers, are localized along traces of the margins of windows in the regionally extensive Roberts Mountains thrust fault. The spatial association between the trace of the Roberts Mountains thrust fault and the localized mineral deposits provided the geologic basis upon which private industry could then focus its exploration efforts. In another example, the Fortitude gold-skarn deposit in the Battle Mountain Mining District, Nev., was not discovered until 1981, some 115 years after the mining district was first organized (Roberts and Arnold, 1965; Wotruba and others, 1986). Before the start-up of mining operations in 1985, the Lower Fortitude gold-skarn orebody contained 5.1 million tonnes of ore at a grade of 10.45 g Au/t, 27.8 g Ag/t, and 0.2 weight percent Cu (Theodore and others, 1991). In fact, no skarns cropped out anywhere in the immediate area of the Fortitude deposit before its exposure during open-pit operations.

As with all applied-exploration methodologies, the discoveries of economic concentrations of metals that are actually brought to the stage of mining operation are substantially limited compared to the number of claim

groups commonly examined. Various estimates suggest that as many as 1,000 prospects are examined for every mine brought into production thus far (1993) in the 1990s. Peters (1978) introduced the concept of “teaser districts” as those areas that include an abundance of small mines and (or) prospects that draw an inordinate amount of exploration effort before eventual rejection by some exploration group. Two possibilities exist in such “teaser districts.” On the one hand, the absence of some fundamental geologic condition from the ore-forming process apparently precludes accumulation of metals into an economic concentration; the process may never have attained that particular intensity required to affect a volume of rock sufficient for an orebody (Peters, 1978). On the other hand, the major orebody may still be there somewhere in the “teaser district,” but it may be found only by a redirection of geologic concepts by the exploration team, a reassessment of economics in the district, or by the application of newly developed exploration tools and concepts.

An assessment of the EMNSA that is based on potential-exploration targets (Menzie and Singer, 1990) for a particular metal or groups of closely related metals can lead to the recognition of new models and, necessarily, to a delineation of geologic terranes that are permissive for those new models. However, the cost of implementing state-of-the-art geochemical and geophysical techniques in a program to determine potential-exploration targets in the 1.5 million acres of the EMNSA would be exorbitant, especially when one considers that geochemical expenditures higher than approximately \$20,000 per 640 acres of bedrock are fairly commonplace in private industry.

Lode-metal mines apparently were first discovered in 1861 in the Clark Mountain Range, at Striped Mountain, and in the Ivanpah Mountains, a region that was subsequently included in the EMNSA (Hewett, 1956). Shortly thereafter, in 1865, these discoveries were followed by others in the Ivanpah Mountains, and, in that same year, the Clark Mountain Mining District was organized. The first shipments of ore from the Copper World Mine took place during 1869, and many small lode mines that have shown sporadic production in the intervening years were discovered between 1865 and 1892 (Hewett, 1956). Subsequently, the region was explored extensively for tungsten, zinc, and lead from 1915 to 1918 during World War I. However, many mines in the EMNSA ceased production at the end of World War I and apparently never produced again (fig. 90; data from U.S. Bureau of Mines, 1990a). Many other mines in the EMNSA, mostly gold producers, ceased production in 1941 and 1942, many with promulgation of U.S. Government Limitation Order L-208 of October 8, 1942, which closed down domestic mining of most gold near the onset of World War II (see Shawe, 1988; Lucas, 1992).

## Definitions

This section follows closely the overall organization of one prepared by John and others (1993) for the Reno 1° × 2° quadrangle, Nev. and Calif., resource-evaluation study by the U.S. Geological Survey. In the present report, the definitions put forth by Cox and others (1986) for the terms “ore deposit,” “mineral deposit,” and “mineral occurrence” are adapted somewhat. Specifically, a “mineral occurrence” is “\*\*\*a concentration of a mineral\*\*\*that is considered valuable by someone somewhere or that is of scientific or technical interest.” However, use of this definition does not imply endorsement of economic value by the U.S. Geological Survey for the mineral occurrences considered in this report. A “mineral deposit” is “\*\*\*a mineral occurrence of sufficient size and grade that it might, under the most favorable of circumstances, be considered to have economic potential,” a necessary corollary being that drilling has tested the system in the third dimension to the point that a grade and tonnage can be assigned to the volume of rock with some level of confidence. An “ore deposit” is “\*\*\*a mineral deposit that has been tested and is known to be of sufficient size, grade, and accessibility to be producible to yield a profit.” The inclusion of the concept of “profit” in this description put forth by Cox and others (1986) and many others is somewhat unfortunate in that it leads to contradictions when applied to estimates of speculative resources present in a given area (H.G. Wilshire and J. E. Nielson, written commun., 1991). We certainly can envision that national needs might require extraction of some metals under circumstances that do not yield a financial profit to society as a whole or even to some segment of society. If we were to attempt some estimate of the numbers of a particular type of deposit either present in a region or present in a favorable area for that deposit, then all existing occurrences, regardless of size and prior mining history, would have to be treated as unknowns if either the grade or the tonnage at the site were not available

to us. An ore deposit is the economic, measured and demonstrated, identified-resource part of the resource-reserve classification scheme adopted by the U.S. Bureau of Mines and U.S. Geological Survey (1980). Furthermore, the grade and tonnage of an ore deposit is not necessarily the same as the “geologic resource” of the deposit. The “geologic resource” is the grade or tonnage of the mineralized volume of rock that has not been constrained by economic-limiting factors such as topography or site location; the mineralized volume of rock is commonly broken down by variable grades and includes the ore deposit itself (see Peters, 1978). The “reserves,” either measured or indicated, are the demonstrated economic portion of the identified resources in a mineralized system (U.S. Bureau of Mines and U.S. Geological Survey, 1980). Additional categories of reserves can be based on the economics and (or) probability of their presence. As pointed out by Bailly (1981), five major factors are generally involved in determination as to whether or not a deposit becomes an economic reserve: (1) existence of the deposit, (2) extractability of the elements of value from the deposit, (3) availability of energy and materials for extraction of the elements of value, (4) acceptable environmental requirements, and (5) favorable economics for a potential mining operation at the site of the deposit. In the EMNSA, recent exploration activities have resulted in discovery of several gold-silver deposits for which both grade and tonnage data have not been released and are considered proprietary by the holder of the claims.

Mineral occurrences, mineral deposits, and ore deposits are classified further into various types on the basis of descriptive mineral-deposit models contained primarily in Cox and Singer (1986), as described previously in this report, but additional references to particular types of other deposits that are not contained in Cox and Singer (1986) are included throughout various sections below. These include gold-bearing breccia pipe, gold skarn, gold-silver quartz-pyrite veins, and several others. The mineral-deposit models are based on groups of mineral deposits that have in common both a relatively wide variety and a large number of attributes, as well as formation in a common geologic environment. Table 15 lists mineral occurrences identified in the EMNSA by model type and the appropriate references to descriptive models for these deposit types. Some deposit types assigned to a given category include a small number of occurrences and deposits that diverge widely from the age and mode of emplacement of the rest of that particular category. For example, although most gold-silver quartz-pyrite veins presumably are Mesozoic in age and are related to the mesothermal batholithic environment in the EMNSA, some deposits of different age and origin, such as those at the Telegraph Mine, also are included under this same category. Mineralization at the Telegraph Mine apparently is Tertiary in age and seems to be associated with wrench-fault-related tectonism (Lange, 1988). This category of gold-silver quartz-pyrite veins is not subdivided further in this report because the age and tectonic environment for the 79 gold-silver quartz-pyrite veins other than those at the Telegraph Mine is not well understood.

Grade-and-tonnage frequency-distribution models contain data on the shape of curves for grades and tonnages for groups of mineral deposits from which grades and (or) tonnages at various percentiles may be extracted. They are useful in numerical resource assessments (Singer, 1990, 1992, 1993; see also, Drew and others, 1986; Singer and Cox, 1988; Root and others, 1992; Brew and others, 1991) by providing information about the potential metal content of undiscovered deposits within a tract of land permissive for a given type or model, and they are used in economic analyses of these resources, provided that (1) estimates may be made with some confidence concerning the number of individual deposits that may be present within that given tract of land and, further, that (2) any undiscovered deposits would show grade and tonnages that are within the limits of the grades and tonnages of the ore-deposit model under consideration. Grade-and-tonnage models typically are frequency cumulations; grade is based on average grades of each metal or mineral commodity for an individual deposit, and the associated tonnage is based on the total of past production, reserves, and resources at the lowest possible cutoff grade (Singer, 1990). However, appropriate care must be exercised in the accumulation of data for a grade-and-tonnage model because the strong possibility of a significant distortion of the grade and (or) tonnage curves exists if one mixes unlike data such as production data for one group of deposits and geologic-resource data from another group of deposits of the same deposit type. In addition, data from geologically mixed populations of deposits can result in distorted grade-and-tonnage distribution curves. Furthermore, prior production data may be influenced heavily by topography in the general area of a deposit that is being exploited presently or has been exploited completely in the past, as well as by price supports during times of national crisis. A “geologic” resource and not an “economic” one, ideally, should make up the individual

grade-and-tonnage data points along the entire distribution curve of a grade-and-tonnage model. However, such information may not be available in the geologic literature for many mined-out deposits.

Grade-and-tonnage distribution models currently are usually developed simultaneously by many workers as part of the descriptive aspects of the models (Cox and Singer, 1986). When sufficient grade-and-tonnage data are available to build a model, the grade-and-tonnage data can help refine descriptive mineral-deposit models (Singer, 1990, 1993). Singer (1990, 1993) discussed in detail the formulation of grade-and-tonnage models and some of the problems associated with their development and use. With regard to the EMNSA, one major shortcoming of present grade-and-tonnage models involves the bulk mineable, volcanic-hosted gold-silver deposits (John and others, 1993) such as are present in the Castle Mountains. A lack of sufficient grade-and-tonnage data for these types of deposits at one time resulted in retention by Cox and Singer (1986) of an artificial division of volcanic-hosted deposits into Comstock (adularia-sericite), quartz-alunite (acid-sulfate), and hot-spring types, and all bulk mineable, volcanic-hosted gold-silver deposits classified as hot-spring deposits (D.A. Singer, oral commun., 1990). However, grade-and-tonnage models for hot-spring gold-silver deposits were derived subsequently by Berger and Singer (1992). In a genetic sense, hot-spring deposits are shallow-level end members of adularia-sericite and quartz-alunite deposits as described by Berger and Henley (1989), and, with continued discoveries of adularia-sericite and quartz-alunite mineralized systems, hot-spring deposits will probably cease to have a separate grade-and-tonnage model (John and others, 1993; see also Albino, 1994).

## **Delineation of Areas Permissive and Favorable For Undiscovered Metalliferous Mineral Resources**

Several subsections that follow present the characteristics of various metalliferous-mineral deposits in the EMNSA and, in addition, delineate those areas where the geology is permissive for as-yet-undiscovered mineral occurrences. For many mineral occurrences identified in the EMNSA, notable characteristics are described and cited, and many well-known deposits of that particular type in the EMNSA are described in detail. Criteria used to delineate areas that may contain undiscovered occurrences are described, as well as the geologic characteristics of these areas. Two types of areas that may contain undiscovered mineral occurrences, permissive terranes and favorable tracts (Menzie and Singer, 1990), are delineated for many model types.

“Permissive terranes” are areas that might contain a certain type of mineral occurrence. Any geologic terrane in the EMNSA that is geologically similar to another terrane containing mineralization that generally formed at the same time as that geologic terrane is considered permissive for the same type of mineralization, whether or not any signs of mineralization are present. Some permissive areas are very broadly outlined because their geologic environments that are conducive to the hosting of mineral occurrences in the EMNSA are wide ranging. For some types of mineral systems, we cannot demonstrate that a particular type of mineral occurrence actually is present within an area shown as permissive for that occurrence type.

“Favorable tracts” are domains within permissive terranes and which are known to contain some positive indications either that a mineralized system, generally irrespective of overall size or grade, is present or that mineralizing processes have occurred. For example, the presence of some known mined deposits and some mineral occurrences, of hydrothermal alteration known to be restricted to a certain type of mineralized system, and of plutons of an age and chemical signature that are associated with known mineralized systems elsewhere are all considered characteristics for the potential presence of that type of mineralized system in an area. Because positive indications that some type of ore-forming processes have occurred are required to designate an area as favorable for a certain type of mineralized system or mineral-deposit model, favorable tracts are commonly of a much smaller areal extent than permissive areas and are more likely, in the judgment of the persons making the mineral evaluation, to contain undiscovered mineral resources of that model type. In all likelihood, many areas judged to be favorable have already been considered as such by exploration geologists in private industry. The absence of any recent discoveries of major mineral occurrences in those areas designated as favorable may be interpreted to indicate a diminished likelihood for the presence of any future additional discoveries of the mineral-occurrence model in question. However, many ore-deposit models are not being sought as viable targets at all times, and the complete history of exploration for the favorable areas outlined

is not available. Thus, numerical judgments concerning probabilities of discoveries in favorable areas versus probabilities of discoveries in the enclosing permissive terrane cannot be made.

Nonetheless, some mineral occurrences in the EMNSA have been judged to constitute an exception to the above-stated rules for delineating a favorable tract within a permissive terrane for a given type of deposit. As has been described, the quartz-molybdenite-vein occurrence at Globe Wash has been judged not to merit classification as being within a surrounding tract that is favorable for the presence of a large stockwork-molybdenum system or systems at depth. By definition, permissive terranes must include all favorable tracts. Thus, these definitions of permissive terrane and favorable tract constitute a two-fold classification that also has been followed in a study currently in preparation that deals with metallic mineral resources of Nevada (Ludington and others, 1993). Refinement of the outlined permissive terranes by deleting parts that can be confidently described as barren of a particular type of mineral occurrence (see Menzie and Singer, 1990) have not been attempted primarily because the needed complete exploration histories and results of detailed studies in the various mountain ranges of the EMNSA are not available.

The permissive-and-favorable classification scheme of mineral resources is not the only one in use. As pointed out by Gair (1989b), an assessment of the mineral-resource potential of an area is an evaluation of the possibility or likelihood that such resources are present in an area; the assessment may or may not include some quantitative measures of the probability of the presence of a given type of mineral occurrence. Gair (1989b) and his associates attached a subjective classification scheme for various degrees of favorability, such as high, moderate, low, and nil categories, for the presence of mineral resources. The permissive terranes and favorable tracts outlined below in the EMNSA are not qualified further because the information needed to differentiate confidently among the above-listed categories is lacking.

It is worth emphasizing again, however, that all positive indications of mineral occurrences were not available, even for those mineral-occurrence types known to be present throughout the EMNSA, primarily because of inherent conditions that severely limited data gathering for the present investigation. Furthermore, the permissive terranes and favorable tracts are presented only for some of the currently recognized ore-deposit models. These include, on the one hand, those that are described formally in the economic-geologic literature together with their grade-and-tonnage distributions and, on the other hand, some additional models that either have not been formally described or are in the process of being described (for example, porphyry gold; see Rytuba and Cox, 1991). Yet, some categories of mineral-occurrence models can provide viable exploration targets in certain permissive terranes. Descriptions by Hewett (1931) of sericitized, unoxidized gold- and pyrite-bearing porphyry at the Red Cloud Mine in the Goodsprings Mining District, Nev., located east of the EMNSA about 13 km from the California-Nevada state line, indicate that a porphyry-gold type of mineralized system should at least be considered as being permissive in intrusive rocks of similar age in the EMNSA. The methodology outlined above, however, cannot consider any types of mineral occurrences that are currently unrecognized as constituting a separate deposit type.

The two-fold permissive-terrane and favorable-tract land-classification scheme used herein for the various types of metal-bearing mineral models is somewhat analogous to the scheme adopted recently by the State of California, as exemplified in its Mineral Land Classification Diagram (fig. 91; also, D.O. Shumway, written commun., 1991). As the term “permissive terrane” is used, it includes both of their sections that are entitled “Areas of Identified Mineral Resource Significance” and “Areas of Undetermined Mineral Resource Significance” of the Mineral Land Classification Diagram. “Favorable tract” is roughly equivalent to their “Areas of Identified Mineral Resource Significance” and “Known Mineral Occurrence” (MRZ-3a, fig. 91).

Geophysical methods described above in the section entitled “Geophysics” that estimate depth to bedrock in those parts of the EMNSA that are covered by valley-fill deposits were used to place limits on extension of permissive terranes and favorable tracts from the mountain ranges into the valleys. A 500-m depth-to-bedrock limit was used to bound the permissive terranes and (or) favorable tracts in the valleys where the bedrock is covered by mostly unconsolidated Tertiary and (or) Quaternary deposits (pl. 3). This depth limit is somewhat arbitrary (for comparison, a recently completed 1:1,000,000-scale state-wide assessment for Nevada used a 1 km depth limit; see Blakely and Jachens, 1990, 1991), but it is believed that extrapolation of bedrock to depths greater than 500 m is subject to such uncertainties in the EMNSA as to have no scientific merit at the

publication scale of our assessment (1:125,000). Also, under present economic conditions, blind exploration for mineral deposits only very rarely exceeds a depth of 200 m, although exploration may extend to much greater depths than this in areas of known mineralization or altered rocks and in areas where specific geophysical targets are calculated to be at great depths.

For evaluation of deposits hosted by Mesozoic and older rocks, a map showing isopachs or depth contours to Mesozoic bedrock was constructed using procedures described by Jachens and Moring (1990) and using some of the data they acquired for partly contiguous regions in Nevada. This isopach map was then modified to reflect the detailed geology available in those areas where lack of gravity stations resulted in a spurious placement of the 500-m-depth contour line (pl. 3). As described by Jachens and Moring (1990), several uncertainties are associated with these contours showing depths to Mesozoic and older bedrock, and the 500-m isopach probably is less accurate than the 1-km isopach for the Cenozoic basin fill used in the study of the entire state of Nevada (R.C. Jachens, oral commun., 1990). Thus, the extent of permissive terranes and favorable tracts buried beneath Cenozoic, nonmagnetic (that is, nonvolcanic) sequences of rock shown on figures 92 and 93 should be viewed with extreme caution and regarded only as estimates subject to further refinement as additional information becomes available. Because of this uncertainty, we show permissive terranes and favorable tracts only at the relatively small scales of figures 92 and 93.

Thickness of nonmagnetic, late Cenozoic basin fill also was semiquantitatively estimated using aeromagnetic data collected by the National Uranium Resource Evaluation (NURE) program over the EMNSA. The NURE data were collected along east-west flightlines flown approximately 5 km apart and 120 m above the ground. These data were analyzed using both qualitative and quantitative techniques by J.D. Hendricks to produce a map showing areas of shallow magnetic sources (approximately <1 km depth to magnetic source) in the EMNSA. The map showing shallow magnetic sources, when combined with the available geologic map (pl. 1) and depths to mostly Mesozoic and older basement rocks, allows separation of areas of thick (>0.5–1.0 km), nonmagnetic Cenozoic deposits (valley-fill sediments) from areas of shallow basin fill. Areas are thus outlined to show the subsurface extent of shallow basin fill and may be considered to be within terranes permissive for the presence of certain types of mineral occurrence on the basis of extrapolation of permissive terranes from adjacent exposed bedrock (pl. 3).

In the following discussion, mineral occurrences are separated by age into three groups: occurrences that may have formed during the Proterozoic, those that may have formed during the Mesozoic, and those that may have formed during the Cenozoic. Some mineral-occurrence types may have formed during both the Mesozoic and Cenozoic (such as mineralized faults and polymetallic-vein deposits). Such deposit types are discussed in detail only with the age group with which they are most closely allied, generally the Mesozoic. This custom was followed even though the characteristics of known deposits elsewhere in the Mesozoic and Cenozoic, as well as the distribution of permissive terranes and favorable tracts for these deposits in the EMNSA, may be somewhat different. In addition, the Proterozoic rare earth element ore deposits at Mountain Pass, which are associated with carbonatite and alkalic intrusions just outside the EMNSA and are currently (1995) in production, were discussed in some detail in the section above entitled “Ultrapotassic Rocks, Carbonatite, and Rare Earth Element Deposit, Mountain Pass, Southern California” and so are not discussed in the sections to follow. Furthermore, also near Mountain Pass on the east flank of the Clark Mountain Range but inside the EMNSA, a breccia-pipe-related gold deposit that was in production during 1993 is present at the Colosseum Mine. This latter mineral deposit is associated genetically with felsic intrusions. Rocks that are similar in age to both of these mineralized systems, Mountain Pass and the Colosseum, also are present elsewhere in the EMNSA.

## **Proterozoic Deposits**

### **Carbonatite-Related, Rare Earth Element Occurrences**

#### ***Known Occurrences***

Although four occurrences in the EMNSA are assigned provisionally to carbonatite-related, REE-type systems (U.S. Bureau of Mines, 1990a, map nos. 48, 156, 351, and 358, pl. 1), only one of these, the Esperanza

Group of claims (map no. 156), is known definitely to be associated with carbonatite or related types of rock. The other three may owe their reported elevated abundances of REE to Early Proterozoic quartz-bearing pegmatite, and so they may not have the resource implications ascribed to them. In the general area of the Esperanza Group of claims, which apparently straddle the boundary of the EMNSA near Mineral Spring in the northeastern Ivanpah Mountains, small bodies of scarce carbonatite and related ultrapotassic rocks crop out in an area of possibly as much as 5 to 6 km<sup>2</sup>.

### ***Permissive Terrane***

The geologic terrane in the EMNSA that is permissive for Middle Proterozoic, carbonatite-related REE deposits and (or) occurrences includes all areas underlain, shallowly or otherwise, by rocks that are Early Proterozoic in age (pl. 1; see also fig. 92).

### ***Favorable Tract***

One tract favorable for the presence of additional discoveries of carbonatite-related REE deposits in and just outside the EMNSA is delineated (fig. 92). This tract is elongated and aligned in a northwest-southeast direction; it extends from the general area of the Mountain Pass REE deposit on the northwest to the general area of the Esperanza Group of claims on the southeast. Criteria used to delineate the favorable-tract boundaries (listed in table 18) primarily reflect the known presence of REE-bearing carbonatite and ultrapotassic rocks in numerous exposures of small bodies throughout the area delineated. According to the U.S. Bureau of Land Management (1982), drilling in the southeasternmost part of this outlined area that is favorable for REE deposits has resulted in discovery of “substantial resources of rare earth and thorium mineralization.” Hodges and Ludington (1991) estimated that 0, 0, 1, 1, and 2 undiscovered carbonatite deposits remain to be discovered, at 90, 50, 10, 5, and 1 percent probability levels, respectively. However, in light of the conclusions of the section above entitled “Ultrapotassic Rocks, Carbonatites, and Rare Earth Element Deposit, Mountain Pass, Southern California,” it is highly probable that the grade-and-tonnage distribution curves used by Hodges and Ludington (1991) to establish their numerical estimates are inappropriate for any REE-bearing carbonatite bodies that might be present in the EMNSA near Mountain Pass and that might be similar petrologically to the carbonatite bodies there.

## **Other Types of Proterozoic Deposits by Clay M. Conway and Ted G. Theodore**

### ***Volcanogenic Massive Sulfide Deposits in Arizona and Nevada***

Massive sulfide deposits are known in the Early Proterozoic rocks of Arizona (Anderson and Guilbert, 1979; Donnelly and Conway, 1988), including several in western Arizona (Stensrud and More, 1980; Conway, 1986; Conway and others, 1986, 1990) that are within the Mojave crustal province (Wooden and others, 1988; Wooden and Miller, 1990). The massive sulfide deposits in western Arizona range in size from small deposits of 1.45 thousand tonnes to as much as 1.5 million tonnes of copper-zinc-lead ore. The larger deposits, such as those located around Bagdad, Ariz., are comparable to a median-sized Cyprus-type massive sulfide deposit, on the basis of compiled grades and tonnages from throughout the world (Singer and Mosier, 1986). In central Arizona, the Early Proterozoic United Verde deposit at Jerome is a large deposit of similar grade and tonnage to some of the largest deposits in the world (Singer and Mosier, 1986). The deposit at Jerome, however, is associated with a sequence of Early Proterozoic rocks different in age and lithology from those found in western Arizona and in the EMNSA.

Massive sulfide deposits are mainly of three types: (1) Cyprus-type deposits, found in marine mafic-volcanic settings that also contain an ophiolite assemblage; (2) Besshi-type deposits, found in sedimentary sequences that consist of clastic terrigenous rocks and tholeiitic to andesitic tuff; and (3) Kuroko-type deposits, associated with marine rhyolite and dacite and subordinate basalt and sedimentary rocks (Cox and Singer, 1986; see also Sangster, 1980). Exhalative silica deposits and chloritized footwall rocks are associated with many of the deposits (Franklin and others, 1981). At high grades of metamorphism, the chloritized footwall rocks are converted to other assemblages, which include cordierite and anthophyllite.

### ***Volcanogenic Massive Sulfide Deposits in the East Mojave National Scenic Area***

Although no volcanogenic massive sulfide deposits are known in EMNSA, certain features that are characteristic of these deposits have been described in the Mojave crustal province, which includes the EMNSA. For example, massive sulfide deposits of varying size, as well as scattered chloritized rocks in the Early Proterozoic gneisses of the Mojave crustal province in western Arizona, suggest that the analogous Proterozoic terrane in the EMNSA may contain more deposits of this type. In addition, possible protoliths for bimodal felsic-gneiss-amphibolite sequences in the Providence Mountains include volcanic rocks (Wooden and Miller, 1990), although these sequences subsequently have been interpreted to have mostly plutonic protoliths (D.M. Miller, oral commun., 1991). Furthermore, cordierite-anthophyllite rocks are reported as small pods in Early Proterozoic gneiss in the Old Woman Mountains, 25 km to the south of the EMNSA (Stoddard and Miller, 1990). Other occurrences of somewhat similar rocks are known farther to the west in the Transverse Ranges of California (Powell, 1981). Howard and others (1988) suggested the possibility of volcanogenic mineralization of Early Proterozoic age at the Virginia May Mine, some 95 km south of EMNSA in the Turtle Mountains. Recent work confirms the volcanogenic character of the ore deposits at the Virginia May Mine (C.M. Conway, unpub. data, 1993). These deposits are likely to be of the Kuroko type. DeWitt and others (1989) recognized features in the McCullough Range, 10 to 20 km northeast of the EMNSA, which suggests the potential there for Besshi-type, sedimentary-hosted massive sulfide deposits.

No permissive terranes or favorable tracts for these types of deposit are delineated in the EMNSA but at least some possibility of volcanogenic massive sulfide occurrences exists in the EMNSA.

### ***Granite-Related Uranium, Thorium, and Rare Earth Element Deposits in Alaska and Elsewhere***

The predominant ore mineral in those granitic rocks favorable for the presence of uranium deposits is uraninite ( $\text{UO}_2$ ). Ballhorn (1989) recognized three types of granite worldwide that have been shown to host uranium deposits: (1) metaluminous anorogenic granite of alaskitic composition, exemplified by those at Rossing, Namibia, whose ore is related primarily to magmatic differentiation; (2) peraluminous granite, exemplified by the Mississippian to Permian, mostly two-mica granites in the Central Massif, France; and (3) alkaline granite, exemplified by the Jurassic granite at Bokan Mountain, Alaska. Uranium-enriched rocks associated with the latter two types of granite apparently are related to circulation of mostly subsolidus fluids. Nokleberg and others (1987) designated uranium-bearing granites in Alaska to be included within a felsic-plutonic type of deposit, and they described this deposit type as follows. Felsic-plutonic uranium deposits in Alaska consist of uranium minerals, thorium minerals, and REE minerals in fissure veins and disseminated in alkaline granite dikes in or along the margins of alkalic and peralkaline granitic plutons or in granitic plutons. The ore-forming environment is mainly in or along the margins of epizonal to mesozonal granitic plutons. Ore minerals in the deposits include allanite, thorite, uraninite, bastnaesite, monazite, uranothorianite, and xenotime, sometimes with galena and fluorite. Notable examples are the Roy Creek (Mount Prindle) deposit in east-central Alaska and the Bokan Mountain deposits in southeastern Alaska.

### ***Granite-Related Uranium, Thorium, and Rare Earth Element Deposits in the East Mojave National Scenic Area***

Certain Early and Middle Proterozoic granitic rocks in the EMNSA are notably enriched in large-ion-lithophile elements (LILE) and high-field-strength elements (HSFE), and they also include somewhat elevated abundances of U, Th, and REE (Miller and others, 1986; Wooden and Miller, 1990). Despite this enrichment, mineral occurrences containing these elements are rare, with the exception of the carbonatite at Mountain Pass. However, allanite-bearing pegmatites that intrude Early Proterozoic gneiss in the New York Mountains have Th and REE concentrations that are anomalous for this region (Miller and others, 1986). Because of these occurrences and the general enrichment in U, Th, and REE in the EMNSA, the potential for deposits associated with the granitic rocks needs to be evaluated. Jurassic granitoids are enriched in LILE and HSFE (Fox and Miller, 1990), and some of the following discussion pertains to rocks of this age.

Geochemical studies at mining-district scale of the levels of overall enrichment(s) of U in rock associated with granite-related uranium deposits provide a basis to which we may compare apparent U concentrations

found in the EMNSA by airborne radiometric surveys described in the section above entitled “Aerial Gamma-Ray Surveys.” Maximum concentrations of fairly widespread U detected in the EMNSA are slightly over 5 ppm (fig. 35C). Most areas showing these highest concentrations of U contain exposures of Proterozoic rocks and, locally, Jurassic rocks. In a comparative study of U concentrations in both uranium-mineralized and barren, peraluminous two-mica granitoids, Friedrich and Cuney (1989) found that 62 unaltered samples of coarse-grained granite in the massif of St. Sylvestre in France had an average U content of 22 ppm and that 45 fine-grained unaltered samples contained an average U content of approximately 17 ppm. The St. Sylvestre granitoid massif contains a proved resource of 38,000 tonnes U. In marked contrast, 90 unaltered peraluminous granitoid samples from the barren Manaslu massif in Tibet contain an average content of 9 ppm U. Therefore, the 5-ppm-maximum U contents over broad regions of the EMNSA suggest that this province is not likely to contain significant granite-related U deposits. Ballhorn (1989) noted that approximately 90 percent of the outcrops sampled within terranes judged to be favorable for the three types of granite-related uranium deposits he recognized showed concentrations of approximately 10 to 20 ppm U. Such large volumes of uranium-enriched rocks provide the source(s) of the uranium that may be subsequently leached and concentrated by oxidizing as well as CO<sub>2</sub>-enriched, subsolidus fluids (Friedrich and Cuney, 1989).

The conclusions above do not preclude the possibility of the existence of some small, high-grade occurrences of uranium in certain areas in the EMNSA. Figure 85 shows the distribution of U concentrations in 1,050 samples analyzed from the EMNSA (U.S. Bureau of Mines, 1990a). The two highest concentrations of U found during this sampling program are 1,570 and 1,590 ppm, the former of which is from the polymetallic vein at the Mammoth Mine (U.S. Bureau of Mines, 1990a, map no. 3, pl. 1) and the latter of which is from the Esperanza Group of claims (U.S. Bureau of Mines, 1990a, map no. 156, pl. 1), both of which are clustered in the general area of carbonatite-related REE occurrences near Mineral Spring in the Ivanpah Mountains. Both highly uranium enriched occurrences yield significant responses when examined by hand-held scintillometers, and both occurrences are in areas showing widespread outcrops of Early Proterozoic rocks. In addition, the Esperanza Group of claims is within the favorable tract we delimit above for the presence of carbonatite-related REE deposits that extends from northwest of the REE deposits at Mountain Pass to the trace of the 500-m depth-to-basement contour southeast of Mineral Spring (fig. 92).

No permissive terranes and favorable tracts for granite-related uranium, thorium, and REE deposits are delineated in the EMNSA because all of the Early and Middle Proterozoic rocks make up a permissive terrane for these types of deposits.

### ***Vein Deposits and Skarn Deposits in the East Mojave National Scenic Area***

As discussed in the section above entitled “Proterozoic Rocks and Their Mineralization,” Hewett (1956) suggested that certain base- and precious-metal vein deposits in the area of the EMNSA might be of Proterozoic age. Preliminary investigations in an area east of the Albermarle Mine in the New York Mountains suggests the possibility that polymetallic veins there predate or, more likely, are the same age as Middle Proterozoic diabase dikes. The time of emplacement of many veins examined by us in Early Proterozoic rocks of the EMNSA can only be constrained to postdate deformation of the foliated host rocks. Thus the possibility remains that some vein deposits might be as old as Early Proterozoic. Nothing has been noted in the literature or discovered during our reconnaissance field investigations of the Early Proterozoic rocks to suggest that many veins predated deformation or were formed during either of the orogenic events. The presence of a ductilely deformed metamorphic fabric in some polymetallic veins in the general area of Mineral Spring, Ivanpah Mountains, can be used as evidence to support emplacement during the Proterozoic, possibly during the Middle Proterozoic. The REE signature of these veins is similar to the REE signature of Middle Proterozoic ultrapotassic rocks at Mountain Pass (T.G. Theodore, unpub. data, 1993). Furthermore, polymetallic skarn at the Butcher Knife Mine, in Butcher Knife Canyon in the New York Mountains, also may be Proterozoic in age (Ntiamoah-Agyakwa, 1987).

Tungsten veins of Early Proterozoic age are an additional type of vein deposit that may be found in EMNSA, although occurrences of these deposits are not presently known in the ENMSA. The possibility of veins of this type in the EMNSA is based on the association of tungsten-bearing veins with Early Proterozoic two-mica granite in the Hualapai Mountains, Ariz., located some 50 km to the southeast of EMNSA. Tungsten

is present there as wolframite in veins. The 1,680– to 1,690–Ma two-mica granite in the Hualapai Mountains is considered to be part of the widespread, postorogenic Early Proterozoic granites (Chamberlain and Bowring, 1990; Conway and others, 1990) that crop out in western Arizona and southern California. They are alkali-calcic in composition and have associated deposits or contain anomalous concentrations of W, Sn, Be, Nb, La, and Y (Conway, 1991). These granites are also found in the region of EMNSA (Bender and others, 1988; Miller and Wooden, 1988; Anderson and others, 1993).

### ***Platinum-Group-Element Occurrences Associated With Ultramafic Rocks in Nevada and Arizona***

Small exposures of ultramafic rocks are reported in Early Proterozoic rocks in the McCullough Range northwest of the EMNSA, the New York Mountains, and elsewhere in Nevada and Arizona. Some of these exposures are associated with somewhat elevated abundances of platinum-group elements. Ultramafic rocks are known in nearby Early Proterozoic sequences in the Gold Butte area of southern Nevada (Volborth, 1962; Dexter and others, 1983), Lost Basin in northwestern Arizona (Page and others, 1986; Theodore and others, 1987a), and near Bagdad, Ariz. (Floyd Gray, oral commun., 1988; C.M. Conway, unpub. data, 1990). Anomalous concentrations of Pt were reported by Lechler (1988) at the Gingerload prospect in the Crescent Peak Mining District, Nev., which is located outside the EMNSA at the north edge of the New York Mountains, approximately 11 km north of Castle Peaks. In the Crescent Peak Mining District, a silicified Early Proterozoic granitoid has probably been mineralized by Cretaceous granite (D.M. Miller, written commun., 1991). The Gingerload prospect is a Pb–Zn–Cu–Ag–Au polymetallic vein (Lechler, 1988).

### ***Platinum-Group-Element Occurrences Associated With Ultramafic Rocks in the East Mojave National Scenic Area***

No platinum-group mineral occurrences are known in the EMNSA. Some small exposures of metamorphosed Early Proterozoic ultramafic rocks in the Ivanpah Mountains in the EMNSA contain as much as 22 weight percent MgO (Wooden and Miller, 1990). However, no platinum-group analyses of these rocks are available. Some potential for copper, cobalt, chromium, and platinum-group elements may be associated with such rocks in the EMNSA in Alaskan platinum-group-element-type or zoned-ultramafic, chromium-platinum-type occurrences (Page and Gray, 1986). These Early Proterozoic ultramafic rocks in the EMNSA should be studied geochemically to evaluate this potential.

## **Mesozoic Deposits**

### **Breccia Pipe and Related Deposits by Carroll Ann Hodges**

#### ***Gold Breccia Pipe***

The Colosseum Mine, in the Clark Mountain Mining District north of Mountain Pass (pl. 2), at one time was the largest gold producer within the EMNSA and, from 1987 to 1992, was the largest metals mine in operation. It produced about 2,188 kg Au and 938 kg Ag per year during peak years of operation. The Clark Mountain Mining District includes the Mountain Pass REE deposit, just outside the EMNSA boundary, as well as numerous abandoned copper, fluorite, and tungsten mines and prospects.

The Colosseum gold deposit, investigated in detail by Sharp (1984), is in a breccia-pipe complex that consists of two connected felsite breccia pipes and outlying felsite dikes in a horst block of Proterozoic younger undivided granitoids (unit Xg, pl. 1). The ore is primarily free gold that is disseminated at the micrometer scale in auriferous pyrite. Surrounding related mineralized rock includes vein silver-copper in brecciated dolostone, tungsten, and fluorite, described in the following sections entitled “Silver-Copper Brecciated Dolostone,” “Tungsten Veins,” and “Fluorite Veins.” Production, initially begun in 1929, was shut down in 1939, but the mine was reopened in 1987 as an open-pit operation. According to the U.S. Bureau of Mines (1990a), ore reserves in 1989 were estimated at 9.5 million tonnes (t), averaging 1.94 g Au/t. About 7 years of mine life were left as of February, 1990, at a production rate of about 219 kg/yr and a gold price of \$400/oz. The following descriptive summary of the deposit largely is modified from Sharp (1984).

Breccia-pipe gold has not been defined formally as a deposit type (Cox and Singer, 1986), and so characteristics of the Colosseum orebody cannot readily be compared with those of other deposits assigned to this specific type, although descriptions of some individual breccia-pipe gold deposits are available (Baker and Andrew, 1991). Sillitoe (1991) included the Colosseum deposit with six other breccia-pipe-hosted gold deposits he described. The overall range in contained gold in those seven gold-bearing breccia pipes is 9 to 101 tonnes Au, and their mean content of Au is about 44 tonnes. Thus, the Colosseum Mine, which has been shown to contain about 20 tonnes Au, is one of the smaller of such systems known.

The Clark Mountain Mining District is in the southernmost tip of the 800-km-long Cordilleran fold and thrust belt, active tectonically from Permian through Cretaceous time. Three major northwest-striking thrust faults transect the region and, together, account for a total west-to-east displacement of 64 to 80 km (Burchfiel and Davis, 1971). Hewett (1956) estimated that 7,000 to 10,000 m of Paleozoic sedimentary rocks originally were thrust over the Proterozoic granitoids that now constitute the horst block in which the breccia pipes are found (fig. 94). Thrusting was followed by normal faulting along the high-angle Clark Mountain and Ivanpah faults, which offset the region during basin-and-range deformation. Only about 500 m of Paleozoic carbonate rocks are exposed presently in the downdropped block to the west. The mineralized breccia pipes, dated at approximately 100 Ma (Sharp, 1984), were intruded after thrusting but before the normal faulting that produced the basin-and-range horst-and-graben structures during the late Tertiary, as interpreted by Sharp (1984).

The breccia pipes and associated felsite dikes, which are exposed as resistant knobs enclosed within the Proterozoic gneisses, are each about 170 by 235 m wide at the surface, elongated to the northeast-southwest, and connected by a narrow dike. The pipes represent multiphase brecciation events, including significant collapse, and the lithologies within them indicate the composition of the overlying Paleozoic sedimentary rocks and the height of stope during the development of the breccia. Overlying rocks included the Cambrian Tapeats Sandstone, Cambrian Bright Angel Shale, and Late Cambrian to Devonian dolomite units (included in units Cd and PDI). The Colosseum orebody is in the western pipe, but both pipes are mineralized. Each pipe consists of early felsite that is disrupted by later igneous breccia; however, the western pipe also contains abundant clasts of the structurally higher Paleozoic rocks that had been thrust over the Proterozoic rocks before onset of breccia-pipe emplacement. The abundance of sedimentary rocks as clasts indicates that the western pipe stopped through the Tapeats Sandstone and Bright Angel Shale, well into the overlying dolomite, whereas the eastern pipe, predominantly containing basement rocks and felsite igneous breccia, did not invade the Paleozoic sedimentary rocks significantly. Height above the current surface that was subjected to stoping was at least 430 to 460 m. Gold is disseminated in breccia and associated closely with pyrite, commonly filling fractures in pyrite. Highest concentrations of gold are in the western pipe where pyrite has replaced carbonate-breccia fragments, greatly increasing the overall concentration of sulfide minerals.

Metal zoning in this part of the Clark Mountain Mining District (fig. 95) is apparently related spatially and genetically to breccia-pipe mineralization. The gold zone is restricted to a circular area around the breccia pipes, in addition to a crescent-shaped area west of and bounded by the Clark Mountain fault. Within the breccia pipes, gold is associated mainly with sulfide minerals, primarily pyrite, whereas outside the pipes, gold is a constituent of quartz-barite and quartz-pyrite veins and veinlets that form a complex network surrounding felsite dikes. Silver is present predominantly in a broadly concentric zone west of, and bounded by, the Keystone thrust fault; the veins make up the Ivanpah Mining District, which had significant production into the early parts of the 20th century. Tungsten is found predominantly in a broad northwest-trending belt, which intersects a part of the gold zone and is bounded on the west by the Clark Mountain fault. Field inspection of the regional distribution of tungsten veins suggests that some of the tungsten veins in the Proterozoic granitoids to the south-southeast of the Colosseum Mine may not be related to the emplacement of the gold-bearing breccia pipe at the mine (pl. 2), inasmuch as known tungsten veins are present in Proterozoic granitoids as much as 6.5 km southeast of the mine. Nonetheless, felsite dikes related to the emplacement of the breccia pipes extend from Clark Mountain to Mountain Pass, a distance of 11 km (Sharp, 1984). Within the gold zone, tungsten is present as wolframite and scheelite in Proterozoic rocks. Fluorite is in veins and shear zones associated with the Keystone and Mesquite Pass thrust faults west of the silver zone.

Sharp (1984) attributed these spatial relations to development of a single hydrothermal system, which was initially stacked vertically but was subsequently displaced by gravity gliding (detachment faulting) on the then-extant Keystone thrust fault and by high-angle normal faulting on the Clark Mountain fault. Epithermal-vein silver, originally closest to the surface in the system, is now horizontally juxtaposed with the deeper gold-rich breccia-pipe complex. Thus, the district zoning from west to east represents the displaced slices of once-vertical zones, the vein silver in the silver-copper brecciated-dolostone occurrences being found at the top (fig. 95). As will be described later in this section, scanning electron microscope (SEM) studies have established the presence of tungsten in ore at the Colosseum Mine, and the presence of tungsten apparently in distal parts of the mineralized system here can only be attributed to mobility of tungsten in a hydrothermal environment, as was documented by Bateman (1965) in some of the retrograde parts of the Pine Creek, Calif., tungsten-skarn system. Alternatively, the Colosseum Mine may represent the superposition of a Cretaceous gold breccia pipe onto an environment already enriched in tungsten during a previous episode of tungsten mineralization.

Felsite, dated at  $99.8 \pm 4$  to  $102 \pm 4$  Ma, is the oldest rock in the breccia pipe (K–Ar dates by Geochron Laboratories, *as quoted* in Sharp, 1984) and consists of equal parts of quartz, K–feldspar, and sericite, plus secondary siderite; carbonate content is about 6 volume percent. The second phase of intrusion caused brecciation of the felsite, producing the igneous breccia that consists mainly of felsite matrix and minor quartzite, granite, gneiss, and andesite clasts. A third phase occurred in the western pipe, producing collapse-rubble breccia that is the most intensely mineralized rock type of the entire breccia-pipe complex. Dolomite breccia fragments are replaced by disseminated pyrite and are accompanied by sphalerite, siderite, and chalcopyrite that hosts gold and silver. As of 1984, commercial values of disseminated gold had been found as deep as 170 m below the surface.

The breccia pipes appear to have been emplaced by fluidization, carbon dioxide being the dominant fluidizing agent (Sharp, 1984). Carbonate content increases with each stage of fluidization and intrusion (6 volume percent in the felsite, 20 volume percent in the igneous breccia, and 30 volume percent in the rubble breccia), indicating that increasing amounts of carbonate rocks were assimilated by the intrusion and incorporated into the breccias as they reached progressively higher levels of stoping into the Late Cambrian to Devonian dolomites. Fluid-inclusion studies of a 751-m-deep drill hole into the breccia-pipe complex indicated that the lower 250 m of the drill hole is dominated by CO<sub>2</sub>-rich fluids (Cook and others, 1992). These studies also suggested that the minimum lithostatic trapping pressures required to yield the observed fluid-inclusion relations range from 2.1 to 3.1 kilobars (kb). These pressures correspond to paleodepths of 7.9 to 11.7 km at the time of emplacement of the breccia-pipe complex, and they are remarkably consistent with the overburden estimated by Hewett (1956) at the time of breccia-pipe development.

Gold mineralization in the breccia pipes is present in an irregular vertical cylinder surrounding a barren core (Sharp, 1984). Depth of oxidation is about 100 m, and degree of oxidation is about 80 percent. Supergene enrichment, however, is of no mineralogic or economic importance. The barren core in the interior of the rubble-breccia pipe is devoid of gold but contains minor to major amounts of pyrite, zinc, and copper in well-silicified impervious rocks. Late gold-bearing fluids were unable to percolate through this impermeable unit to reach the favored sulfide sites for gold deposition. Gold content varies directly with depth, and gold is commonly alloyed with silver (as electrum) as fracture fillings in pyrite or along grain boundaries. According to Sharp (1984), Au/Ag ratios averaged 1.5 to 1, in marked contrast to the Au/Ag ratios found in the surrounding vein deposits (see following section entitled “Silver-Copper Brecciated Dolostone”). Gangue minerals, in order of decreasing abundance, are siderite, goethite, quartz, and sericite. Pyrite is the most susceptible host for precipitation of gold, apparently because of its ease of fracturing (Sharp, 1984).

The four principal vein types in the ore at the Colosseum Mine are quartz-pyrite, quartz-barite, calcite-barite, and calcite-dolomite, in addition to occasional veins of unknown source and genetic significance that contain lead, antimony, tungsten, and zinc, as well as minor silver. According to Sharp (1984), mineral paragenesis and sequence of events took place in the following stages: (1) early, coarse-grained, barren pyrite and minor quartz; (2) coarse-grained, second-stage pyrite that has gold, chalcopyrite, sphalerite, bornite(?), and pyrrhotite; (3) shattering and fracturing of coarse-grained pyrite; (4) major phase of gold mineralization, which filled fractures and interstices in pyrite, accompanied by apparently stable sphalerite, chalcopyrite, and galena;

(5) fine-grained, barren pyrite; (6) siderite replacement and flooding of the breccia matrix; and (7) localized veining by quartz and fine-grained pyrite. Gold is disseminated throughout the deposit; electrum mineralization was later paragenetically than the main-stage sulfide mineralization and its accompanying major amounts of gold.

Two examples of gold included in pyrite were identified in SEM micrographs, which were obtained from one polished thin section of felsite breccia from the Colosseum Mine (fig. 96A, B, D), and also were verified by an X-ray spectrogram (fig. 96C). The largest grain of gold (about 7–8  $\mu\text{m}$ ; see fig. 96B) was clearly deposited along a fracture and possibly represents the major gold-mineralizing phase (stage 4) of Sharp's (1984) paragenetic sequence. The smaller grain (about 4  $\mu\text{m}$ ; see fig. 96D) may represent the second phase (Sharp's (1984) stage 2) of included gold associated with pyrrhotite. Examination by SEM also revealed grains of monazite and other rare earth element minerals that have been localized in cracks between euhedral pyrite crystals (figs. 96E, F). Additional minerals identified within pyrite include the following: small grains of wolframite (fig. 96A); bismuth and silver tellurides (fig. 96G); possibly resorbed chalcopyrite, pyrrhotite, and sphalerite (fig. 96H); and sphalerite that has small euhedral pyrite inclusions and conspicuous replacement rim of covellite surrounded by feldspar (fig. 96I). The relation shown in figure 96A seems to confirm the genetic gold-tungsten association in the ore-forming system at the Colosseum Mine.

### ***Silver-Copper Brecciated Dolostone***

Silver veins in the Clark Mountain Mining District are categorized as silver-copper brecciated dolostone; they are peripheral to the gold breccia pipes of the Colosseum orebody which was emplaced in Proterozoic rocks to the east of the silver veins (pl. 2). The veins are restricted to Late Cambrian to Devonian dolomite, which was downdropped to the west from its earlier overthrust position above the Proterozoic rocks (pl. 1).

According to the U.S. Bureau of Mines (1990a), the veins are present in fractured, sheared, and brecciated zones in gray-yellow dolostone. Ore mineralization is reported as stromeyerite (ideally,  $(\text{CuAg})_2\text{S}$ ) in pods and blebs that contain minor azurite and malachite, and a gangue of calcite-dolomite and quartz (Hewett, 1956). Most individual vein systems strike northwestward and dip steeply to the northeast. More than \$4 million in silver was produced from the Clark Mountain Mining District in the late 1800s, primarily from the Beatrice, Monitor, Stonewall, and Lizzie Bullock Mines (Sharp, 1984); production from the Monitor Mine continued until 1942.

The U.S. Bureau of Mines (1990a) analyzed 92 samples from the silver-copper brecciated-dolostone deposits. Maximum Ag content was 3,080 ppm; maximum Au, 946 ppb. In 32 samples, Cu content was well over 1,000 ppm, and was greater than 10,000 ppm in 11 of them. Forty-seven samples contained more than 1 ppb Au and more than 1 ppm Ag; the average Ag/Au ratio was 4,660, which is notably high and contrasts with the Ag/Au ratio of approximately 0.67 at the Colosseum gold deposit. Zinc content was greater than 10,000 ppm in only three samples and greater than 1,000 ppm in 18 samples. Lead content was greater than 10,000 ppm in four samples and was 1,000 ppm or greater in 32 samples.

Sharp (1984) developed an intriguing hypothesis for the origin of the Ivanpah silver deposits, relating them genetically to the gold mineralization of the Colosseum breccia pipe. By this hypothesis, silver-bearing hydrothermal fluids accompanying the felsite breccias rose through the Proterozoic granitoid rocks, in which the gold orebodies are now present, into the overthrust Paleozoic sedimentary rocks. The fluids stopped upward well into the Cambrian to Devonian dolomite units; height of stoping is demonstrated by the presence of abundant carbonate fragments within the Colosseum breccia pipe. Mesothermal gold mineralization is richest in this pipe because of selective massive replacement of carbonate minerals by sulfide minerals. Epithermal-vein silver, however, emplaced in the overlying dolomite, was subsequently downdropped to the west along high-angle normal fault(s) and low-angle detachment fault(s) during a postmineralization extensional event localized along a preexisting thrust plane. Thus, the breccia pipe was effectively decapitated, juxtaposing the silver-copper occurrences in the dolomite on the west with the gold mineralization in lower parts of the pipe to the east (fig. 97). The mineral zoning and fault pattern as described by Sharp (1984) fit this explanation.

Although not exact analogues, the silver-copper deposits in the Ivanpah Mining District exhibit some characteristics of polymetallic-vein and polymetallic-replacement occurrences, which generally are related to

felsic igneous intrusions (Cox and Singer, 1986). They are particularly common in areas of high permeability, such as breccia veins and pipes, and may form replacement bodies in carbonate rocks. It seems unlikely that economic, large-tonnage deposits of a type similar to the silver veins of the Ivanpah Mining District will be discovered in the EMNSA.

### ***Tungsten Veins***

Tungsten is present in veins and skarns within the EMNSA. Veins are primarily in Proterozoic schist and gneiss and are localized in a northwest-trending belt south of and overlapping the gold and silver zones of the Colosseum breccia pipes (fig. 95B). Other small occurrences are present in presumed 70–Ma Cretaceous monzogranites, mostly in the Signal Hill Mining District near the south end of the Piute Range (area VI, fig. 92). Tungsten veins in the Signal Hill Mining District may be significantly younger than those associated with the ores at the Colosseum Mine. According to the U.S. Bureau of Mines (1990a), the Mojave Tungsten Mine, south of the Colosseum Mine, produced 29,090 kg of 60 percent WO<sub>3</sub> concentrates in 1915 and 1916; elsewhere, production has been minor or nil, although one sample (from the Old Boy prospect, lat 35°00' N., long 115°02' W.) analyzed by the U.S. Bureau of Mines (1990a) contains 2.59 weight percent W.

Tungsten veins in both the Ivanpah-Colosseum Mining District and the Cretaceous intrusive bodies farther south are in fault and shear zones that strike generally to the northwest. Tungsten mineralized rocks consist mainly of wolframite in vein quartz; scheelite is present in some veins. At the Mojave Mine, gold, silver, pyrite, azurite, and malachite, in a gangue of quartz and subsidiary calcite, are accessory to the iron-manganese and calcium tungstates. Limonite is common in some veins. Consistent detection of tungsten in veins within the Late Cambrian to Devonian dolomites, as well as in quartz veins of the Proterozoic granitoids, prompted extension of the tungsten zone around the Colosseum breccia pipes west of the Keystone thrust fault and Clark Mountain fault (fig. 95; Sharp, 1984).

Sharp (1984) concluded that the tungsten mineralization surrounding the Colosseum Mine was genetically related to the breccia-pipe complex. Tungsten was deposited in a zone both vertically and laterally intermediate between mesothermal gold and epithermal silver.

The descriptive model of tungsten veins by Cox and Bagby (1986) fits closely with characteristics of the tungsten veins in the EMNSA. Such deposits typically contain wolframite and base-metal sulfide minerals in quartz veins associated with granitoid rocks emplaced in sedimentary or metamorphic rocks. The deposits consist generally of swarms of parallel veins. Grade-and-tonnage models that are based on data from 16 deposits worldwide indicate that a 90 percent chance exists for any new discovery to contain at least 45,000 tonnes of ore, as well as a 90 percent chance that any newly discovered deposit will have at a grade of as much as 0.6 percent WO<sub>3</sub>, whereas only a 10 percent chance apparently exists for a new deposit to contain as much as 7,000,000 tonnes of ore (Jones and Menzie, 1986a).

### ***Fluorite Veins***

Fluorite veins are present at scattered localities in the EMNSA, most notably throughout the entire Clark Mountain Mining District (Sharp, 1984) where the mineralization is in low-angle shears and fractures parallel to the Keystone and Mesquite Pass thrust fault zones (fig. 95). In this northernmost part of the EMNSA, veins commonly contain varying amounts of pyrite, copper-carbonate minerals, silver, and tungsten, all of which are associated also with the Colosseum breccia-pipe gold mineralization. Because fluorite is much more broadly distributed than the mineralized zones adjacent to the breccia pipes, it is not clear that the fluorite is related genetically.

According to the U.S. Bureau of Mines (1990a), minor fluorite production occurred only at the Pacific and Juniper Mines, and no production has taken place since 1961. At the Pacific Mine, about 3.2 km southwest of the Colosseum orebody, fluorite is concentrated in zones as much as 2 m wide along low-angle, north-striking, west-dipping faults that crop out within Late Cambrian to Devonian dolomites. It also is present in high-angle shear zones together with quartz, sericite, limonite, stibnite, and copper minerals. Analyses of 11 samples showed metal contents as high as 122,000 ppm Sb, 367 ppm Mo, 592 ppm Ag, 190 ppm W, and 56,300 ppm Zn. One sample contained 3.07 weight percent Cu and 26.1 weight percent Pb; three others contained 3.68,

3.94, and 5.26 weight percent fluorine. The U.S. Bureau of Mines (1990a) concluded from these analyses that significant resources exist at the Pacific Mine. At the Juniper Mine, about 1.6 km south of the Pacific Mine, massive purple and green fluorite is present in sheared, brecciated zones 2 m thick or more within surrounding carbonate rocks. The zones are partly silicified, showing minor amounts of limonite and copper carbonate minerals. On the basis of sample analyses, the U.S. Bureau of Mines (1990a) estimated resources of approximately 272,000 tonnes (t) containing 20 to 30 weight percent fluorite, 3 weight percent Cu, and 312 g Ag/t. The fluorite veins at both the Pacific and Juniper Mines are associated with polymetallic veins, as are a number of fluorite prospects in the area. Scattered fluorite veins also are present in shear zones in Proterozoic granite gneiss near the Albemarle Mine in the northeast corner of the EMNSA in the Castle Peaks Wilderness Study Area (Miller and others, 1986). Production was insignificant from these veins, but 15 analyzed samples ranged from 1 to 5.9 weight percent fluorine (U.S. Bureau of Mines, 1990a). Miller and others (1986) did not identify any potential for resources in the general area of the Albemarle Mine. In addition, fluorite veins are present in dolomite near the contact with the informally named Mid Hills adamellite of Beckerman and others (1982), which is associated with the Big Hunch stockwork-molybdenum system in the southern New York Mountains (pl. 2). Select samples of mineralized Mid Hills adamellite in the general area of the Giant Ledge Mine (U.S. Bureau of Mines, 1990a, map no. 296, pl. 1) show flooding by fluorite to as much as 20 volume percent. Polymetallic veins that cut the Mid Hills adamellite at this locality in Caruthers Canyon also show assemblages of galena, chalcopyrite, quartz, pyrite, fluorite, and white mica. In the southern Providence Mountains, the Golden Nugget prospect includes blue and green fluorite veins in association with quartz and polymetallic veins in fault- and shear-breccia zones. Production from this prospect has been nil, but of 111 samples analyzed by the U.S. Bureau of Mines (1990a), 15 contained 100 to 620 ppm Pb, 25 contained 26 to 600 ppm Zn, 89 contained 20 to 990 ppm Cu, 56 contained 6 to 270 ppm Mo, 61 contained trace to 88 g Au/t, 59 contained trace to 44 g Ag/t, and 7 chip samples contained 0.08 to 25 weight percent fluorine. If the Golden Nugget prospect is developed for other metals, fluorite could be a possible by-product. However, most ore deposits of hydrothermal fluorite veins and mantos contain more than 35 volume percent fluorite (Worl and others, 1973).

No descriptive or grade-and-tonnage model exists for fluorite veins (Cox and Singer, 1986). If, however, future production of fluorite in the EMNSA is contingent upon development of associated polymetallic veins, the probability is not high that large-tonnage economic orebodies of that type remain to be discovered in the EMNSA.

### ***Known Occurrences***

The only known occurrence of gold-bearing breccia pipes is at the Colosseum Mine. Silver-copper brecciated dolostone is present in a broad area, generally west of the orebodies at the Colosseum Mine, within Paleozoic rock sequences (pl. 1). The silver-copper brecciated-dolostone mineralization, which presumably developed at the same time as the orebodies at the Colosseum Mine were emplaced, forms a halo of petrogenetically linked deposits. Tungsten veins are present in Proterozoic granitoids in and around the general area of gold ores at the Colosseum Mine (pl. 2); most are presumably linked to the emplacement of the gold-bearing breccia pipe (Sharp, 1984) but some may not be related to the pipe development during the Cretaceous. In addition, scattered occurrences of tungsten veins are found elsewhere in the EMNSA, including widespread veins in the Signal Hill Mining District near the south end of the Piute Range (pl. 2) and minor occurrences hosted by the Mid Hills adamellite. Vein-type fluorite is associated with the Colosseum breccia pipes and is present in Paleozoic sequences of carbonate rocks west of the Colosseum Mine (pl. 2).

### ***Permissive Terrane and Favorable Tract***

A permissive terrane and a favorable tract for gold-bearing breccia pipes are largely coextensive and are defined in the northern part of the EMNSA by the outer limit of silver-copper brecciated-dolostone occurrences in Paleozoic rocks and the outer limit of tungsten veins in Proterozoic younger granitoids (pl. 2; see also fig. 92). The terrane outlined for gold-bearing breccia pipes also is shown as being both permissive and favorable for tungsten veins, as is another small area near the south end of the Piute Range (fig. 92). Hodges

and Ludington (1991) estimated that one tungsten-vein deposit, at a 1 percent probability level, remains to be discovered in the EMNSA at a size and grade comparable to the grade-and-tonnage model for these types of deposit.

No permissive terranes or favorable tracts specifically for silver-copper brecciated dolostones or fluorite veins are delineated in the EMNSA. Because silver-copper brecciated dolostones are probably related to Mesozoic magmatism, the common presence of Mesozoic igneous rocks in the EMNSA makes all carbonate sequences exposed there permissive hosts, which are largely coextensive with the permissive terranes discussed below for skarn.

Geologic factors controlling ore deposition at the Colosseum gold mine include the presence of Proterozoic crystalline host rocks overlain by reactive carbonate sequences at the time of emplacement of a CO<sub>2</sub>-rich magmatic-hydrothermal system during the Cretaceous (fig. 97). Exposure of the mesothermal gold-bearing ores adjacent to the epithermal-silver veins was dependent on a complex sequence of tectonic and erosional events (Sharp, 1984). The vein silver is the downfaulted top of the Clark Mountain breccia-pipe system, emplaced adjacent to the Colosseum ore zone as a result of relative vertical uplift and tilting of the Proterozoic basement. This was then followed by detachment faulting that decapitated the breccia pipe and juxtaposed the vertically stacked precious-metal zones. The western breccia pipe was particularly favorable to ore mineralization because it stopped high into Late Cambrian to Devonian limestones and includes large volumes of carbonate fragments within the breccia. This reactive rock type was susceptible to replacement by pyrite, whose low strength and brittle character resulted in fracturing in response to continued brittle-style strain, thereby providing a receptive host for late gold-mineralizing fluids (Sharp, 1984).

## **Low-Fluorine Porphyry-Molybdenum Deposits**

### ***Classification of the Deposits***

The Big Hunch stockwork-molybdenum system in the southwestern part of the New York Mountains in the EMNSA is one of a number of molybdenum deposits and molybdenum-enriched systems that are associated with Jurassic to Pliocene calc-alkaline magmatic arcs in the western North America Cordillera (this section of the report is modified from Theodore and others, 1992). In addition, several molybdenum-enriched porphyry systems of Paleozoic age (Schmidt, 1978) and presumed Paleozoic age (Ayuso and Shank, 1983) crop out in eastern North America and bear many similarities to the calc-alkaline ones in western North America. Such stockwork-molybdenum systems generally have low fluorine contents relative to deposits of the better known Climax-type molybdenum deposits in Colorado (Theodore and Menzie, 1984). The fluorine-deficient porphyry-molybdenum systems have been included in different ways in the several classifications of porphyry-molybdenum deposits (Woodcock and Hollister, 1978; Sillitoe, 1980; Mutschler and others, 1981; White and others, 1981; Cox and Singer, 1986; Carten and others, 1993). Guilbert and Park (1986) considered the low-fluorine stockwork-molybdenite deposits as a subset of porphyry base-metal systems. The one striking characteristic of all these systems is their minor-element signature, especially when compared to the better known stockwork-molybdenum systems exemplified by the one at Climax, Colo. (see for example, Westra and Keith, 1981; White and others, 1981; Carten and others, 1993). Thompson (1982b), in a further modification of the classification scheme for stockwork-molybdenum deposits, suggested that alkali-calcic and the alkali stockwork-molybdenum deposits of Westra and Keith (1981) be subdivided into a monzonite-syenite subtype and into a leucogranite subtype. The Climax-type systems are characterized by highly differentiated, high-silica rhyolite magmas that are enriched in F (locally as much as 2–3 weight percent), Nb, Rb, Mo, Sn, and W and are nearly depleted in Cu and Sr (Ludington, 1981). The Climax-type systems are present in rifted cratons, whereas the low-fluorine or quartz-monzonite type of systems are related to geologic processes associated with continental margins.

Fluorine-deficient porphyry-molybdenum systems generally show overall F contents of less than 0.1 weight percent, and many of these systems also include significant concentrations of Cu and Ag (Czehura, 1983); some include significant W and Au (Theodore and Menzie, 1984; Theodore and others, 1992). At Buckingham, Nev., gold skarns at the Surprise Mine and at the Carissa Mine probably are temporally and genetically related

to the Buckingham stockwork-molybdenum system (Schmidt and others, 1988). Westra and Keith (1981, fig. 9) showed a continuity of hypogene copper and molybdenum grades between porphyry-copper deposits and fluorine-deficient porphyry-molybdenum deposits.

Fluorine-deficient porphyry-molybdenum systems, which are widespread throughout the geologic provinces of the North American Cordillera, are present in magmatic arcs that generally parallel the Mesozoic batholiths. In the Basin and Range Province, several Late Cretaceous fluorine-deficient porphyry-molybdenum deposits in Nevada (for example, Buckingham or Hall) and many other prospects are related to small granitic bodies peripheral to the Sierra Nevada batholith. These prospects include the Magruder Mountain (Sylvania), Nev., and, in the EMNSA, the Big Hunch, Calif., systems, both of which may have been emplaced sometime in the Mesozoic.

### ***Big Hunch Stockwork-Molybdenum System***

The Big Hunch stockwork-molybdenum system is an extremely large system that at one time was inferred to encompass approximately 1.63 billion tonnes of mineralized rock that has an estimated grade of approximately 0.025 weight percent Mo (U.S. Bureau of Land Management, 1980; most of this section of the report is modified from Ntiamoah-Agyakwa, 1987). However, recently completed evaluations of this system suggest that the volume of significantly mineralized rock is about 43,000,000 tonnes (Wetzel and others, 1992). Nonetheless, mineralized rock at the surface here is widespread, and the main center of alteration associated with this system is the area of the Big Hunch Mine (pl. 2). A second center east of the Lighthouse Mine (also known as the Dorr Tungsten Mine; see also U.S. Bureau of Mines, 1990a, map no. 291, pl. 1) is much less strongly developed. The best developed alteration zones are silicic, phyllic (quartz-sericite), and argillic. No propylitic stage of alteration has been observed. A questionable potassic stage is poorly represented by an erratic, apparently relict, K-feldspar stable assemblage found in one vein. Intensity of silicification declines away from the core of the system, and concentrations of sericite and clay minerals increase successively. Ore mineralogy is simple, consisting chiefly of pyrite, chalcopyrite, sphalerite, galena, and molybdenite and minor amounts of magnetite, specularite, bornite, and wolframite-heubnerite. Two samples of diamond drill core from DDH York no. 9, which was drilled into the core of the Big Hunch system, were taken from depths of approximately 68 m below the surface and examined by SEM. The purpose of this examination was to determine the mineral phase(s) that hosts most of the silver in the system. Silver was not detected during any spot analyses of the polished surfaces. However, it was determined that many of the quartz-molybdenite veins in the Big Hunch system also contain tetrahedrite, as well as some minor amounts of galena as minute blebs in stout crystals of pyrite. None of the tetrahedrite was found to contain detectable silver, which is common in the tetrahedrite present in many low-fluorine stockwork-molybdenum systems elsewhere (Theodore and Menzie, 1984). In places, tetrahedrite seems to predate paragenetically the crystallization of minor amounts of sphalerite. In addition, some tetrahedrite in close proximity to chalcopyrite shows notable concentrations of As and some Zn. Growth zones of tetrahedrite against quartz suggest that some of the earliest crystallized tetrahedrite is more arsenian than the latest crystallized varieties. Fluorite is ubiquitous. Although the presence of fluorite in the Big Hunch system suggests highly elevated concentrations of fluorine during the metallogenesis here, the overall abundance of fluorine in these types of systems is still less than that found in the much higher grade, rift-related Climax-type systems (White and others, 1981; Westra and Keith, 1981; Theodore and Menzie, 1984; Carten and others, 1993).

The surficial and vertical extent of the Big Hunch system was established by Ntiamoah-Agyakwa (1987) from surface mapping on a scale of 1:4,800, as well as data from over 2,000 m of drill cores representing nine drill holes. All holes were drilled from the surface and went through the mineralized zones. The Big Hunch system is semielliptical, a hook-shaped (pseudoannular) compound system made up of two nested concentric patterns about 3.2 by 4 km. The larger outer system is incomplete, thought at one time by Ntiamoah-Agyakwa (1987) to be cut off on the west by the Cliff Canyon fault, but phyllic alteration associated with the Big Hunch system has since been determined to extend well beyond the trace of the Cliff Canyon fault (D.M. Miller, oral commun., 1993). On the north, the Big Hunch system appears to be bounded by an east-northeast-striking fault (pl. 1). The exposed vertical extent of the system is about 250 m, from 5,700 ft (1,737 m) to 6,500 ft (1,981 m) in elevation.

In the Big Hunch stockwork-molybdenum system, quartz-sericite or phyllic alteration is not only the most conspicuous but also the best developed alteration product in the informally named Mid Hills adamellite of Beckerman and others (1982) (unit Kmh, pl. 1), which hosts the system (Ntiamoah-Agyakwa, 1987). This type of alteration is characterized by a preponderance of quartz veins that have sericite selvages. Pyrite is not ubiquitous in this alteration; fluorite is commonly present. Muscovite is characteristically coarse grained. Development of the quartz-sericite veins apparently took place during three episodes, the second of which seems to have been the episode during which the bulk of the molybdenite was introduced. The second episode of quartz veining also involved intense hydroxyl metasomatism. Clay minerals and fine-grained hydrothermal quartz are replaced by quartz veins. This second-generation quartz is massive, compact, milky quartz. In most cases, veining is episodic, resulting in rhythmic bands of quartz and sulfide minerals and (or) oxide minerals. In its most advanced stage, silicification is the most destructive event, obliterating most of the earlier stages of alteration. In areas where development stages can be traced, such as at Lecyr Well, alteration proceeds from closely spaced fractures to quartz veins that have sericite selvages. Influx of altering fluids depended on either the extent of fracturing or permeability of the initially argillized host. Where extensive microfracturing preceded fluid influx, the result is near complete silicification. Fluorite, molybdenite, or pyrite may accompany this second stage. Locally, sparse orthoclase-microcline veins developed, as is described later in this section.

Although the geochemistry of the Big Hunch stockwork-molybdenum system has been described by Ntiamoah-Agyakwa (1987) and the U.S. Bureau of Mines (1990a), additional analyses of 36 rocks in the general area of the system are included in this report (table 19). Analyses show the overall intensity of fluorine metasomatism (as fluorite and micas mostly in veins) and the sporadic intensity of molybdenum introduction. Furthermore, the large number of samples that show F abundances greater than 1,000 ppm, together with their locations throughout an area of approximately 5 km<sup>2</sup>, emphasize that the emplacement of this system during the Late Cretaceous has affected significantly a very large volume of rocks.

Potassic alteration is either very weakly developed or absent throughout much of the Big Hunch system, in contrast to the extent of potassic alteration at other stockwork-molybdenum systems (Ntiamoah-Agyakwa, 1987). Secondary biotite was noted only in a 1-m-long section in one drill hole. Here, it is poorly developed at a depth of about 3 m as a thin vein about 0.1 mm wide. Pervasive argillic alteration is crosscut by 1- to 2-mm-wide sericite veinlets and 0.1-mm-wide, fine-grained, amorphous biotite microveins. Biotite in the original porphyritic to equigranular adamellite is in varying stages of degradation. Primary magmatic orthoclase is still preserved, however, which is suggestive of intermediate argillic-alteration assemblages.

No correlation has been made at the regional scale between density of deposits or nearby mineral occurrences and intensity or overall volume of metal introduced. As described above, the subeconomic (at 1994 market conditions) Big Hunch stockwork-molybdenum system hosts one of the largest concentrations of metal known to date (1995) in the EMNSA. However, the grade of this type of molybdenum system is the limiting factor that results in many of such systems in the western North American Cordillera being economically marginal. Nonetheless, some zoning of types of veins is present peripheral to the Big Hunch system. As pointed out by Ntiamoah-Agyakwa (1987), some of the more important polymetallic-vein occurrences in the general area of the Big Hunch System include Lighthouse (Dorr?) (copper-tungsten), Giant Ledge (lead-copper, with silver), and Sagamore (copper-lead, with zinc, silver, and tungsten); smaller prospects include Garvanza (copper-tungsten), Hard Cash (copper-zinc-fluorine, with tungsten?), Lecyr Well (copper, with zinc-molybdenum?), and Live Oak (copper-zinc, with tungsten). Thus, this area of the New York Mountains was classified by Ntiamoah-Agyakwa (1987) as a polymetallic molybdenum-copper-tungsten porphyry center that has varying amounts of silver, lead, and zinc in its surrounding veins.

Potassium-argon ages were obtained by Ntiamoah-Agyakwa (1987) on six samples spatially and (or) temporally associated with emplacement of the Big Hunch stockwork-molybdenum system. The six ages cluster into two groups, 67 to 71 Ma and 59 to 66 Ma; the short time interval between the two clusters suggested to Ntiamoah-Agyakwa (1987) that all dated samples are part of one continuous process during the Late Cretaceous magmatic event associated with emplacement of the Mid Hills adamellite. However, U-Pb data for zircons from the Mid Hills adamellite indicate that the rocks crystallized about 93 Ma (E. DeWitt, oral commun., 1985). The Late Cretaceous ages ascribed by Ntiamoah-Agyakwa (1987) to the alteration associated

with the Big Hunch system in the area of Fourth of July Canyon have been verified by others (69 to 88 Ma on biotite, Beckerman and others, 1982; 69 Ma on biotite in sericitized rocks, D.M. Miller, written commun., 1991). Thus, either the polyphase emplacement of the Mid Hills adamellite took place over approximately 25 m.y. or the alteration and emplacement of the Big Hunch system was related to a Late Cretaceous hydrothermal event that was discrete from emplacement and crystallization of the major part of the Mid Hills adamellite.

### ***Known Occurrences***

The presence of molybdenum in the general area of the New York Mountains has been known since the 1950s (Ntiamoah-Agyakwa, 1987), and, nearby, relatively small veins have achieved some production of note in the general area of the Big Hunch system. As indicated by the maps showing the classification of deposit types in the EMNSA (pl. 2), in fact only a small number of vein-type occurrences are known in the general area of the Big Hunch system. The petrogenetic linkage of polymetallic veins and other types of deposits to low-fluorine, porphyry-molybdenum systems is indicated schematically on figure 89. It cannot be precluded that linkages exist elsewhere in the EMNSA, but outside the general area of the Big Hunch system, such as between polymetallic veins and some buried porphyry-molybdenum system. A corollary from this schematic linkage is the fact that one does not need to observe enhanced abundances of Mo and F to indicate the possible presence of a porphyry-molybdenum system at depth, although F and Mo anomalies might be additional positive signatures. A number of samples analyzed from polymetallic veins in the EMNSA by the U.S. Bureau of Mines (1990a) were shown to include more than 500 ppm Mo. The pervasive character of veining, fractures, and alteration patterns, if present, are the diagnostic features that one must first consider before making a qualified judgment about the potential presence of a porphyry system, either a molybdenum or a copper-molybdenum one.

### ***Permissive Terrane***

One terrane is delineated as being permissive for stockwork-molybdenum systems in the EMNSA (fig. 92). This terrane follows generally the inferred and mapped outline of the informally named Mid Hills adamellite of Beckerman and others (1982). As such, the localities of possible stockwork-molybdenum mineralization at Globe Canyon, described above in the section entitled "Delineation of Areas Permissive and Favorable for Undiscovered Metallic Mineral Resources," also are included within this permissive terrane. The mineralization at Globe Canyon apparently is associated spatially with two small outliers of the Mid Hills adamellite that crop out approximately 0.5 km south of the main mass of the body (pl. 1). The mineralized rocks at Globe Canyon are categorized as being the possible site of a low-fluorine stockwork-molybdenum system (pl. 2). Jurassic plutonic rocks are excluded from the permissive terrane for stockwork-molybdenum systems primarily because most contain relatively reduced contents of silica relative to those stockwork-molybdenum systems known elsewhere in the western North American Cordillera. The Jurassic plutonic rocks in the EMNSA as a group are apparently not that highly evolved, and Westra and Keith (1981) showed that nearly all host intrusions for low-fluorine types of stockwork-molybdenum systems are apparently peraluminous, regardless of silica content. However, some of the least altered igneous rocks associated genetically with the Buckingham stockwork-molybdenum system, Nevada, are slightly metaluminous (Theodore and others, 1992). In addition, all Cretaceous plutons other than the Mid Hills adamellite are excluded because of either their low-silica chemical composition or the absence of a widespread composite mode of emplacement. The informally named Rock Spring monzodiorite of Beckerman and others (1982) (Krs) generally has an overall low silica content (54–64 weight percent) compared with igneous rocks that are associated with most of these types of molybdenum systems; the rocks are essentially porphyritic and compositionally variable, including mostly monzodiorite, quartz monzodiorite, and some quartz monzonite (pl. 1). Estimates of 0 to 3 kb pressures of emplacement for the Teutonia batholith by Anderson and others (1988, 1992) were obtained from the Kessler Springs adamellite (Kks), the Mid Hills adamellite, and the Rock Spring monzodiorite, all informally named units of Beckerman and others (1982). The 3–kb pressures of the Rock Spring monzodiorite suggest that its currently exposed levels may be well below those depths commonly ascribed to most porphyry systems, both molybdenum and copper-

molybdenum, in the Southwest, which are generally less than about 1.5 kb. The Kessler Springs adamellite is seemingly shallow seated (0–0.5 kb, Andersen and others, 1992), but it apparently shows minimal evidence of a wide-ranging, composite nature for its emplacement mode, as does the phase of the batholith represented by the informally named Teutonia adamellite of Beckerman and others (1982) (Kt) (D.M. Miller, oral commun., 1991).

### ***Favorable Tract***

A relatively small area in the general area of the Big Hunch system is delineated as being favorable for the presence of stockwork-molybdenum systems (fig. 92). The general area of Globe Canyon is not considered to be a favorable tract, which reflects the judgment that the occurrences there should not be ranked as equivalent to those at the Big Hunch system. Hodges and Ludington (1991) estimated that one low-fluorine porphyry-molybdenum system, at a probability level of 1 percent, remains to be discovered in the EMNSA.

## **Porphyry Copper and Skarn-Related Porphyry Copper**

### ***Known Occurrences***

No known occurrences of porphyry-copper systems or skarn-related porphyry-copper systems, as defined by Cox and Singer (1986), are known in the EMNSA. In the exposed upper parts of many of these systems, the rocks commonly are intensely fractured and altered to various combinations of potassic, phyllic, intermediate-argillic, argillic, and advanced-argillic assemblages across widespread areas, sometimes as much as 20 to 30 km<sup>2</sup>. Many systems include quartz-stockwork veins that also are commonly widespread, as well as distinctive pyritic halos, together with elevated abundances of many metals. Many of these features are shared with stockwork-molybdenum systems, and these features are present in the general area of the Big Hunch system. In addition, the porphyry-copper and the skarn-related porphyry-copper systems would show the same genetic relations to other types of mineral occurrences depicted for the stockwork-molybdenum systems (fig. 89). In the general region of the EMNSA, porphyry-copper systems have been inferred to be present in the area of Turquoise Mountain, 5 km north of the EMNSA, in the hills near Halloran Spring (Hall, 1972), as well as in the Crescent Peak Mining District, about 10 km northeast of the EMNSA in Nevada (D.M. Miller, oral commun., 1991). North of the Horse Hills, near the southern end of the Providence Mountains, Miller and others (1985) assigned a low potential for the presence of a gold-rich porphyry-copper system in iron-oxide-stained Jurassic igneous rocks. However, field examinations for the present report did not reveal the presence there of widespread altered and shattered rocks that are typical of the upper parts of many of these types of porphyry systems. In addition, the exposed iron oxide minerals appear to be related to mineralized dilational fractures that opened in response to displacements along the regionally extensive Bighorn fault about 3 km to the east. Finally, examination of about 10 thin-sectioned rocks from this area failed to show the presence of any alteration phenomena that are characteristic of these systems.

### ***Permissive Terranes and Favorable Tract***

All of the EMNSA that is underlain by Mesozoic igneous rocks is permissive for the presence of porphyry-copper systems. The areas where these igneous rocks are near or in contact with sequences of Paleozoic carbonate rocks also are permissive for the presence of skarn-related porphyry-copper systems. Excluding alteration associated with the Big Hunch system, the most likely porphyry-style alteration of igneous rocks noted during the study is in the general area of New Trail Canyon, in the northeastern part of the Ivanpah Mountains. Here, some outliers of the informally named Ivanpah granite of Beckerman and others (1982) (unit Ji, pl. 1), which crop out away from its major exposures farther south in the Ivanpah Mountains, are intensely fractured, iron stained, and hydrothermally altered across several square kilometers. The outlined favorable tract for porphyry-copper and skarn-related porphyry-copper systems (fig. 93) coincides with one of the tracts also classified as favorable for the occurrence of various other types of skarn and polymetallic replacement occurrences in the EMNSA. Hodges and Ludington (1991) estimated that one porphyry-copper deposit at each of the 5 and 1 percent probability levels remains to be discovered in the EMNSA.

## Skarn

Smirnov (1976) suggested that classification of skarns be based on the composition of the original protolith of the skarn, either calcareous, magnesian, or silicate. However, the nongenetic definition of skarn proposed by Einaudi and others (1981) is followed in this report:

\*\*\* replacement of carbonate [or other sedimentary or igneous rocks] by Ca–Fe–Mg–Mn silicates [resulting from] (1) metamorphic recrystallization of silica-carbonate rocks, (2) local exchange of components between unlike lithologies during high-grade regional or contact metamorphism, (3) local exchange at high temperatures of components between magmas and carbonate rocks, and (4) large-scale transfer of components over a broad temperature range between hydrothermal fluids \*\*\* and predominantly carbonate rocks.

Most metallized skarns owe their genesis to processes largely involving the fourth classification. Thus, we follow an overall classification of skarns that is based on their sought-after metal content (see also, Zharikov, 1970; Shimazaki, 1981).

### **Known Occurrences**

Known metallized skarns in the EMNSA are classified into the following types, the number of each shown in parentheses: polymetallic (18), zinc-lead (6), tungsten (3), iron (10), tin-tungsten (1), and copper (26) (table 14). Almost all skarns apparently formed during emplacement of either Jurassic or Cretaceous magmas into the carbonate sequences of Paleozoic rocks that crop out in the EMNSA (pl. 1). A small number of relatively minor occurrences of skarn in the New York Mountains may be Proterozoic in age. Examination of the regional distribution of the types of skarn in the EMNSA suggests that no readily apparent clustering by type of skarn is evident in the immediate area of any particular type of granitoid body. Jurassic granitoids, however, seem to be associated preferentially with some of the largest and highest grade iron-skarn deposits in the EMNSA, such as those at the Vulcan Iron Mine (pl. 2). Skarns are distributed widely across most exposed carbonate sequences of rocks in the EMNSA (pl. 2). Some of the most conspicuous skarns in the EMNSA are at the following locations: (1) along the west flank of the Clark Mountain Range in the general area of the Mohawk and Copper World Mines, presumably Cretaceous in age; (2) in the Ivanpah Mountains in the general area of the Evening Star Mine and Standard Mine No. 2 and along the east edge of Striped Mountain, presumably Jurassic in age; (3) near the central Providence Mountains at the Vulcan Iron Mine, Jurassic in age; and (4) in the general area of Cowhole Mountain, Little Cowhole Mountain, and Old Dad Mountain (pl. 2).

Of the 197 rock samples analyzed by the U.S. Bureau of Mines (1990a) that contain greater than 500 ppb Au, 36 are from mineralized skarns of all types in the EMNSA. This particular data base does not include rocks from the area of the Providence Mountains, which has been shown to host six skarn occurrences (pl. 2). Nonetheless, a small number of samples in the RASS and PLUTO heavy-mineral-concentrate and rocks data bases obtained from the Providence Mountains show anomalous concentrations of Au (figs. 57, 58). All skarns, regardless of type, in the EMNSA can thus be characterized as being potential sites for the deposition of at least some gold, in significant concentrations in some places. The highest concentration of Au reported by the U.S. Bureau of Mines (1990a, map no. 163) is from copper skarn at the New Trail Mine (pl. 6) in the Ivanpah Mountains (51,700 ppb Au). In addition, our limited sample base collected during this study (tables 10, 11) includes a small number of samples from five occurrences of mineralized skarn in the EMNSA (Evening Star, Copper King, Vulcan Iron, Mohawk, and Copper World Mines). Four samples from the Evening Star Mine area show Au contents that range from 26 to 450 ppb (table 11, analysis nos. 1–4). The highest recorded Au content from the Mohawk Mine area is 42 ppb in four select samples (analysis no. 72); from the Vulcan Iron Mine, 150 ppb (analysis no. 7). The highest content of Au found at the Vulcan Iron Mine is in marble less than 0.5 m beyond the magnetite front, suggesting a buildup of precious-metal content at the fringes of this iron-skarn system.

The geologic environments of gold-bearing skarn worldwide were examined by Ray and others (1990), Ray and Webster (1990), and Theodore and others (1992b). Korobeinikov (1991) listed the following criteria for granitoid intrusions that are associated with productive gold-bearing skarns, mostly in the Soviet Union: (1) Na predominating over K by approximately 1 to 2 weight percent; (2) high Cl/F ratios in the evolved fluids; and (3)

wide-ranging gold-bearing contact zones in the surrounding hornfels, marbles, and magnesian skarns.

As recognized by Meinert (1983, 1988a, b, 1989, 1993), many deposits referred to as gold skarns in the literature have been classified, or could be classified, under skarn-deposit models as copper and iron skarns by their dominant base- or ferrous-metal contents. For these deposits, gold production may be considered a by-product of base- or ferrous-metal mining. Furthermore, gold-bearing skarn deposits commonly may be gradational into skarn that contains no gold but does contain significant other metal(s), including the silver-rich skarns as defined by Ray and others (1986), possibly sediment-hosted disseminated gold-silver deposits (also known as carbonate-hosted and Carlin-type), porphyry-copper or copper-molybdenum deposits, or polymetallic-replacement deposits (exemplified by the McCoy megasystem, Nev.), as well as other deposit types related to felsic- and (or) intermediate-composition plutonic emplacement or volcanic activity. Mineralized skarns show genetic linkages to a wide variety of deposit types, of which some linkages are well established by geologic relations in the EMNSA (fig. 89). The Cove deposit, McCoy Mining District, Nev., which has been shown to include proven and probable reserves of 48.7 million tonnes (t) with an average grade of 1.85 g Au/t and 87.1 g Ag/t (Kuyper and others, 1991), has been classified recently by Cox and Singer (1990) as a distal disseminated silver-gold deposit. Polymetallic veins, the most common type of deposit in the EMNSA, are another deposit type that may be present on the fringes of gold-bearing skarn deposits (pl. 2; see also table 12). Other commodities produced by gold-bearing skarns include silver, copper, zinc, iron, lead, arsenic, bismuth, tungsten, and tin, as principal or by-product commodities, and cobalt, cadmium, and sulfur, as by-products (Theodore and others, 1991).

Gold-bearing skarns are generally calcic exoskarns that have gold associated with intense retrograde hydrosilicate alteration, although gold-bearing magnesian skarns are known and in some areas are dominant. Some economically significant gold-bearing skarns, however, are partly in endoskarn (Knopf, 1913; Pardee and Schrader, 1933) (for example, Hedley, British Columbia, 2.986 million tonnes at 13.46 g Au/t, Theodore and others, 1991; Suian, South Korea, 0.53 million tonnes at 13.0 g Au/t, Theodore and others, 1991). Significant concentrations of gold-bearing endoskarn also are present at the Nambija, Ecuador, gold-skarn deposit (McKelvey and Hammarstrom, 1991). Gold-bearing skarns can show diverse geometric relations to genetically associated intrusive rocks and nearby premetallization structures (Theodore and others, 1992b). Similar relations are present in some of the skarns in the EMNSA that have been shown to contain some gold.

### ***Permissive Terranes and Favorable Tracts***

Permissive terranes and favorable tracts for the presence of metallized skarn of all types, including gold-bearing skarn, are considered to be coextensive and to include all exposed areas of Paleozoic carbonate sequences in the EMNSA (fig. 93). In addition, some small parts of the Proterozoic rocks also may be permissive for the presence of mineralized skarn, especially in the New York Mountains, where a single favorable tract, mostly including Paleozoic carbonate strata, is shown. This favorable tract also is coextensive with the permissive terrane for metallized skarn in this area. On figure 93, a favorable tract for iron skarn is delineated, primarily on the basis of magnetic anomalies in the general area of the Vulcan Iron Mine in the Providence Mountains; in addition, the presence of magnetite-bearing skarn at two localities, the BC prospect and the Adams-Ikes Hope prospect, both in the Colton Hills, are categorized as being permissive for the presence of additional iron-skarn occurrences (Goldfarb and others, 1988). However, the amplitude of the magnetic anomaly in the general area of these latter two occurrences, about 2,000 nanoTeslas, is somewhat lower than that in the general area of the Vulcan Iron Mine, and Jurassic igneous rocks in the general area of the two prospects have a high magnetic susceptibility (Goldfarb and others, 1988). An extensive permissive terrane for iron skarn in the general area of Old Dad Mountain is delineated on the basis of wide-ranging positive magnetic anomalies that extend well into areas covered by unconsolidated gravels (fig. 93).

In established mining districts in the EMNSA that are zoned from mostly proximal, copper-dominant deposits to distal, precious-metal- and base-metal-dominant veins, all stratigraphic sequences favorable for development of skarn in the zone of precious-metal deposits should be considered as permissive hosts for development of gold-bearing skarn. One area in the EMNSA that seems to show some of these zonal relations between a copper-enriched part and a lead-zinc-enriched part is the general setting of the Mohawk and Copper

World Mines in the southwestern part of the Clark Mountain Range. In another area, a gold-copper-iron zone is distal to the iron skarn at the Vulcan Iron Mine in the Providence Mountains (Goldfarb and others, 1988). In addition, Ray (1990) and Ray and Webster (1990) included the Jurassic arc-related rocks in the EMNSA as being favorable hosts for the development of gold skarns.

Gold placers in regions permissive for the formation of skarn also may be suggestive of the presence of gold skarn (R.G. Russell, written commun., 1989), especially if the placer gold is intergrown with bismuth minerals, including bismuth oxides or bismuth tellurides (Theodore and others, 1987b; Theodore and others, 1989). However, only nine placer localities in the EMNSA show the presence of visible free gold (table 15). Even in some of the most heavily mineralized areas of the EMNSA, such as the northern parts of the Providence Mountains (pl. 2), only a small number of placer operations are developed in drainages whose upper reaches head in the heavily mineralized areas (Moyle and others, 1986).

Anomalous values of Bi, Te, As, Se, and Co, on the one hand, are useful geochemical signatures for some gold-bearing skarns (Brooks and Meinert, 1989). However, some economically important gold skarns are notably deficient in Bi, As, and Te (McKelvey and Hammarstrom, 1991).

Hodges and Ludington (1991) estimated that the following numbers of various types of skarn deposit remain to be discovered in the EMNSA at the ensuing probability levels (--, not determined):

<i>Probability level</i> -----	90%	50%	10%	5%	1%
<i>Deposit type</i>	<i>Number of deposits</i>				
Copper skarn-----	1	2	4	--	--
Lead-zinc skarn-----	0	1	2	5	7
Iron skarn -----	0	0	1	3	5

## **Polymetallic Replacement, Distal Disseminated Gold-Silver, and Vein Magnesite**

### ***Known Occurrences***

Twenty-three polymetallic-replacement deposits, one distal disseminated gold-silver occurrence, and one vein-magnesite occurrence are known in the EMNSA (table 15; see also pl. 2). Most polymetallic-replacement deposits are in the western part of the Clark Mountain Range where some are present distal to well-developed lead-zinc skarn at the Mohawk Mine. Another notable concentration of polymetallic-replacement deposits is near the south end of the Mescal Range, an area that was being evaluated for its mineral potential by private industry in 1991. Only one occurrence (U.S. Bureau of Mines, 1990a, map no. 161, pl. 1) in the Ivanpah Mountains has been classified tentatively as belonging to a distal-disseminated gold-silver type of occurrence, and it is described as a pyrite-bearing, iron-oxide-stained jasperoid developed in dolomite. The magnesite-vein occurrence is present in the New Trail Canyon area of the Ivanpah Mountains (fig. 98), near the copper and iron skarns at the New Trail Mine. These latter mineral occurrences are just to the north of a large mass of the informally named, Jurassic Ivanpah granite of Beckerman and others (1982) (unit Ji, pl. 1), which is a porphyritic monzogranite, and so mineralization is presumably Jurassic in age in the general area of New Trail Canyon.

Polymetallic-replacement deposits as classified and analyzed in Cox and Singer (1986) showed median tonnages of 1.8 million tonnes, and median grades of 5.2 weight percent Pb, 3.9 weight percent Zn, and approximately 0.1 weight percent Cu.

### ***Permissive Terranes and Favorable Tracts***

All areas of the EMNSA that are underlain by Paleozoic carbonate rocks are designated to be permissive for the presence of polymetallic-replacement deposits, distal-disseminated gold-silver occurrences, and magnesite-vein occurrences (fig. 93). As such, the areas so designated are coextensive with those that we consider to be permissive for the presence of various types of skarn. However, available data are not refined to the point that we can confidently discriminate favorable tracts for polymetallic replacement within the outlined permissive

terrane. Figure 89 depicts graphically the genetic linkages among all these deposits. Hodges and Ludington (1991) estimated that one polymetallic-replacement district remains to be discovered in the EMNSA at each of the 5 and 1 percent probability levels.

## **Polymetallic Vein, Polymetallic Fault, and Gold-Silver Quartz-Pyrite Vein**

### ***Known Occurrences***

At least 206 polymetallic-vein occurrences, 79 polymetallic faults, and 80 occurrences classified as gold-silver quartz pyrite veins are known in the EMNSA (table 15; pl. 2). All three types of occurrences are essentially cogenetic. The major differences between the polymetallic-vein occurrences and the gold-silver quartz-pyrite veins are differences in the relative amounts of galena, sphalerite, and chalcopyrite. Polymetallic veins generally show high concentrations of all these minerals, even though they may have been exploited primarily for their precious metals. One of the most economically significant concentrations of polymetallic veins in the EMNSA apparently is at the Morning Star Mine (pl. 2; U.S. Bureau of Mines, 1990a, map no. 178, pl. 1). Mining operations at the Morning Star Mine were placed on standby during 1991, although gold continued to be produced from a 1.8-million-tonne heap-leach pad at the property (Keith Jones, Vanderbilt Gold Corp., oral commun., 1991). Some ore apparently was shipped in 1992 from polymetallic veins at the Golden Quail Mine (pl. 2; see also U.S. Bureau of Mines, 1990a, map no. 417, pl. 1), which was reported to contain 12,500 kg Au (Wetzel and others, 1992); operations at the Golden Quail Mine were suspended in 1993. As noted by Ausburn (1988) and Sheets and others (1989), proven reserves at the Morning Star Mine in 1988 included about 7.26 million tonnes (t) of ore at a grade of 1.88 g Au/t. The deposit is hosted by the informally named, Jurassic Ivanpah granite of Beckerman and others (1982) (unit Ji, pl. 1) and primarily is present along the hanging wall of a low-angle thrust fault related to the Mesozoic thrust belt (Burchfiel and Davis, 1971; Sheets and others, 1989). Early-stage quartz-carbonate veins in the deposit include pyrite, sericite, hematite, ilmenite, galena, electrum, chalcopyrite, sphalerite, and tetrahedrite (Sheets and others, 1988, 1989, 1990). According to these authors, mineralization at the Morning Star Mine appears to be associated spatially and genetically with metamorphic fluids. In addition, textural relations suggest that primary electrum was deposited and then remobilized by secondary supergene fluids (Sheets and others, 1995). The tonnage of the mineralized system at the Morning Star Mine is larger than any of the deposits used in the base-metal-silver category of polymetallic veins plotted by Bliss and Cox (1986). As pointed out by Bliss and Cox (1986), apparently two types of polymetallic veins are known: (1) base-metal-silver veins, and (2) gold-silver polymetallic veins that contain significant concentrations of Cu, Pb, and Zn. The Morning Star deposit probably belongs to the latter of these two categories. Some major mining districts elsewhere that show significant production from gold-bearing polymetallic vein have been described by Morris (1990), Fisher (1990), Shawe (1990), and Thompson (1990).

The gold-silver quartz-pyrite veins in the EMNSA typically do not show visible presence of galena, sphalerite, or chalcopyrite, and, as such, they commonly have low contents of Pb, Zn, and Cu. The classification scheme adopted during study of the EMNSA for those occurrences that were not examined in the field and that do not report presence of galena, sphalerite, or chalcopyrite involved use of available analyses of mineralized rock reported by the U.S. Bureau of Mines (1990a). Those mineralized-vein samples reported to contain in excess of several hundred ppm Pb, Zn, or Cu were included with the polymetallic veins. Analyses are available for 97 mineralized rock samples from the sites of 47 gold-silver quartz-pyrite veins in the EMNSA (table 20). In these 97 rock samples, average contents are approximately 1,800 ppb Au, approximately 7 ppm Ag, 17 ppm As, 3 ppm Sb, and approximately 100 ppm Zn; Ag/Au ratios are approximately 4. The apparently low average contents of Sb in these veins probably are a reflection of emplacement of most of these veins in a mesothermal, base-metal-deficient environment, although Sb can be present in fairly large concentrations in some deep-seated geologic environments (Berger, 1993). The polymetallic veins seem generally to contain more As and Sb (fig. 86). The strongest elemental association of Au in these 97 rock samples is for Ag; calculation of Spearman's correlation coefficient yields a value of +0.4. Some gold-silver quartz-pyrite veins in the EMNSA may be Tertiary in age and epithermal rather than mesothermal (Lange, 1988). No grade-and-tonnage models are

available for gold-silver quartz-pyrite veins in the EMNSA. These types of veins in the EMNSA most likely are analogous to the gold-silver polymetallic veins of Bliss and Cox (1986). However, preliminary compilations by Bliss and Cox (1986) did not yield an adequate grade-and-tonnage sampling of gold-silver polymetallic veins, and they, therefore, present no plots showing their cumulative frequency distributions for grade and tonnage. Some gold-bearing quartz veins elsewhere bear some similarities to the gold-silver quartz-pyrite veins delineated in the EMNSA. Gair (1989a), in a comprehensive evaluation of the mineral resources of the Charlotte 1° × 2° quadrangle, North Carolina and South Carolina, described some gold-quartz and gold-pyrite-quartz veins there that were important sources of gold from about 1825 to 1910. As pointed out by Gair (1989a), the gold-quartz and gold-pyrite-quartz veins he studied are epigenetic fissure fillings, many of which crosscut the foliation in the enclosing schists and gneisses. Many veins are in the upper parts of apparently subvolcanic intrusions, and some of the gold grades in the mined veins apparently were as much as 344 g Au/t, but probably grades of 9.4 to 15.6 g Au/t were more typical at some of the more significant deposits (Gair, 1989a).

Polymetallic faults are mostly brittle-type gouge and fracture zones along structures of variable regional importance. Such mineralized fault zones typically do not include a silicate-gangue mineralogy common to veins; quartz is not reported. Most of the brittle-type polymetallic faults in the EMNSA were exploited some time in the past primarily along their near-surface traces of gouge. Elsewhere, Wallace and Morris (1986) documented the highly variable geometric relations between gouge and the trace of the associated fault zones (fig. 99). Most importantly, however, these authors showed the complex geometry that some mineralized faults may attain at relatively great depths below the present erosion surface (fig. 100). Similar relations also may be found at some future time along the seemingly geometrically simple East Providence fault in the EMNSA (pl. 1). Some mineralized strands of the East Providence fault may be as complex at depth as those depicted in the Coeur d'Alene Mining District, Idaho, by Wallace and Morris (1986) and, in fact, to this date (1995) have not been deciphered properly to show the massive fluid-flow patterns suggested by the presence of many small mineral occurrences in the general area of the fault.

All three types of mineralized occurrences may be related spatially and genetically to mineralized skarn, polymetallic-replacement deposits, and any centers of porphyry-type mineralization. Distribution patterns of polymetallic veins and gold-silver quartz-pyrite veins were examined in the EMNSA to determine whether or not their distribution may, in places, have followed the proximal-to-distal copper-gold (silver)-lead (zinc) zonation recognized in many porphyry-type metallization centers elsewhere in the Southwest. However, the spatial relations between these two types of vein occurrence in the EMNSA seem to be highly erratic (pl. 2).

### ***Permissive Terranes and Favorable Tracts***

All areas of the EMNSA that mostly include outcrops of Proterozoic, Paleozoic, and Mesozoic rocks (including both igneous and sedimentary protoliths) are designated to be permissive for the presence of Mesozoic polymetallic veins, polymetallic faults, and gold-silver quartz-pyrite veins (pl. 1). Favorable tracts within the outlined permissive terranes could not be delineated on the basis of data available. Hodges and Ludington (1991) estimated that 3, 8, and 20 polymetallic-vein deposits, respectively, at 90, 50, and 10 percent probability levels, comparable to those in the published grade-and-tonnage curves (Bliss and Cox, 1986), remain to be discovered. No grade-and-tonnage models are available for the gold-silver quartz-pyrite vein or the polymetallic-fault occurrences.

## **Tertiary Deposits, by James J. Rytuba and Robert J. Miller**

### **Volcanic-Hosted Epithermal-Gold Deposits**

#### ***Known Occurrences***

Tertiary volcanic rocks in the Castle Mountains, located near the California-Nevada border, hosted one of the largest mineable reserves of gold in southern California (pl. 2). These gold deposits are located in the easternmost part of the EMNSA and are economically the most important Tertiary deposits in the EMNSA. Development drilling in the Hart Mining District by Viceroy Gold Corporation from the mid-1980s

to the present (1993) delineated six individual orebodies in the southernmost part of the Castle Mountains (Linder, 1989). Total combined reserves were 34 million tonnes of ore containing more than 62,500 kg Au. Commercial production at Castle Mountains Mine by Viceroy began in April, 1992, and, in its first six months, approximately 1,600 kg Au had been produced (The Northern Miner, 1993, v. 79, p. 14). The volcanic-hosted gold deposits in the Hart Mining District are similar to other economically important volcanic-hosted deposits being mined in Nevada, such as Rawhide and Round Mountain; the latter, which has reserves of over 312,500 kg Au, is the largest volcanic-hosted deposit in the United States. The large tonnage and grade of these orebodies makes them amenable to open-pit and heap-leach methods, and this class of deposits constitutes a significant component of gold reserves in the United States. Gold was first located in the Hart Mining District in 1907 (Ausburn, 1991).

Similar-age middle Miocene volcanic rocks are present elsewhere in and west of the EMNSA, and, in the vicinity of the cities of Mojave and Lancaster, Calif., several rhyolite dome complexes host economically important gold deposits that were being mined in 1993. These deposits are characterized by widespread acid-sulfate and argillic alteration. Closely associated in time and space with these gold deposits is the largest borate deposit in North America at Boron, Calif., which formed from hot-spring systems that were active during volcanism. These hot springs vented into basins developed peripheral to the volcanic-dome field. On the basis of this association, a model for the gold deposits in the Hart Mining District must include the potential for B, as well as other lithophile elements (Li, Mo, F, U) peripheral to the gold deposits.

Tertiary volcanic rocks in the Castle Mountains are middle Miocene in age and range from 18.5 to 14 Ma (see section above entitled "Tertiary Rocks"). The volcanic rocks unconformably overlie a basement composed of Proterozoic metamorphic rocks covered by a thin sequence of Paleozoic carbonate rocks (Capps and Moore, 1990) and Miocene sedimentary rocks (pl. 1). Capps and Moore (1990) divided the volcanic rocks in the Castle Mountains into the following four informally named units (from oldest to youngest): (1) Castle Mountains tuff unit, rhyolitic ash-flow tuff; (2) Jacks Well unit, latite, basalt, and ash-flow tuff; (3) Linder Peak unit, rhyolite flow-dome complex; and (4) Hart Peak unit, basalt and intermediate-composition flows and volcanoclastic rocks (these four units are not shown on plate 1). The Linder Peak (rhyolite flow-dome) unit, which has an age of about 15.5 Ma, hosts the gold deposits that formed just after dome emplacement (Capps and Moore, 1990). North of the known orebodies, these rhyolitic rocks are present in a north-trending zone on the west side of the Castle Mountains, and they are potential hosts for volcanic-hosted gold deposits, in addition to those orebodies already delineated.

Gold mineralization is present in structurally controlled, silicified fracture zones and more permeable lithologies that have been silicified (Ausburn, 1991). Argillic alteration and local zones of advanced argillic alteration are associated with the orebodies, and adularia and pyrite are present in close association with the gold. The ore minerals are native gold and electrum. The geochemical suite associated with the ore consists of As, Sb, and Hg (Capps and Moore, 1990). Quartz-adularia alteration is associated with the main stage of gold mineralization.

Eleven specific localities in the EMNSA are shown as being volcanic-hosted epithermal gold occurrences (table 14; see also pl. 2), all of which are in the Castle Mountains. Although mineralized occurrences in the area of Hackberry Mountain have been classified as polymetallic-fault-related deposits, these occurrences are volcanic hosted and are directly analogous with those in the Castle Mountains. However, the mineralization at Hackberry Mountain may be confined to generally northeast striking fault zones.

Tertiary volcanic rocks of similar age to those hosting gold deposits in the Hart Mining District are present in a large area in the south-central part of the EMNSA and are associated with the Woods Mountain volcanic center (McCurry, 1988). These volcanic rocks consist of regionally extensive ash-flow tuffs and rhyolitic domes and flows. The ash-flow tuffs include the 15.8-Ma Wild Horse Mesa Tuff of McCurry (1988) (unit Tw, pl. 1), a compositionally zoned, metaluminous to mildly peralkaline tuff, and the possibly younger Tortoise Shell Mountain Rhyolite of McCurry (1988) (Tts), which may be a lava flow. Large-amplitude, circular gravity (about -30 mGal) and magnetic (about -600 nT) anomalies are centered over the Woods Mountain volcanic center and reflect a caldera and associated, buried felsic stock about 9 km in diameter. McCurry (1985, 1988) suggested the presence of a trap-door style of collapse for a 10 km-diameter caldera, and the magnetic anomaly may reflect the outline of the caldera structure. However, the magnitude of the gravity anomaly and estimated depth to pre-Tertiary basement, about 7 km, indicate a symmetrical zone of subsidence that has a much larger component of collapse than previously postulated.

Similar-age volcanic rocks at Hackberry Mountain to the east of the Woods Mountain volcanic center consist of ash-flow tuffs, flows, and domes (pl. 1). These volcanic rocks are altered over a large area in the southern part of Hackberry Mountain. The alteration pattern is coincident with an east-west-trending magnetic-low anomaly, which probably reflects the oxidation or sulfidation of magnetic iron-oxide minerals during alteration. In the alteration zone, drilling indicated the presence of disseminated native gold, as much as 2.75 g Au/t, as well as stibnite and hematite in argillically altered and partly silicified ash-flow tuff that is cut by chalcedonic veinlets (Gottlieb and Friberg, 1984). Similar volcanic rocks are present around the north and west margins of the Woods Mountain volcanic center and have potential for volcanic-hosted gold deposits.

Volcanic-hosted gold deposits can be present in association with porphyry-type gold deposits (Rytuba and Cox, 1991). Most known porphyry-gold deposits are characterized by a stockwork of quartz and pyrite veins in subvolcanic intrusive rocks. These deposits form at greater depths and are lateral to volcanic-hosted gold deposits such as those in the Hart Mining District. The gold orebodies in porphyry-type gold deposits are generally low grade, 1.5 to 2.5 g Au/t, but are known to contain a very large tonnage of ore, as much as several hundred million tonnes. The subvolcanic intrusive rocks associated with the flow-dome complex in the Castle Mountains and the Woods Mountain volcanic center are permissive for porphyry-gold deposits, and those areas outlined below as being favorable for volcanic-hosted gold deposits also have potential for porphyry-gold deposits at depth.

### ***Permissive Terranes***

Three terranes in the EMNSA are delineated as permissive for Tertiary, volcanic-hosted epithermal-gold deposits of the quartz-alunite and (or) quartz-adularia variety (fig. 93). One is a north-northeast-trending terrane in the general area of the Castle Mountains. The northeast boundary of this terrane is based on the outermost limit of small numbers of rhyolite and (or) latite intrusions emplaced into Proterozoic basement rocks (pl. 1). The south boundary of the terrane is defined by our estimate of the southernmost extent of altered, demagnetized volcanic rocks under the overlying Quaternary gravels (fig. 93). The overall configuration of these apparently demagnetized rocks under the gravels is inferred from the available aeromagnetic data (pl. 5). The second of the two permissive terranes is a broadly ovoid one in the general area of Hackberry Mountain and the Woods Mountains, which includes the Miocene Hackberry Spring Volcanics of McCurry (1988) and Wild Horse Mesa Tuff of McCurry (1988) (units T<sub>hs</sub> and T<sub>w</sub>, respectively) in the area of Hackberry Mountain and the mostly Miocene Tortoise Shell Mountain Rhyolite of McCurry (1988) (T<sub>ts</sub>) in the area of Woods Mountains. Relation of these rocks to a caldera is described above. The third terrane permissive for Tertiary, volcanic-hosted epithermal gold deposits is marked by sequences of ash-flow tuffs near the south-central edge of the EMNSA in the area of Van Winkle Mountain (fig. 93).

### ***Favorable Tracts***

A favorable tract for Tertiary, volcanic-hosted epithermal-gold deposits of the quartz-adularia or quartz-alunite type is delineated within each of the first two above-outlined permissive terranes (fig. 93). These favorable tracts are outlined using the presence of magnetic lows, mineralized occurrences, and alteration anomalies detected by Landsat Thematic Mapper. Within these zones, deposits of B and Li, F, and U also may be present. Hodges and Ludington (1991) estimated that 0, 1, 2, 3, and 3 hot-spring-gold deposits, at 90, 50, 10, 5, and 1 percent probability levels, respectively, remain to be discovered in the EMNSA using the tonnage and grade distributions for these types of deposits derived by Berger and Singer (1992). The tonnage and grade distributions of the hot-spring-gold type of Berger and Singer (1992) did not discriminate between the quartz-adularia and quartz-alunite subtypes of these systems that have been distinguished petrogenetically.

## **Speculative Associations, by Richard M. Tosdal and Ted G. Theodore**

Some associations among known types of deposits in the EMNSA, as described above and as depicted schematically in figure 89, apparently have still not been utilized fully in the search for additional exploration targets. Recognition of linkages among some deposits, including gold skarn and the association of boron

and other lithophile elements with gold, might impact significantly exploration concepts in the Mesozoic and Tertiary magmatic-hydrothermal environments in the EMNSA. Application of an exploration concept based on linkages among deposit types is by no means a guarantee of an exploration success. Exploration failures far outnumber exploration successes. We recognize, furthermore, that no gold skarns, as defined by Theodore and others (1992b), are currently known in the EMNSA. As compiled, 39 gold skarns show median tonnages worldwide of 213,000 tonnes (t) of ore and median grades worldwide of 8.6 g Au/t; these include the 13.2-million-tonne McCoy and the 5.1-million-tonne Fortitude deposits in Nevada. Domestic primary-gold production in 1989 was approximately 240 tonnes of contained gold (U.S. Bureau of Mines, 1990b).

Lastly, we examine two recently recognized deposit-type linkages as examples of how discoveries elsewhere can impact future concepts of exploration, which might be applied to the EMNSA. First, we will examine the possible linkage between distal sediment-hosted gold deposits and their presumed proximal variants, including skarn of all types and porphyry-stockwork systems, and, second, we will examine the possible association between some possibly wrench-fault-related Tertiary gold mineralization in the EMNSA and hot-spring-gold deposits similar to the Mesquite deposit in southern California.

Local mineralized Mesozoic skarn environments in the EMNSA should be examined from the perspective of (1) a location proximal to magma-equilibrated fluids exsolving from a progenitor intrusive complex and (2) a position interior to sediment-hosted gold systems in the surrounding sedimentary sequences. Sillitoe and Bonham (1990) proposed that most gold in many sediment-hosted gold deposits, in particular the distal-disseminated silver-gold type of deposit, originates in magma-derived fluids and may be deposited on the peripheries of base- and precious-metals mining districts as much as several kilometers from the mineralizing plutons. Gold-bearing skarns, of which several are known in the EMNSA, may be “indicator” occurrences for sediment-hosted gold deposits (Tingley and Bonham, 1986). The schematic model proposed by Sillitoe and Bonham (1990) that shows such linkages is applicable to some of the more shallow-seated magmatic-hydrothermal pulses associated with emplacement of the Teutonia batholith (fig. 101). As noted by Sillitoe and Bonham (1990), the fringes in most carbonate-rock sequences beyond many intrusion-centered base- and precious-metal districts have been minimally explored for gold. Such conclusions are probably applicable also to the EMNSA. The Navachab, Namibia, gold deposit may be an example of a type of mineralized system that might be present in the EMNSA. At Navachab, 9.5 million tonnes of gold ore with an average grade of 2.6 g Au/t is hosted by steeply dipping marbles that include mottled dolomitic marble, biotite hornfels, and calc-silicate marble (Wyllie, 1991). However, all of the above conclusions with regards to linkage between a porphyry-magmatic environment and the sediment-hosted gold environment are proposed on the basis of magmatic-hydrothermal fluids forming a significant component of the fluid regime in each environment during mineralization. This relation may not be true. Hofstra and others (1988, 1989) showed that nonmagmatic fluids, which are instead apparently equilibrated isotopically with deep-seated rocks, were heavily involved in generation of some of the largest sediment-hosted gold deposits in Nevada.

Gold-quartz veins at the Telegraph Mine in the north-central part of the EMNSA (pl. 2; Lange, 1988; U.S. Bureau of Mines, 1990a, map no. 121, pl. 1) apparently are related to wrench or strike-slip faults, suggesting that additional deposits of this type may be present elsewhere in the EMNSA. Mineralization at the Telegraph Mine is associated spatially with structures interpreted by Lange (1988) as Riedel shears (see Riedel, 1929; Tchalenko, 1970; Ramsay and Huber, 1987). These types of secondary shears are oriented generally at low angles to the general trace of a broad zone of shear. Prominent geomorphic and structural features trending N. 20° to 40° E. in the general area of the Telegraph Mine acted as open conduits or as breccia-filled high-permeability zones during mineralization, which has been dated by the K–Ar method at  $10.3 \pm 0.4$  Ma (Lange, 1988). This type of mineralization is particularly significant in terms of resource evaluation because of its geologic similarity to the world-class gold deposit at the Mesquite Mining District, Calif. No volcanism has been documented close to 10.3 Ma in the area of the Telegraph Mine; some andesite in the vicinity has been dated at 12.8 Ma, and the oldest alkaline basalts in the area are 7.5 Ma (H.G. Wilshire, written commun., 1991). Nonetheless, as Lange (1988) concluded, mineralization at the Telegraph Mine may be related to regional right-lateral, north-south-directed shortening strains that, in turn, resulted in the opening of low-angle, en echelon tension gashes oriented approximately northeasterly. These mineralized tension gashes at the Telegraph Mine

probably are related to post-20–Ma combined wrenching across the San Andreas, Death Valley, and Soda-Avawatz fault zones. Recent studies in the general area of the Telegraph Mine suggest that a regional wrench fault that strikes approximately N. 70° E. may pass through the general area of the mine (D.M. Miller, oral commun., 1995). Although we assigned mineralization at the Telegraph Mine to a gold-silver quartz-pyrite type of occurrence, the mineralization there seems to be of an epithermal variety, showing relatively high Au/Ag ratios for the ores (Lange, 1988). Total production from the Telegraph Mine has been 1,976 tonnes of ore that included 68 kg Au, 169 kg Ag, and 227 kg Cu; 1948 was the last recorded year of production (U.S. Bureau of Mines, 1990a). Hewett (1956) showed production from the Telegraph Mine to include a total of 79 kg Au. Drilling in 1968, which was sponsored by the Office of Mineral Exploration of the U.S. Geological Survey, resulted in the blocking out of 66,016 tonnes at a grade of 15.6 g Au/t and 36.3 g Ag/t at the Telegraph Mine (U.S. Bureau of Mines, 1990a).

The Mesquite Mining District is located in southeastern California about 150 km south-southeast of the south border of the EMNSA and 60 km east of the Salton Sea. Large-scale gold production from the mining district began in 1985; announced reserves were 40.5 million tonnes at an average grade of 1.75 g Au/t (Lindquist, 1987). By 1988, the mining district had become one of the largest producers of gold in California (Burnett, 1990), and continued exploration through 1989 increased the known reserves to 52.3 million tonnes at an average grade of 1.34 g Au/t (Higgins, 1990).

Gold-bearing veins in the Mesquite Mining District formed in an epithermal setting within a few hundred meters of the surface (Willis and Holm, 1987; Manske and others, 1987; Willis, 1988; Manske and Einaudi, 1989; Manske, 1990; Willis and Tosdal, 1992). Gold-bearing quartz-adularia-sericite and ferroan-carbonate veins are the mineralized structures within the district (Willis, 1988; Manske, 1990). Quartz-cemented breccias are contemporaneous with the simple veins and are common in the parts of the deposit that have the highest economic grades. Younger, barren calcite veins and chalcedonic-quartz veins are present locally. Vein deposition occurred by episodic open-space filling, as indicated by vuggy and comb quartz and carbonate minerals, multiple banding of chalcedonic quartz, and clasts of silica-matrix breccia within other breccias. Veins vary from thin microcracks to breccias a meter or so thick. Little hydrothermal alteration of host lithologies accompanied mineralization (Manske and others, 1987; Willis, 1988). Weakly anomalous, sporadic concentrations of Au, Ag, As, Sb, Hg, W, Zn, and Te were found in surface-rock exposures before mining (Tosdal and Smith, 1987).

The veins are steeply dipping and are strongly controlled by right-lateral strike-slip faulting (Willis, 1988), as indicated by the vein geometry in complex dilational jogs (Sibson, 1990), by negative and positive flower structures (Harding, 1985), and by kinematic evidence for strike-slip faulting along the major mineralized faults (Willis and others, 1989; Willis and Tosdal, 1992). Mineralization in the mining district is hosted mostly by gneissic rocks that were metamorphosed at amphibolite grade and, to a lesser extent, by granite, pegmatite, and aplite that intrude the gneissic rocks (Willis, 1988). The ages of these rocks and their subsequent metamorphism have been established as Jurassic and Cretaceous, respectively (R.M. Tosdal, unpub. data, 1987–90). K–Ar and  $^{40}\text{Ar}/^{39}\text{Ar}$  geochronologic studies indicate an Oligocene age of mineralization sometime between 37 and 27 Ma (Willis, 1988; see also D.L. Martin, *as quoted in* Shafiqullah and others, 1990), or a minimum of 60 m.y. after the host rocks were formed. The apparent age of the orebodies is, however, somewhat similar to the age of nearby volcanic and plutonic rocks in the Chocolate Mountains (Miller and Morton, 1977; Crowe and others, 1979). No Tertiary volcanic or plutonic rocks are known within the Mesquite Mining District, although they may have provided a heat source to drive the hydrothermal system (Manske, 1990).

The large gold deposit in the Mesquite Mining District is a typical epithermal precious-metal deposit similar to many of those hosted by volcanic rocks or by other rocks that are intruded by hypabyssal stocks elsewhere. Major distinctions between orebodies in the Mesquite Mining District and typical epithermal deposits include the gneissic host rocks, the large difference in age between the host rocks and the orebodies, and the lack of volcanic or plutonic rocks of the appropriate age within the district. The strike-slip environment is not unique, although it does provide a structural setting into which hydrothermal fluids could flow away from any associated heat source (Sibson, 1987).

Within the EMNSA, the Telegraph Mine appears to have an analogous setting to Mesquite. At this locality, gold-bearing epithermal veins and breccias, which consist of quartz-sericite-adularia-pyrite and quartz-carbonate, cut the informally named, Cretaceous Teutonia adamellite of Beckerman and others (1982) (unit Kt, pl. 1) (Lange, 1988). Veins in this mine are interpreted to have formed within a dextral strike-slip environment, the strike of which is now to the north-northeast, at a high angle to trends of regionally extensive strike-slip faults. A single K–Ar age on adularia implies that the main stage of mineralization occurred in the late Miocene, at about  $10.3 \pm 0.4$  Ma (Lange, 1988). No late Miocene volcanic rocks of this age are known in the immediate area of the Telegraph Mine (pl. 1), although Miocene felsic volcanism of similar age is present within the region, some 40 km to the east-southeast, and late Miocene to Pleistocene basaltic volcanism is present also in the Cima volcanic field to the immediate south (pl. 1). Some basaltic rocks elsewhere are known to host significant concentrations of gold. The Buckhorn deposit, the Mule Canyon deposit, and the Fire Creek occurrence, all in Nevada, apparently are hot-spring gold deposits in basaltic andesite above complexes of basaltic dikes associated with the middle Miocene northern Nevada rift. The Mule Canyon deposit initially was described as including a geologic resource of approximately 26.5 tonnes Au at an average grade of 3.75 g Au/t (Consolidated Gold Fields Defense Document Against Minorco, Sept. 1989); this was revised subsequently to 32.8 tonnes Au at a grade of 4.25 g Au/t (Bonham and Hess, 1993).

The question of mineral-resource potential for these types of gold-bearing epithermal deposits of Tertiary age within the EMNSA is difficult to address at this time. Information is inadequate for us to outline reasonably constrained permissive terranes, or favorable tracts, on the large pediments in the EMNSA. Select mineralized samples from gold-silver quartz-pyrite veins that show relatively high Au/Ag ratios might be one method that could be used to discriminate middle Miocene veins from older ones. Surface expressions of the orebodies at Mesquite on the pediment before exploration were small and consisted of local high-grade gold-quartz veins that had small amounts of reported production, as well as various small placer mines (Morton, 1977). In addition, weak and very limited geochemical expression, and no known geophysical expression, is associated with the orebodies. Only thorough exploration around these small occurrences in the Mesquite Mining District could define the large orebodies now identified there.

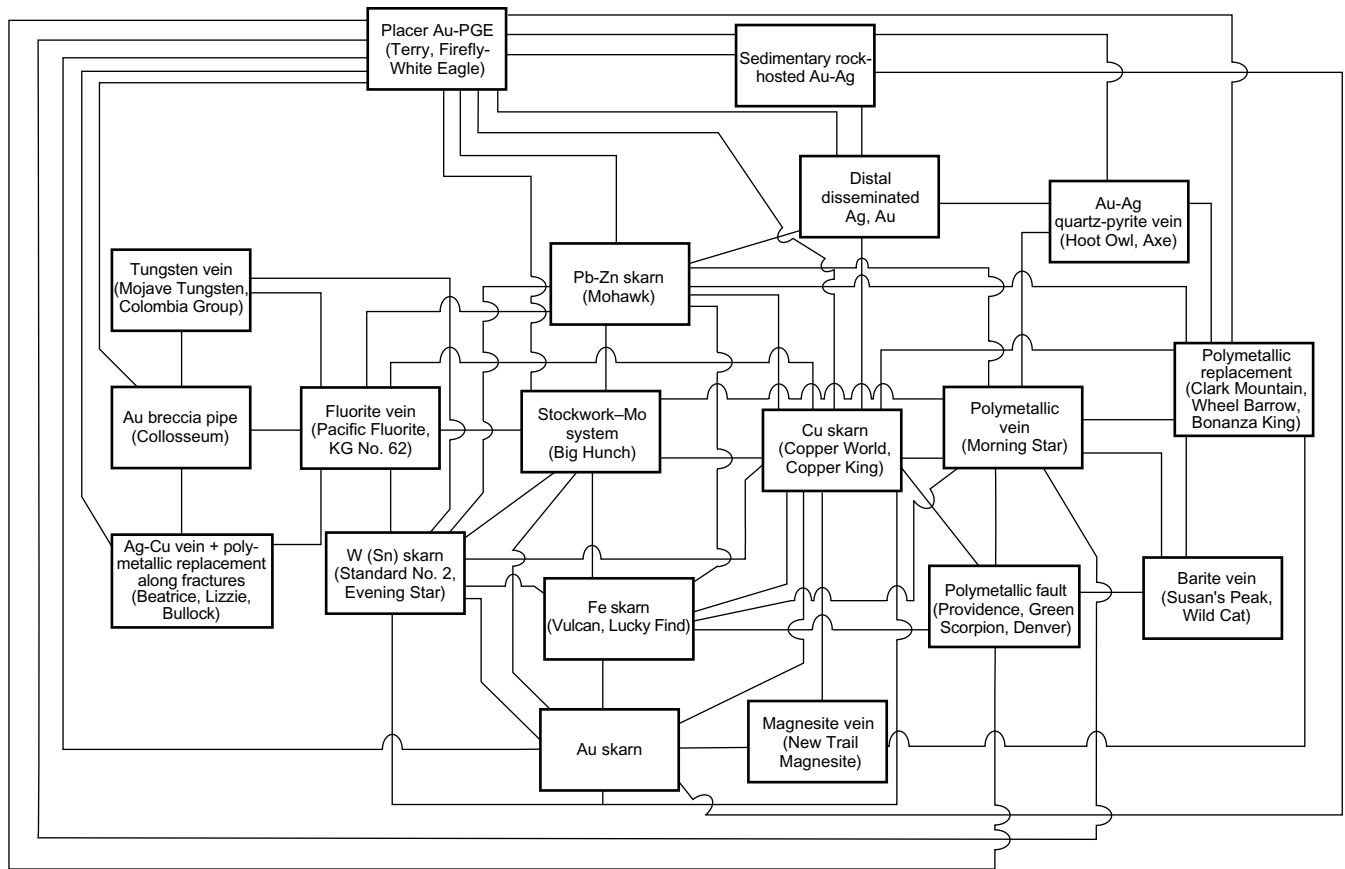


**Figure 89.** Possible linkages among some types of mineral occurrences that are associated with felsic intrusive rocks in the East Mojave National Scenic Area, Calif. Most linkages are inferred from mineral zonation established in mining districts elsewhere. Examples of mineral occurrences in East Mojave National Scenic Area are shown in parentheses.

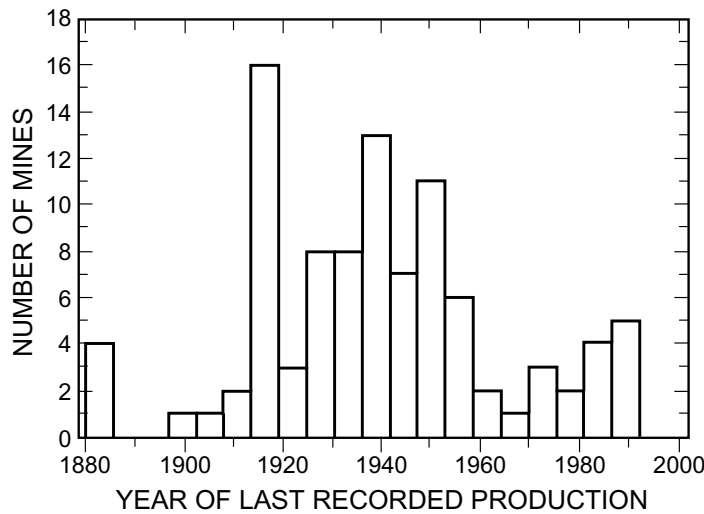


**Figure 90.** Plot showing number of formerly active mines in the East Mojave National Scenic Area, Calif., versus year of their last recorded production activity. Data for 97 mines from U.S. Bureau of Mines (1990a).

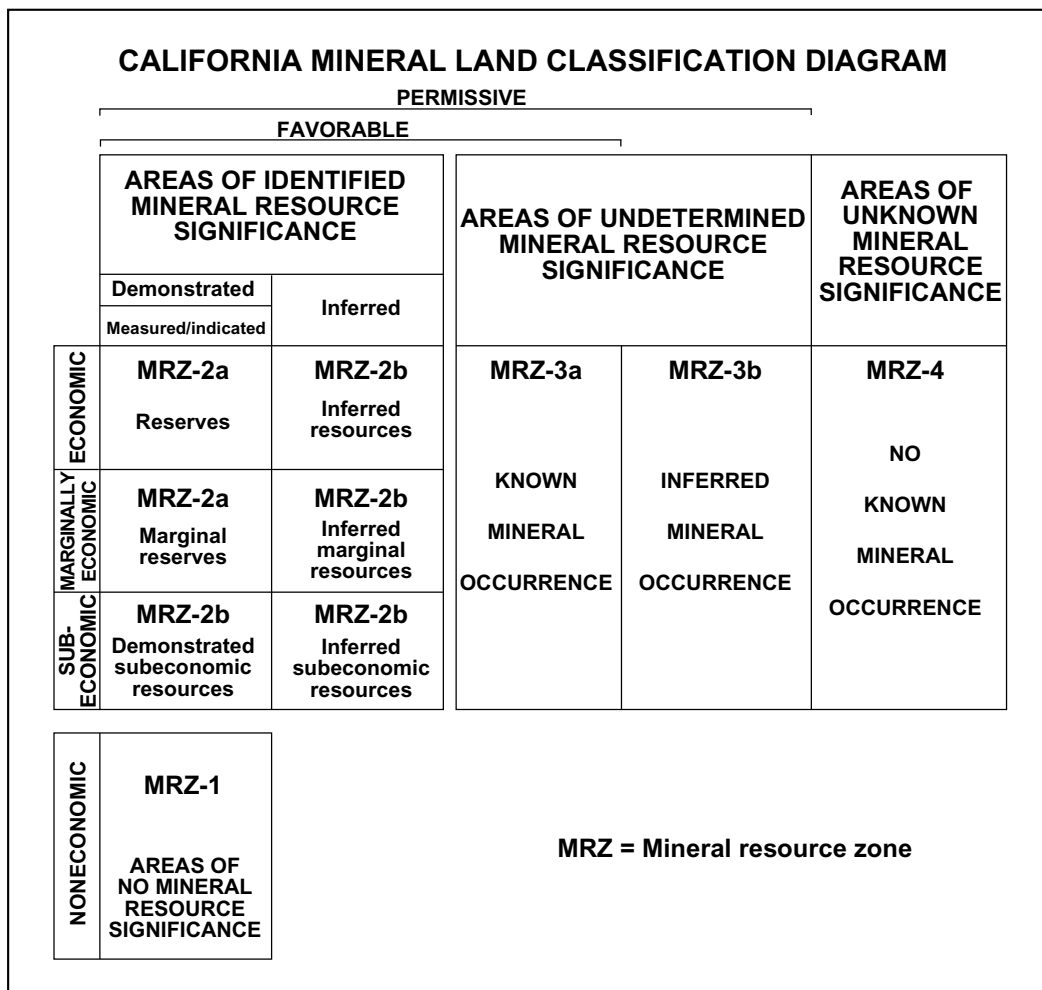
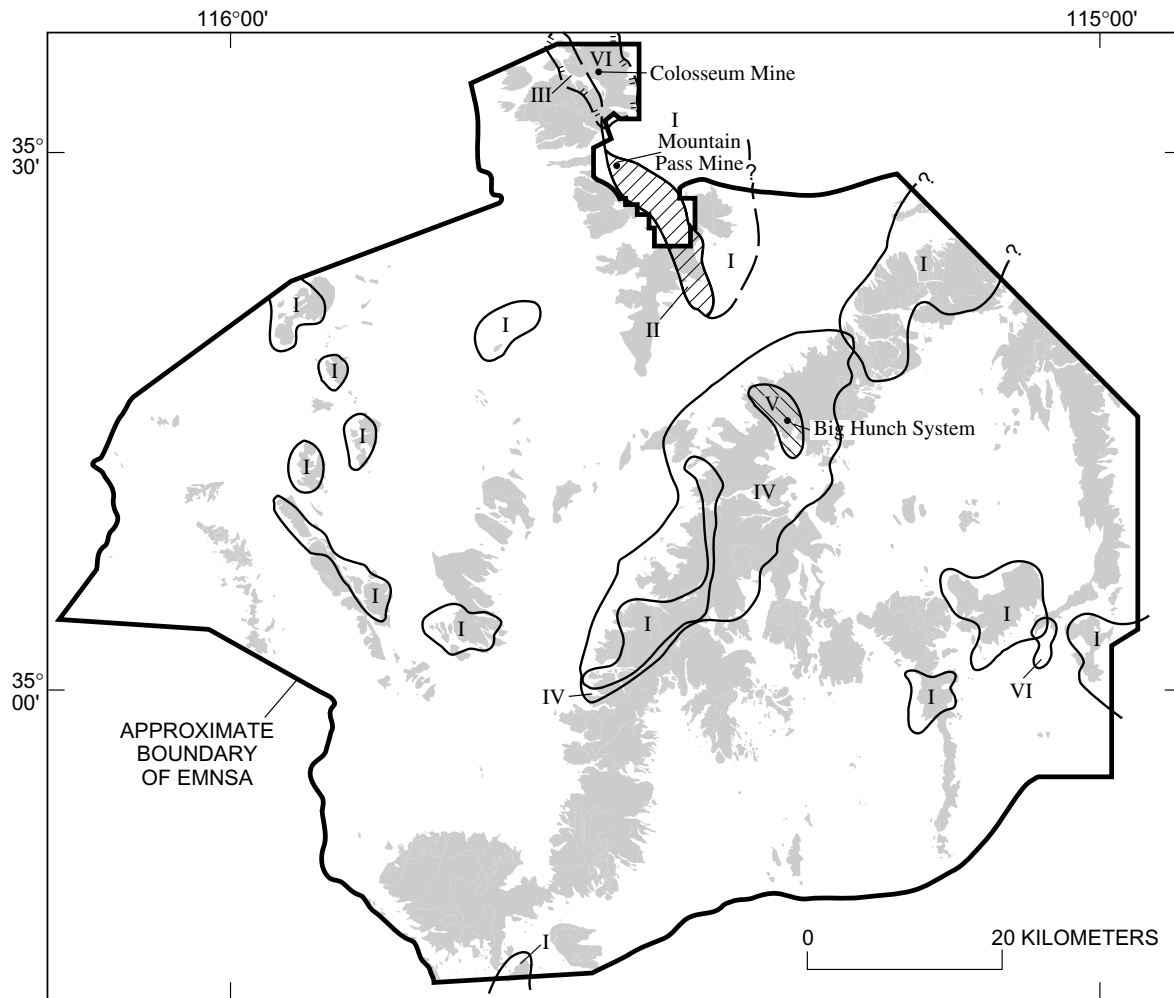


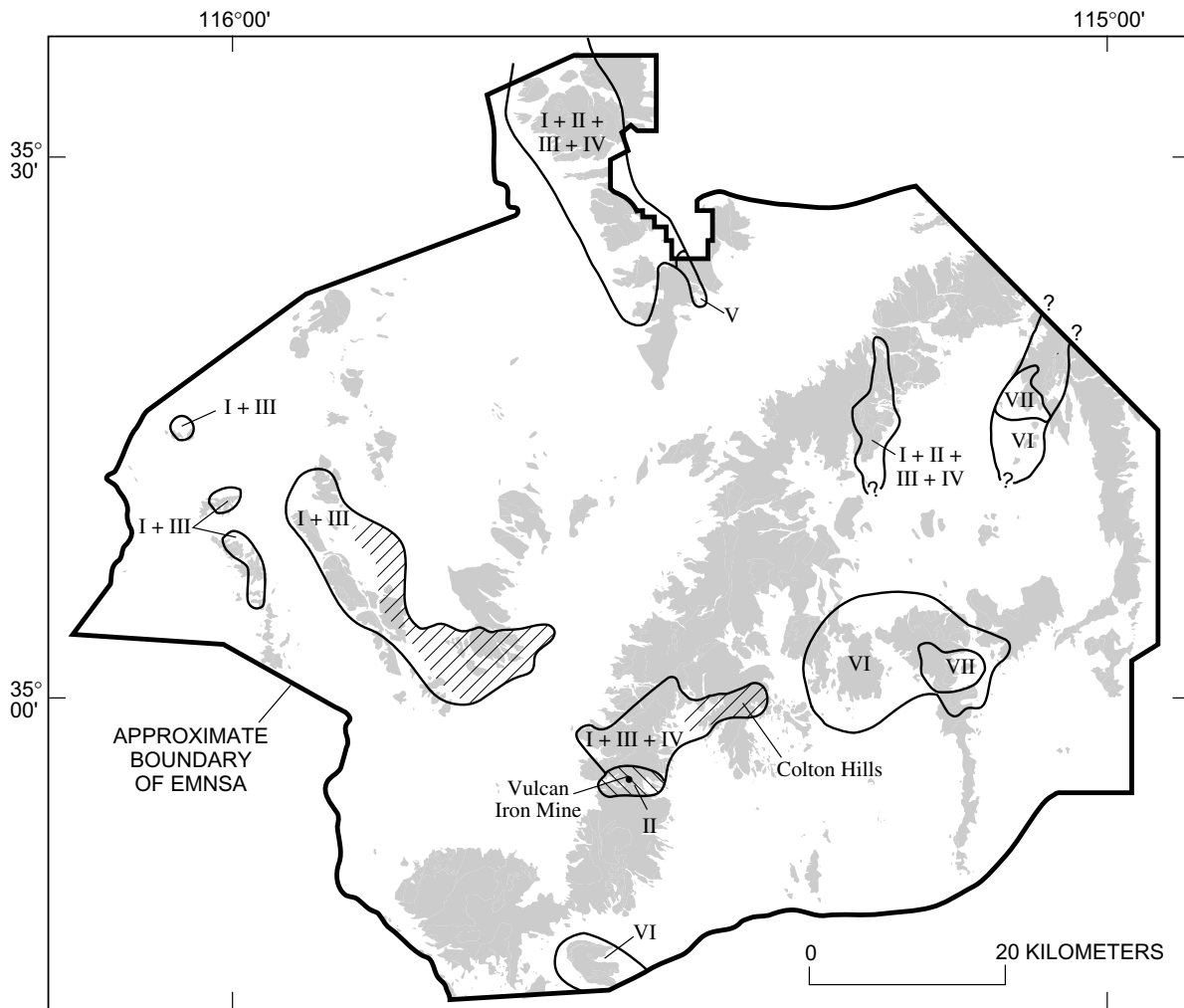
**Figure 91.** Mineral land-classification diagram adopted by State of California, showing diagrammatic relations of mineral-resource-zone categories to resource-reserve classification system. From D.O. Shumway (written commun., 1991). Major elements of mineral-resource classification modified from McKelvey (1972) and U.S. Bureau of Mines and U.S. Geological Survey (1980).



EXPLANATION

- — — — ? Outline of permissive terranes and favorable tracts—Dashed where approximately located; queried where uncertain
- — — — — Outline of permissive terranes and favorable tracts for Mesozoic gold breccia pipe plus related occurrences, including Mesozoic tungsten vein occurrences—Hachures point toward interior of terranes and tracts
- Permissive terranes and favorable tracts
- Proterozoic carbonatite-related REE occurrences
- I Permissive
- II Favorable
- Mesozoic gold breccia pipe plus related occurrences
- III Permissive and favorable
- Mesozoic stockwork-molybdenum occurrences
- IV Permissive
- V Favorable
- Mesozoic tungsten-vein occurrences
- VI Permissive and favorable

**Figure 92.** Map of East Mojave National Scenic Area (EMNSA), Calif., showing permissive terranes and favorable tracts for Proterozoic carbonatite-related rare earth element (REE) occurrences, Mesozoic gold-bearing breccia pipes, Mesozoic stockwork-molybdenum systems, and Mesozoic tungsten veins. Outlines of permissive terranes and favorable tracts established independently for specific mineral-occurrence models, and some terranes and (or) tracts may overlap or be nested within one another, because of the mineral-occurrence implications of the geology of the terranes and (or) tracts on that particular model. See figure 91 for explanation of terminology. Mountain areas shaded.



EXPLANATION

- ? Outline of permissive terranes and favorable tracts—Queried where location uncertain
- Permissive terranes and favorable tracts
- Mesozoic skarn occurrences—Pattern indicates area particularly favorable or permissive for iron skarn
  -  I Permissive
  -  II Favorable
- Mesozoic polymetallic-replacement occurrences
  - III Permissive
  - IV Favorable
- Mesozoic porphyry-copper and skarn-related porphyry-copper occurrences
  - V Favorable
- Tertiary volcanic-hosted gold occurrences
  - VI Permissive
  - VII Favorable

**Figure 93.** Map of East Mojave National Scenic Area (EMNSA), Calif., showing major permissive terranes and favorable tracts for Mesozoic mineralized skarns of all types and iron skarns in particular, Mesozoic skarn-related porphyry copper and porphyry copper systems, Mesozoic polymetallic-replacement occurrences, and Tertiary volcanic-hosted, gold-silver occurrences. See figure 91 for explanation of terminology.

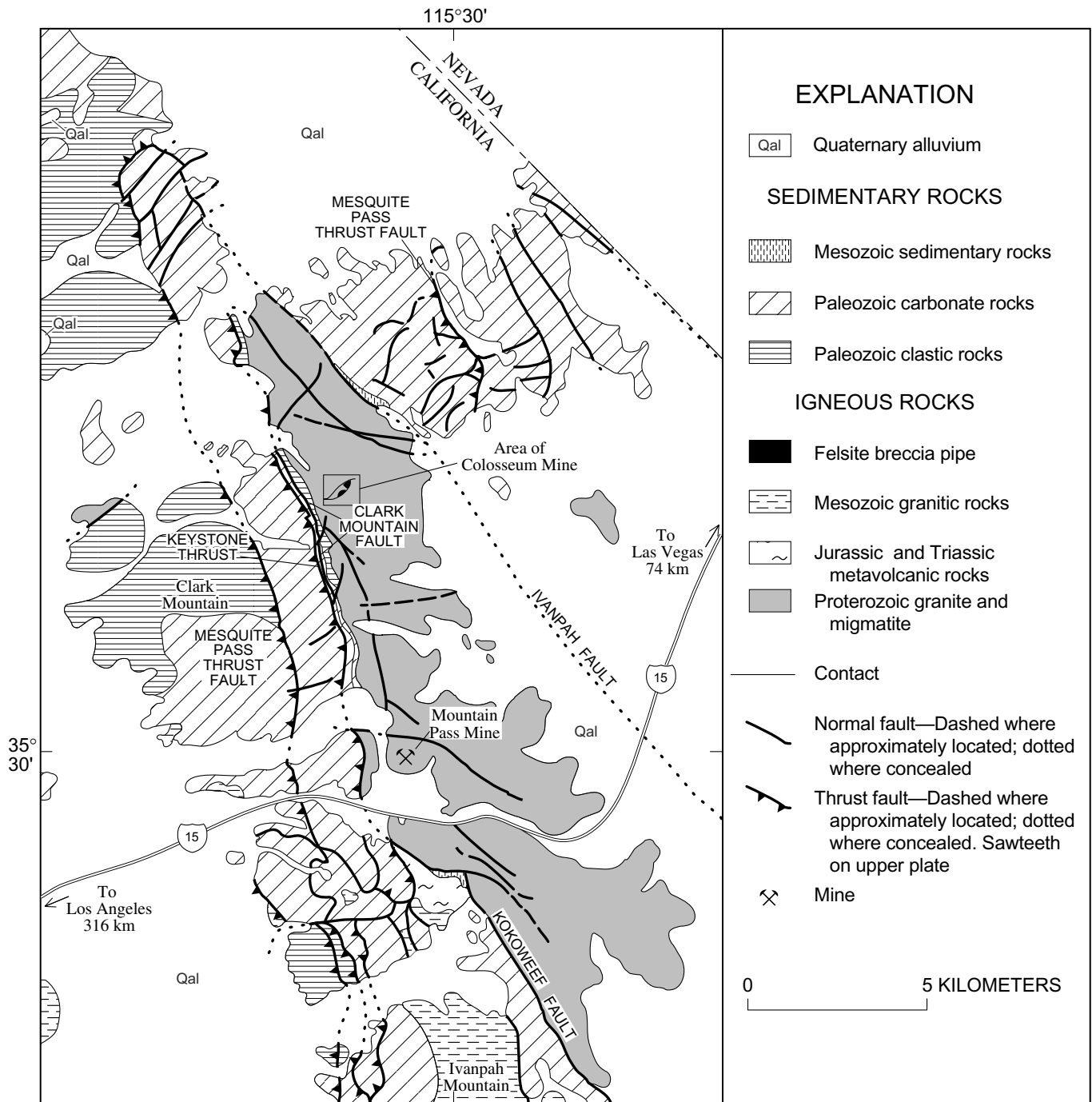


**Figure 94.** Geologic map of area surrounding Cretaceous gold-bearing breccia pipes at Colosseum Mine, in north-central part of East Mojave National Scenic Area, Calif. Modified from Sharp (1984).

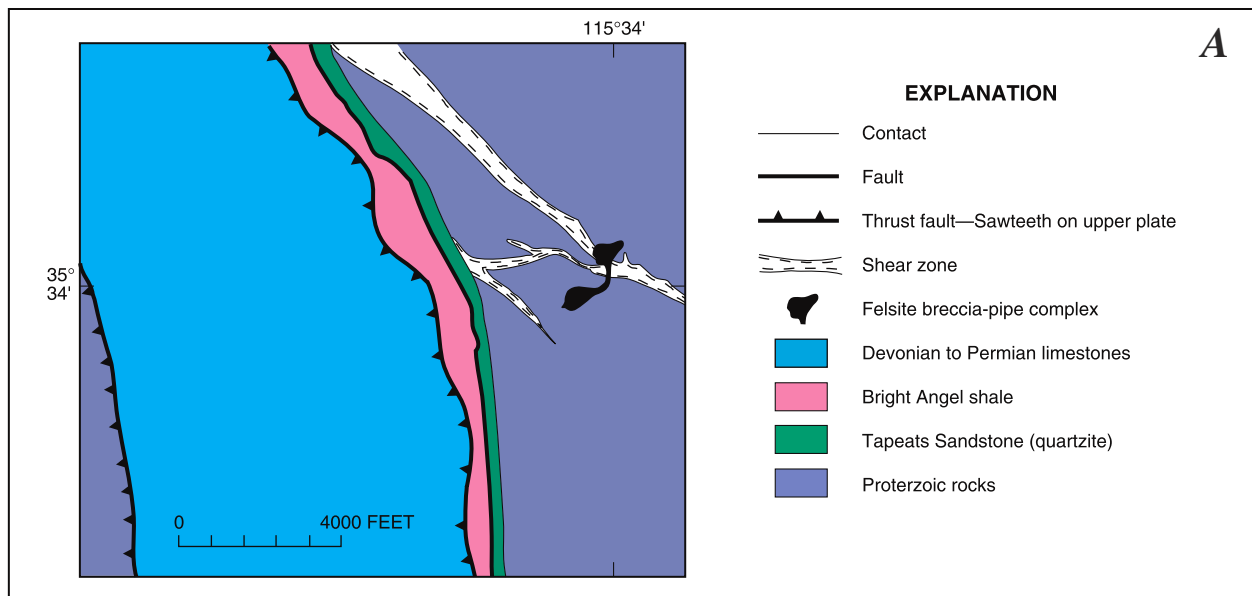
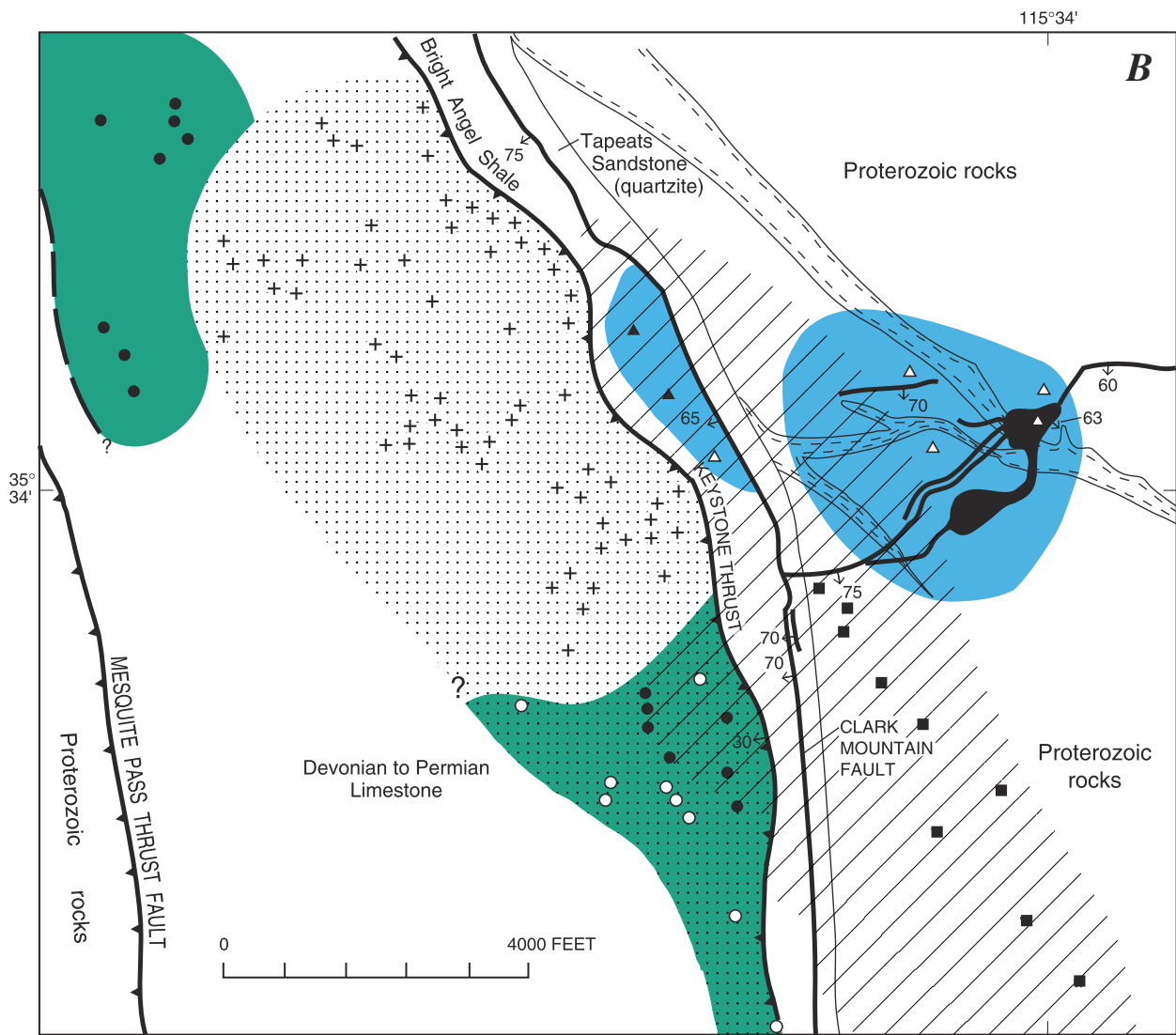


**Figure 95.** Northeastern part of Clark Mountain Mining District, north-central East Mojave National Scenic Area, Calif (see fig. 94 for location). *A*, Generalized geologic map of Clark Mountain Mining District. Some faults omitted for simplicity. Cambrian Bright Angel Shale, Cambrian Tapeats Sandstone, and Proterozoic rocks are included in unit CZs (pl. 1); Devonian to Permian limestones are in unit PDI (pl.1). *B*, Map showing metal zoning in Clark Mountain Mining District (modified from Sharp, 1984).



**EXPLANATION**

- |  |  |  |          |
|--|--|--|----------|
|  | Contact  |  | Fluorite |
|  | Fault—Dashed where approximately located; queried where uncertain. Showing dip where known |  | Silver   |
|  | Thrust fault—Showing dip where known; sawteeth on upper plate                              |  | Gold     |
|  | Shear zone   |  | Tungsten |
|  | Felsite breccia-pipe complex—Showing dip where known                                       |  | Ag       |
|  | Metal zones  |  | Au       |
|  |  |  | W        |
|  |  |  | AuW      |
|  |  |  | FCuAg    |
|  |  |  | FCuAgW   |
- Metal occurrences at prospects or small mines—When more than one metal is shown, metals are listed in decreasing order of abundance

**Figure 95.** Northeastern part of Clark Mountain Mining District, north-central East Mojave National Scenic Area, Calif (see fig. 94 for location). A, Generalized geologic map of Clark Mountain Mining District. Some faults omitted for simplicity. Cambrian Bright Angel Shale, Cambrian Tapeats Sandstone, and Proterozoic rocks are included in unit €Zs (pl. 1). B, Map showing metal zoning in Clark Mountain Mining District (modified from Sharp, 1984)—Continued.

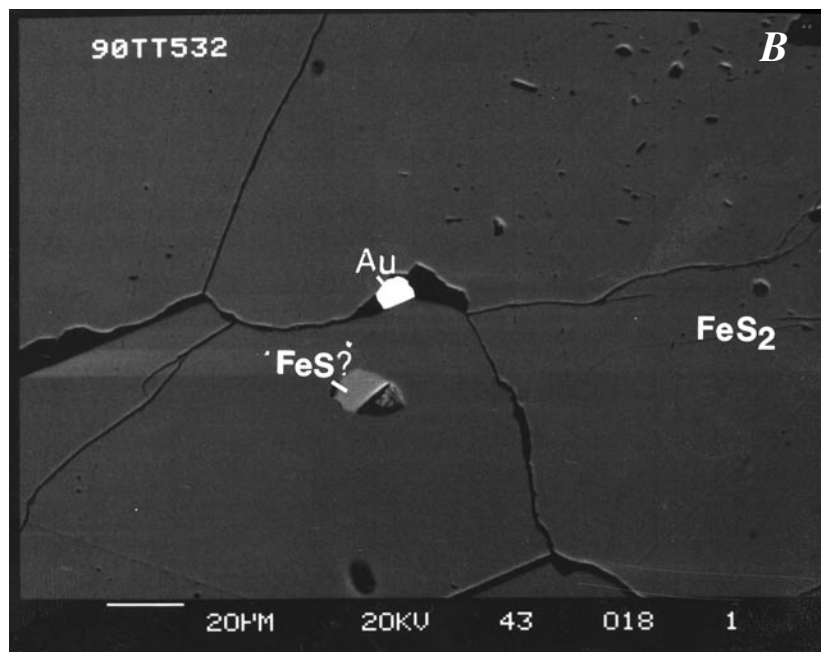
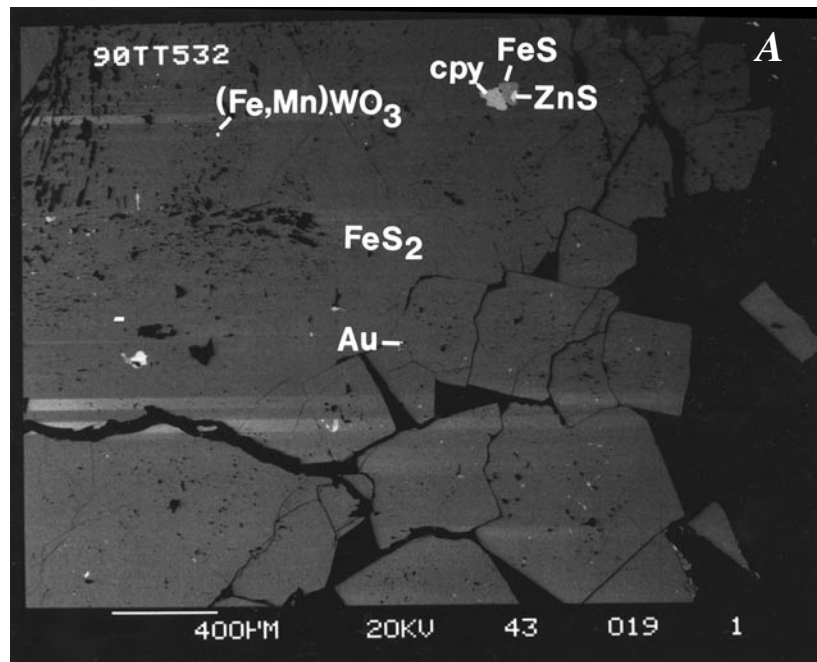


**Figure 96.** Scanning electron micrographs of gold-bearing breccia pipe at the Colosseum Mine, East Mojave National Scenic Area, Calif (fig. 94). Abbreviations: Ag, silver; AgTe, silver telluride; Au, gold; BiTe, bismuth tellurides; (Ce,La,Nd)PO<sub>4</sub>, monazite; cpy, chalcopyrite; CuS, covellite; (Fe,Mn)WO<sub>3</sub>, wolframite; FeS, pyrrhotite (queried where uncertain); FeS<sub>2</sub>, pyrite; Kf, K-feldspar; Py, pyrite; SiO<sub>2</sub>, quartz; ZnS, sphalerite. *A*, General morphology of pyrite hosting various minerals, including gold. *B*, Enlargement of part of 96A, showing argenteriferous gold along microcrack in pyrite; some possible pyrrhotite also in the field of view. *C*, Energy-dispersive X-ray spectra of argenteriferous gold grain in 96B. *D*, Gold associated with pyrrhotite in pyrite. *E*, Euhedral outlines of pyrite (py) crystals, common throughout sample. *F*, Enlargement of part of 96E, showing monazite crystals along margins between pyrite crystals. *G*, Silver tellurides and bismuth tellurides in pyrite. *H*, Enlargement of part of 96A, showing clot of chalcopyrite, pyrrhotite, and sphalerite in pyrite. *I*, Sphalerite surrounded by covellite in K-feldspar.

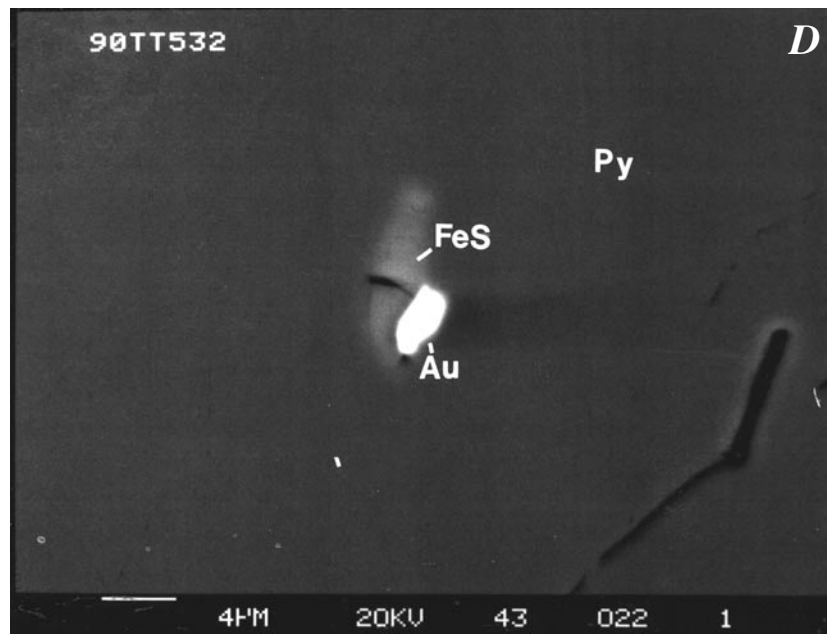
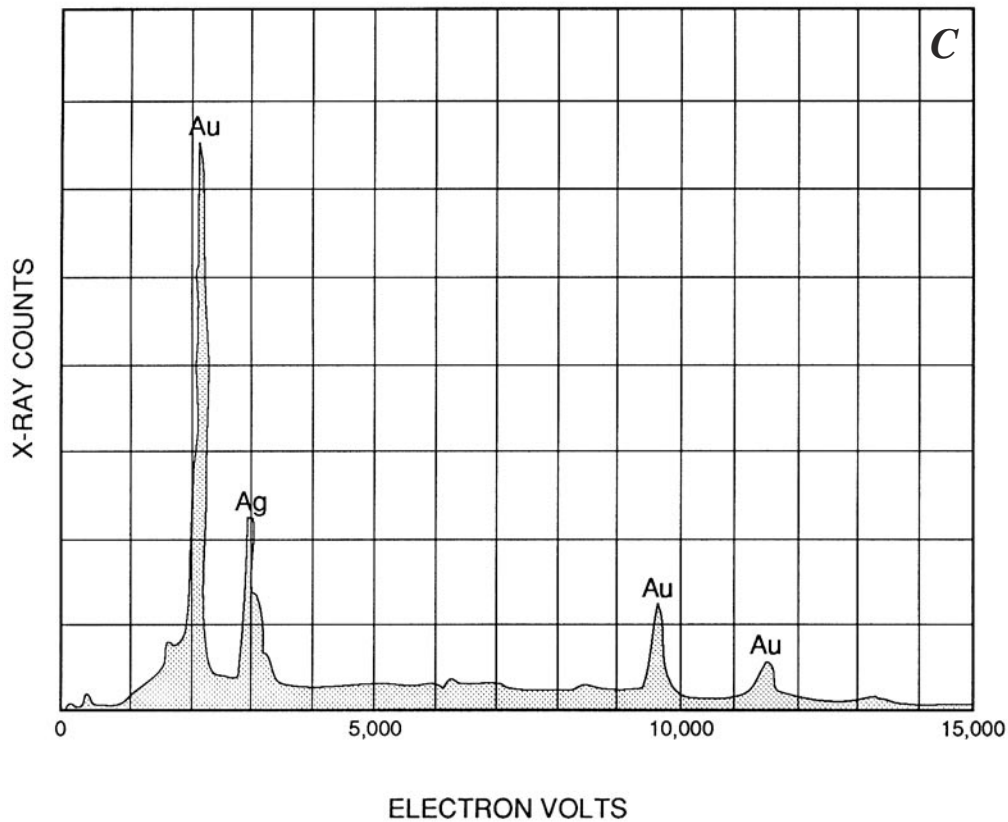


**Figure 96.** Scanning electron micrographs of gold-bearing breccia pipe at the Colosseum Mine, East Mojave National Scenic Area, Calif (fig. 94). Abbreviations: Ag, silver; AgTe, silver telluride; Au, gold; BiTe, bismuth tellurides; (Ce,La,Nd)PO<sub>4</sub>, monazite; cpy, chalcopyrite; CuS, covellite; (Fe,Mn)WO<sub>3</sub>, wolframite; FeS, pyrrhotite (queried where uncertain); FeS<sub>2</sub>, pyrite; Kf, K-feldspar; Py, pyrite; SiO<sub>2</sub>, quartz; ZnS, sphalerite. *A*, General morphology of pyrite hosting various minerals, including gold. *B*, Enlargement of part of 96A, showing argentiferous gold along microcrack in pyrite; some possible pyrrhotite also in the field of view. *C*, Energy-dispersive X-ray spectra of argentiferous gold grain in 96B. *D*, Gold associated with pyrrhotite in pyrite. *E*, Euhedral outlines of pyrite (py) crystals, common throughout sample. *F*, Enlargement of part of 96E, showing monazite crystals along margins between pyrite crystals. *G*, Silver tellurides and bismuth tellurides in pyrite. *H*, Enlargement of part of 96A, showing clot of chalcopyrite, pyrrhotite, and sphalerite in pyrite. *I*, Sphalerite surrounded by covellite in K-feldspar—Continued.

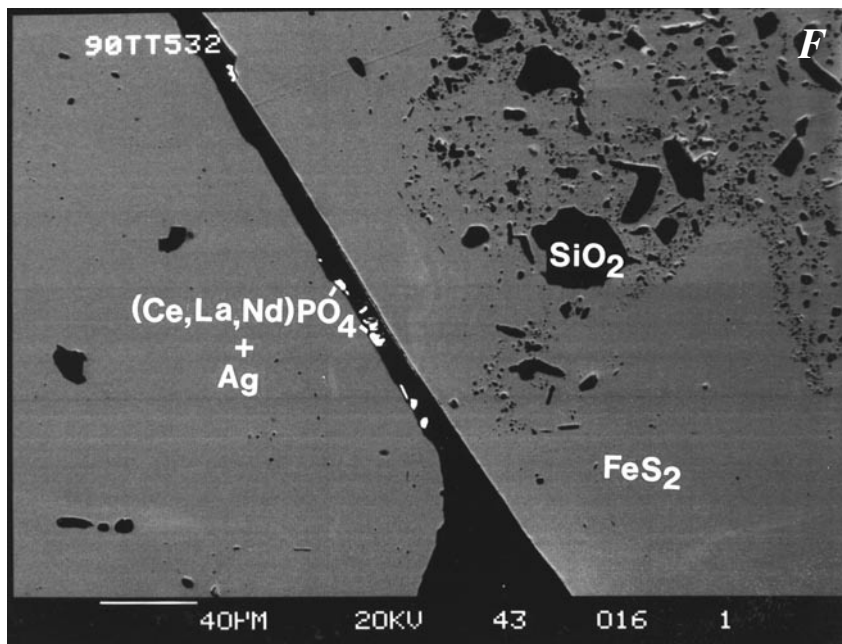
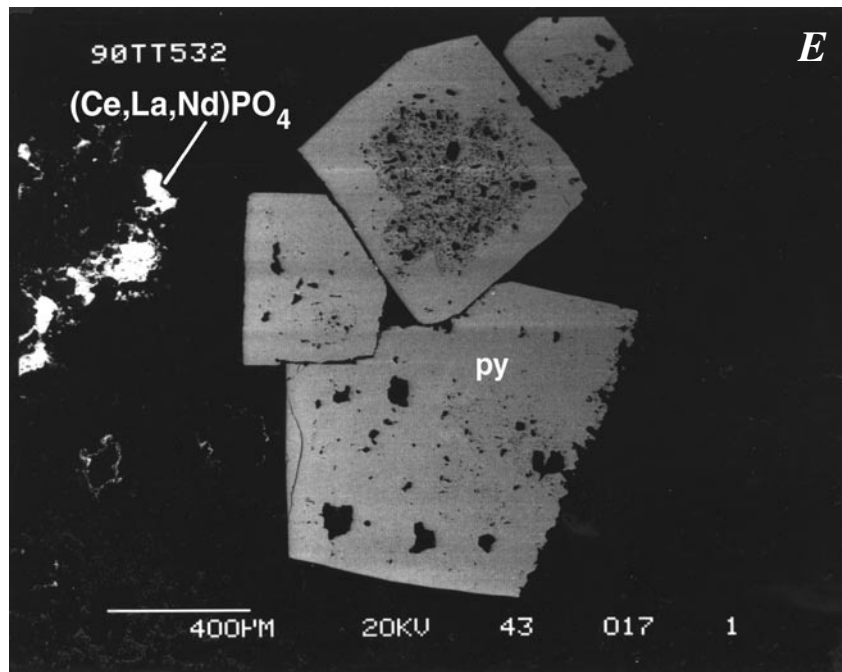


**Figure 96.** Scanning electron micrographs of gold-bearing breccia pipe at the Colosseum Mine, East Mojave National Scenic Area, Calif (fig. 94). Abbreviations: Ag, silver; AgTe, silver telluride; Au, gold; BiTe, bismuth tellurides; (Ce,La,Nd)PO<sub>4</sub>, monazite; cpy, chalcopyrite; CuS, covellite; (Fe,Mn)WO<sub>3</sub>, wolframite; FeS, pyrrhotite (queried where uncertain); FeS<sub>2</sub>, pyrite; Kf, K-feldspar; Py, pyrite; SiO<sub>2</sub>, quartz; ZnS, sphalerite. *A*, General morphology of pyrite hosting various minerals, including gold. *B*, Enlargement of part of 96A, showing argentiferous gold along microcrack in pyrite; some possible pyrrhotite also in the field of view. *C*, Energy-dispersive X-ray spectra of argentiferous gold grain in 96B. *D*, Gold associated with pyrrhotite in pyrite. *E*, Euhedral outlines of pyrite (py) crystals, common throughout sample. *F*, Enlargement of part of 96E, showing monazite crystals along margins between pyrite crystals. *G*, Silver tellurides and bismuth tellurides in pyrite. *H*, Enlargement of part of 96A, showing clot of chalcopyrite, pyrrhotite, and sphalerite in pyrite. *I*, Sphalerite surrounded by covellite in K-feldspar—Continued.

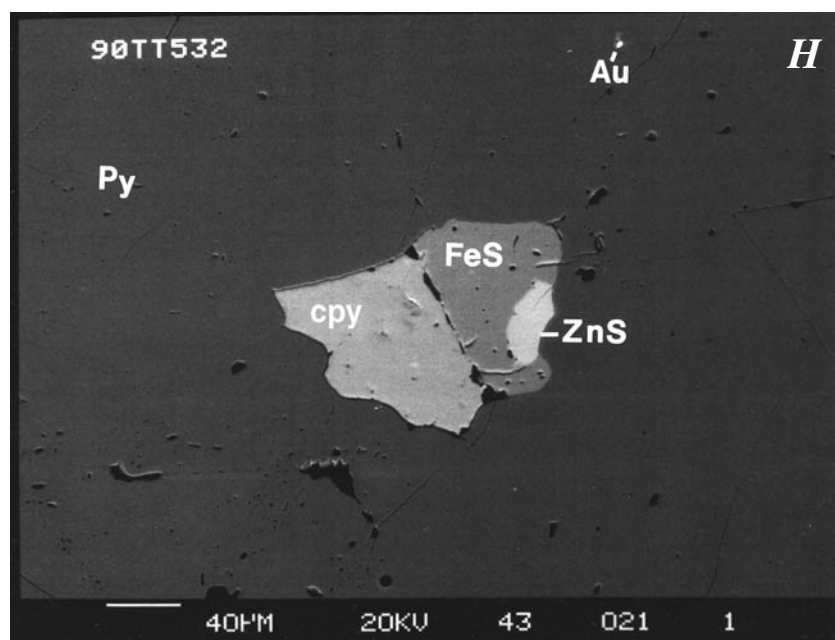
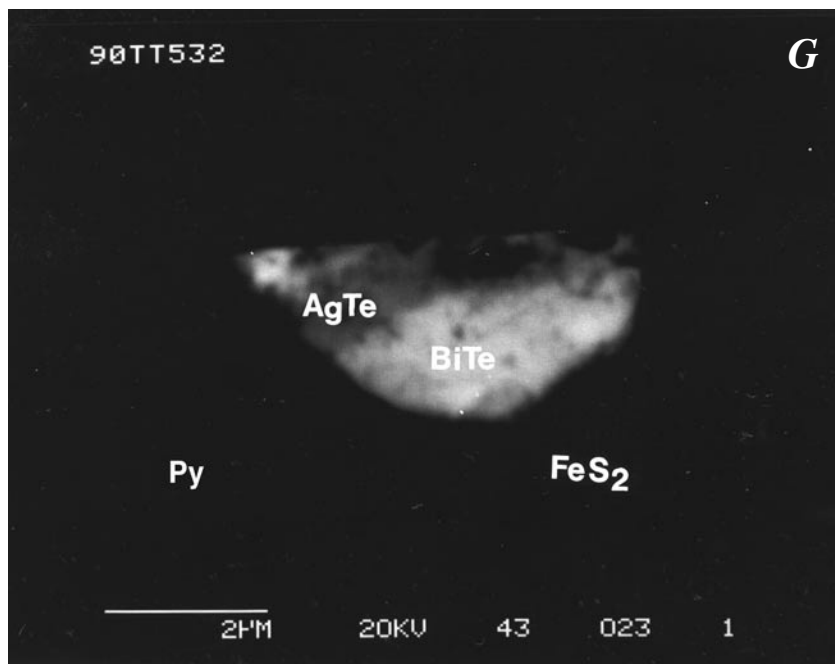


**Figure 96.** Scanning electron micrographs of gold-bearing breccia pipe at the Colosseum Mine, East Mojave National Scenic Area, Calif (fig. 94). Abbreviations: Ag, silver; AgTe, silver telluride; Au, gold; BiTe, bismuth tellurides; (Ce,La,Nd)PO<sub>4</sub>, monazite; cpy, chalcopyrite; CuS, covellite; (Fe,Mn)WO<sub>3</sub>, wolframite; FeS, pyrrhotite (queried where uncertain); FeS<sub>2</sub>, pyrite; Kf, K-feldspar; Py, pyrite; SiO<sub>2</sub>, quartz; ZnS, sphalerite. *A*, General morphology of pyrite hosting various minerals, including gold. *B*, Enlargement of part of 96A, showing argentiferous gold along microcrack in pyrite; some possible pyrrhotite also in the field of view. *C*, Energy-dispersive X-ray spectra of argentiferous gold grain in 96B. *D*, Gold associated with pyrrhotite in pyrite. *E*, Euhedral outlines of pyrite (py) crystals, common throughout sample. *F*, Enlargement of part of 96E, showing monazite crystals along margins between pyrite crystals. *G*, Silver tellurides and bismuth tellurides in pyrite. *H*, Enlargement of part of 96A, showing clot of chalcopyrite, pyrrhotite, and sphalerite in pyrite. *I*, Sphalerite surrounded by covellite in K-feldspar—Continued.

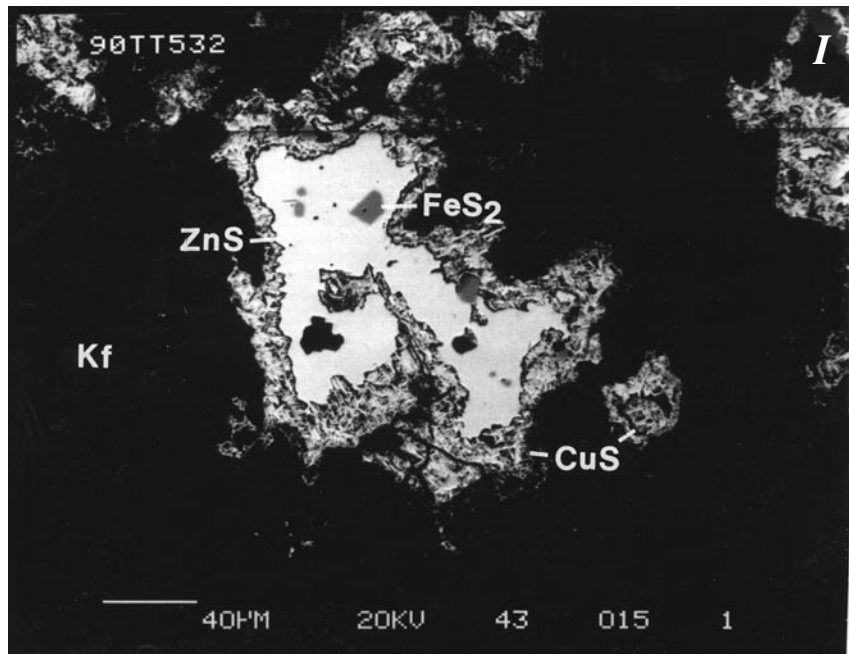


**Figure 96.** Scanning electron micrographs of gold-bearing breccia pipe at the Colosseum Mine, East Mojave National Scenic Area, Calif (fig. 94). Abbreviations: Ag, silver; AgTe, silver telluride; Au, gold; BiTe, bismuth tellurides; (Ce,La,Nd)PO<sub>4</sub>, monazite; cpy, chalcopyrite; CuS, covellite; (Fe,Mn)WO<sub>3</sub>, wolframite; FeS, pyrrhotite (queried where uncertain); FeS<sub>2</sub>, pyrite; Kf, K-feldspar; Py, pyrite; SiO<sub>2</sub>, quartz; ZnS, sphalerite. *A*, General morphology of pyrite hosting various minerals, including gold. *B*, Enlargement of part of 96A, showing argentiferous gold along microcrack in pyrite; some possible pyrrhotite also in the field of view. *C*, Energy-dispersive X-ray spectra of argentiferous gold grain in 96B. *D*, Gold associated with pyrrhotite in pyrite. *E*, Euhedral outlines of pyrite (py) crystals, common throughout sample. *F*, Enlargement of part of 96E, showing monazite crystals along margins between pyrite crystals. *G*, Silver tellurides and bismuth tellurides in pyrite. *H*, Enlargement of part of 96A, showing clot of chalcopyrite, pyrrhotite, and sphalerite in pyrite. *I*, Sphalerite surrounded by covellite in K-feldspar—Continued.

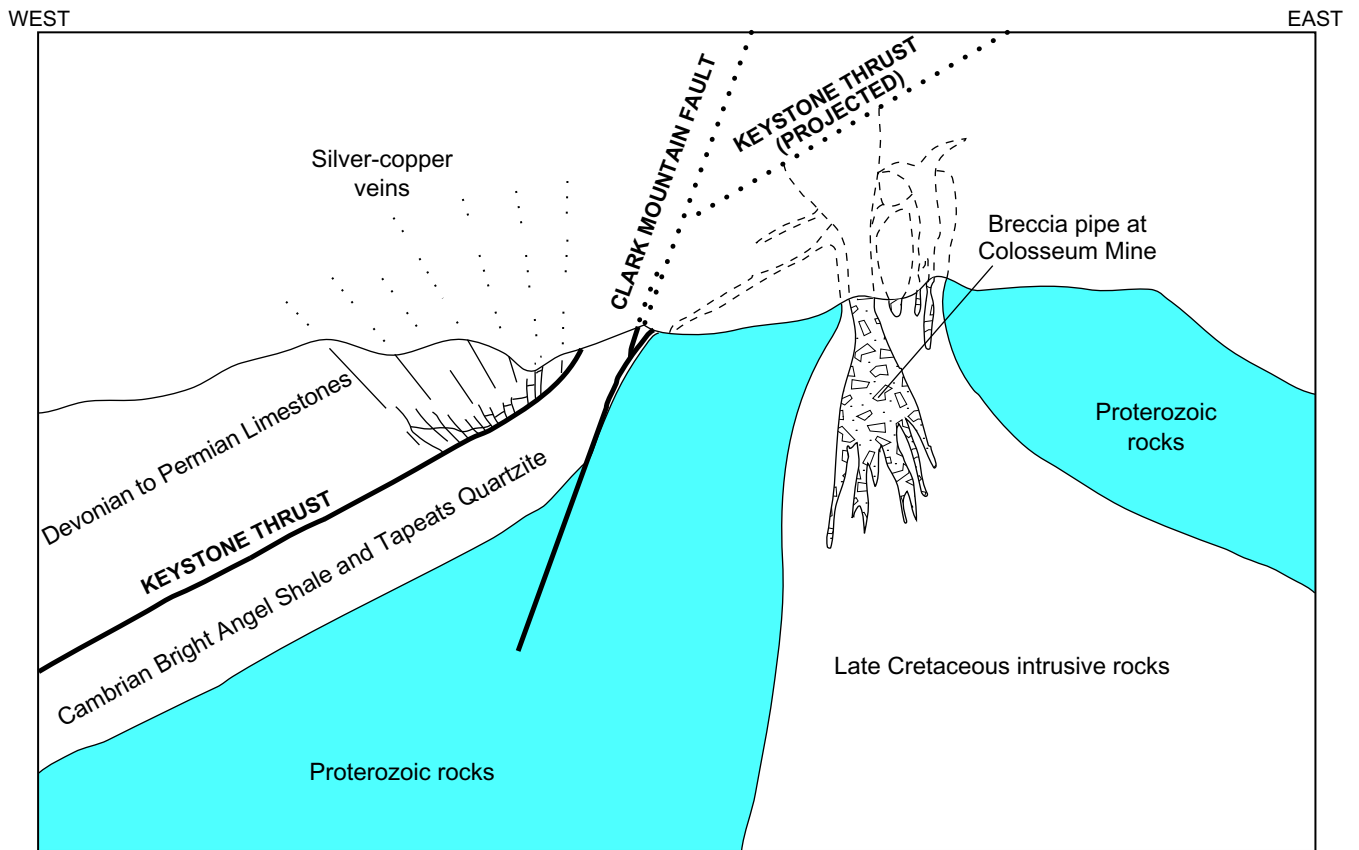


**Figure 97.** Schematic cross section showing displacement down to west along Clark Mountain fault (fig. 94) of silver-copper brecciated-dolostone vein-type occurrences from their initial positions at top of gold-bearing breccia pipes at Colosseum Mine, East Mojave National Scenic Area, Calif. Modified from Sharp (1984).



**Figure 98.** New Trail Canyon area, northern Ivanpah Mountains, East Mojave National Scenic Area, Calif. (figs. 2, 26). *A*, Workings at New Trail Canyon Mine (at head of arrow), which explore copper and iron skarn. View to N. 40° W. from general area of Bullion Mine. *B*, Narrow veins of magnesite (*m*) cutting altered Paleozoic carbonate rocks (*ac*). Approximately 1 m from 1-m-wide main vein at New Trail Magnesite Mine, approximately 2.5 km southeast of the New Trail Mine.

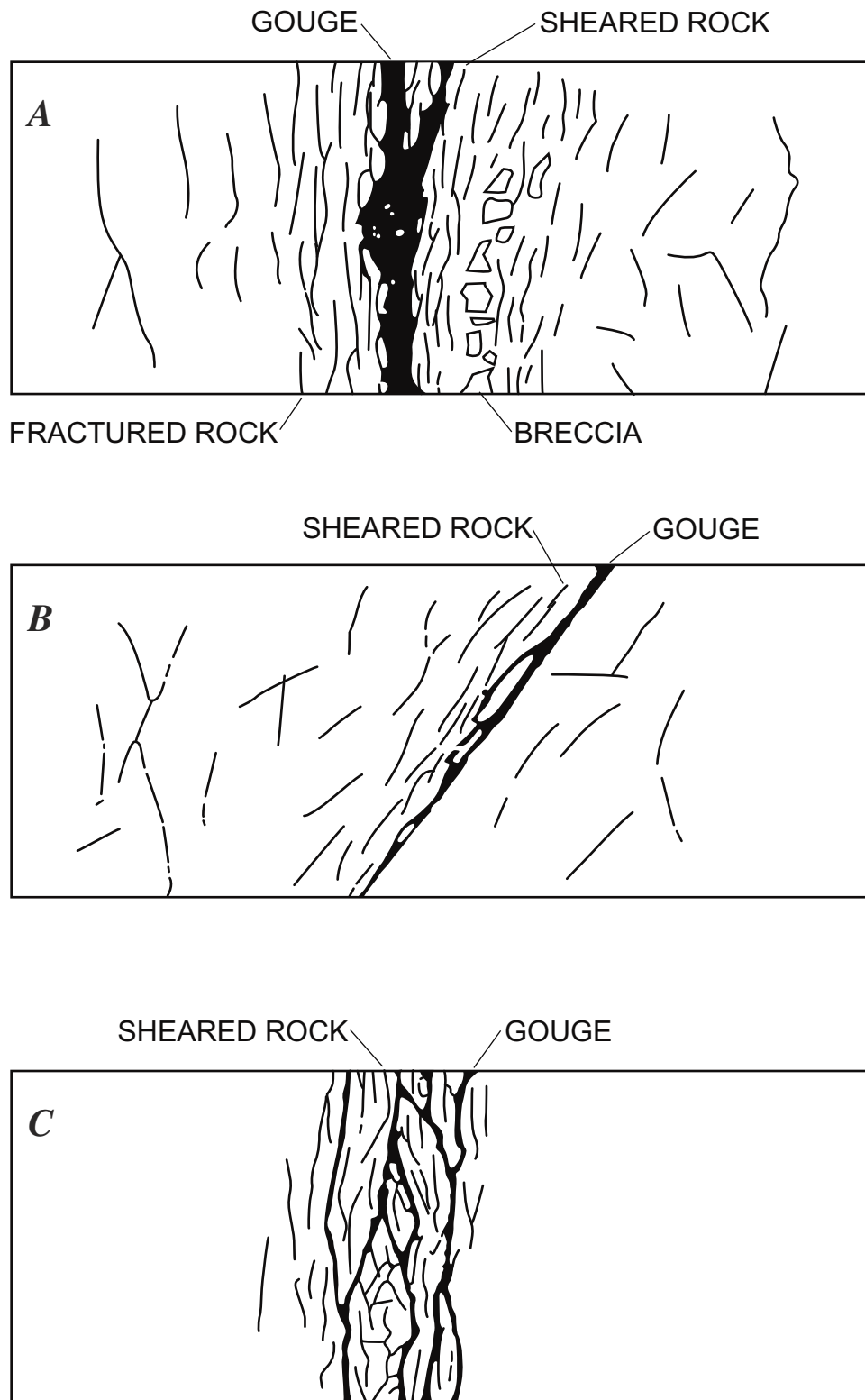


**Figure 99.** Schematic diagrams showing various relations of gouge within a fault zone (from Wallace and Morris, 1986). *A*, Gouge zone near center of trace of a fault zone. *B*, Gouge zone preferentially located near one boundary of a fault zone. *C*, Thin seams of gouge developed throughout zone of sheared rock that define overall width of a fault zone.

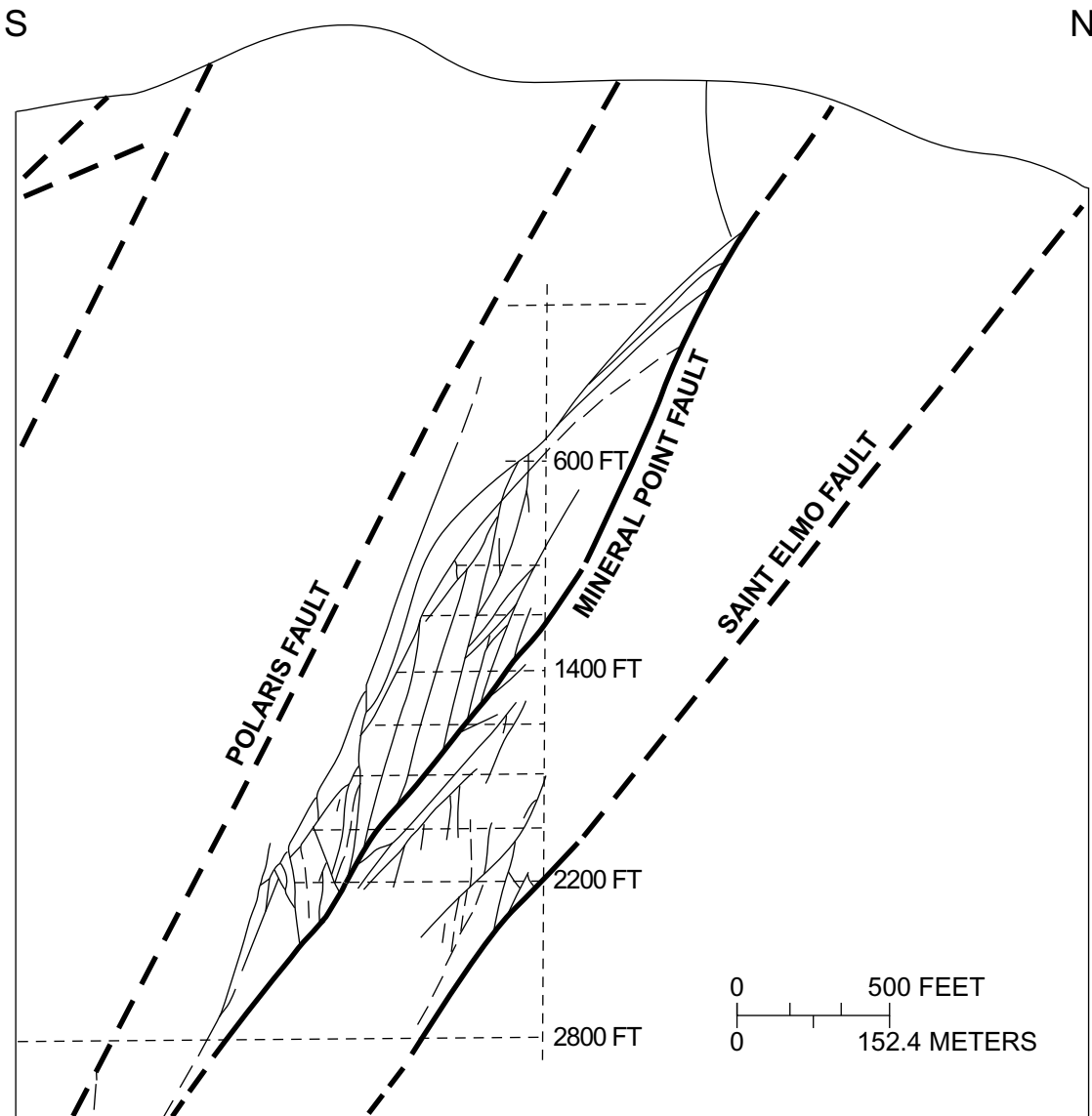


**Figure 100.** Cross section through Coeur d'Alene Mine, Idaho, showing complex anastomosing pattern of traces of fault found in approximately 70-m intervals of underground mine workings. Faults, dashed where approximately located; short-dashed lines, shaft and underground mine levels projected to plane of section. From Wallace and Morris (1986).

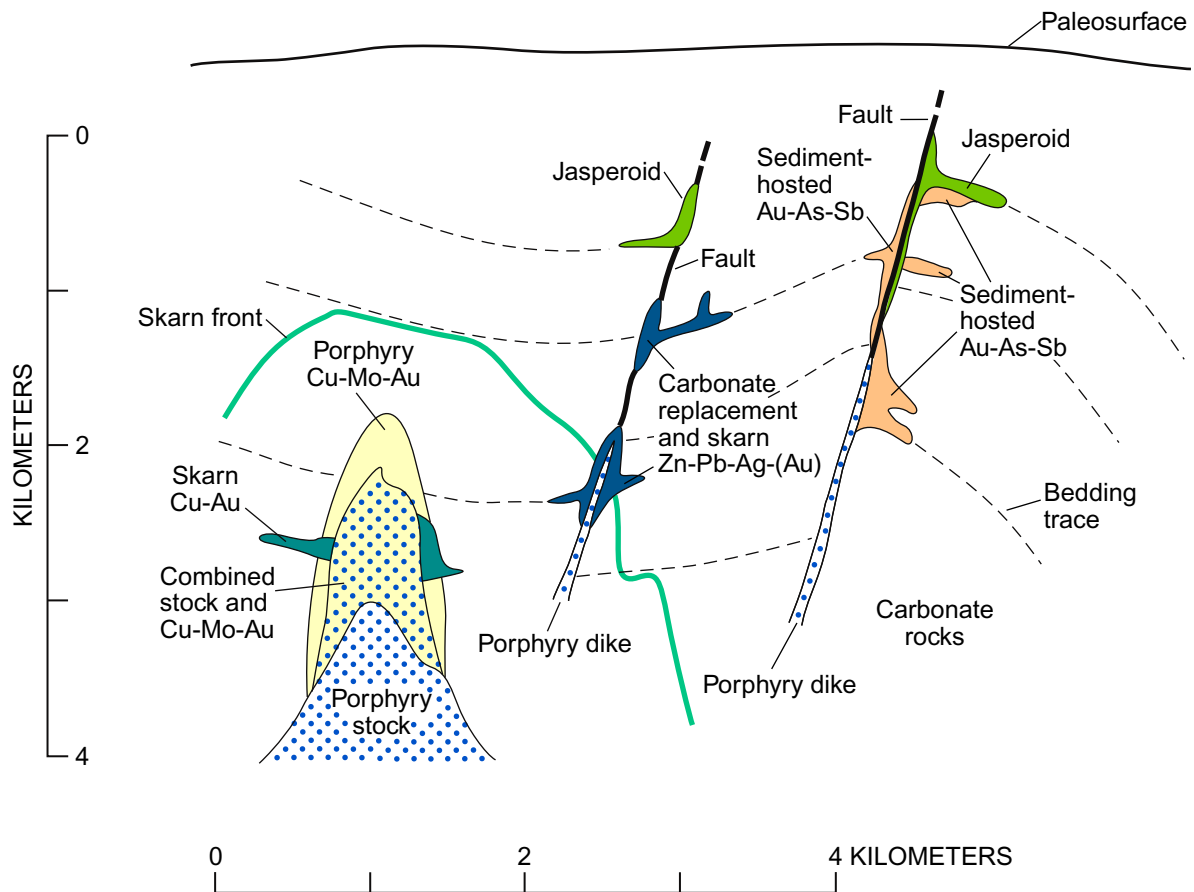


**Figure 101.** Schematic cross section showing inferred general relations of sediment-hosted gold deposits on fringes of base- and precious-metal mining districts. Porphyry Cu–Mo–Au deposits may include significant proportions of upper parts of associated stocks. Metals potentially present shown parenthetically. Short-dashed lines, schematic form lines of bedding in sedimentary strata. From Sillitoe and Bonham (1990).

**Table 18.** Characteristics of permissive terranes and favorable tracts for Proterozoic carbonatite-related, rare earth element (REE) deposits; Mesozoic gold-bearing breccia pipes; Mesozoic stockwork-molybdenum systems, and other types of deposits in the East Mojave National Scenic Area, Calif.

[-----do-----, same as above; --, not available; n.a., possibly not applicable]

Deposit type	Permissive terrane	Favorable tract	Criteria used to delineate favorable tract <sup>1</sup>	Age	Worldwide Characteristics <sup>2</sup>	
					Median tonnage (million tonnes)	Median grade
Proterozoic						
Proterozoic carbonatite-related, REE deposit	All Early Proterozoic rocks	Belt of ultrapotassic rocks and carbonatite	1, 2, 3	1.4 Ga	60	<sup>3</sup> 0.58 percent Nb <sub>2</sub> O <sub>5</sub>
Mesozoic						
Gold-bearing breccia pipe	Shallow-level magmatic hydrothermal environment	Area delineated by petrogenetically linked veins	1, 4, 5, 6, 9	~100 Ma	--	--
Stockwork molybdenum deposits	Area underlain by Mid Hills adamellite of Beckerman and others (1982)	Widespread alteration	1, 4, 5, 7, 8	~59–71 Ma	94	0.085 percent Mo
Copper skarn	Sequences of Paleozoic carbonate rocks <sup>4</sup>	Sequences of Paleozoic carbonate rocks <sup>4</sup>	1, 4, 5, 9, 10	Jurassic and Cretaceous	0.56	1.7 percent Cu
Lead-zinc skarn	-----do-----	-----do-----	-----do-----	-----do-----	1.4	5.9 percent Zn 2.8 percent Pb
Tungsten skarn	-----do-----	-----do-----	-----do-----	-----do-----	1.1	0.67 percent WO <sup>3</sup>
Tin (tungsten) skarn	-----do-----	-----do-----	-----do-----	-----do-----	<sup>5</sup> 9.4	<sup>5</sup> 0.31 percent Sn
Iron skarn	-----do-----	-----do-----	1, 4, 5, 9, 10, 11	-----do-----	7.2	50 percent Fe
Gold skarn	-----do-----	-----do-----	4, 5, 9, 10	-----do-----	<sup>6</sup> 0.213	<sup>6</sup> 8.6 g/tonne Au
Polymetallic replacement	-----do-----	-----do-----	1, 4, 5, 9, 10	-----do-----	1.8	5.2 percent Pb 3.9 percent Zn
Polymetallic vein	All Mesozoic and older rocks	All Mesozoic and other rocks	1, 4, 5, 6, 12	-----do-----	n.a.	n.a.
Tertiary						
Epithermal volcanic-hosted gold	Rhyolitic flow domes and caldera	Hydrothermally altered and demagnetized rocks	1, 4, 5, 7, 11, 12	15.5 Ma	<sup>7</sup> 1.6	<sup>7</sup> 8.4 g/tonne Au

<sup>1</sup>Criteria: 1, Presence of mines and prospects; 2, presence of ultrapotassic and carbonatite rocks; 3, anomalous concentrations of REE in rock geochemistry, concentrate samples, and National Uranium Resource Evaluation (NURE) samples; 4 geochemical anomalies of base and precious metals in various sample media; 5 presence of petrogenetically linked metal occurrences; 6, presence of major premineralization structure; 7, widespread hydrothermal alteration of host igneous phase; 8, widespread presence of quartz-sulfide stockworks; 9 presence of reactive, premineralization rocks; 10, skarn alteration in carbonate rocks together with widespread occurrences of polymetallic veins, polymetallic veins, polymetallic faults, and gold-silver quartz-pyrite veins; 11, aeromagnetic data; 12, widespread alteration detected using Thematic Mapper image.

<sup>2</sup>From Cox and Singer (1986), except as noted.

<sup>3</sup>World-class REE deposit at Mountain Pass, just outside EMNSA, includes sparse Nb and extraordinary contents of light rare earth elements.

<sup>4</sup>Includes copper, lead-zinc, iron, tungsten, tin (tungsten), and gold skarns in EMNSA.

<sup>5</sup>Based on only grade and tonnage information from four deposits.

<sup>6</sup>From Theodore and others (1991).

<sup>7</sup>From epithermal quartz-alunite vein deposit model in Cox and Singer (1986).

**Table 19.** Analyses of rocks in the general area of the Big Hunch stockwork-molybdenum system, New York Mountains, East Mojave National Scenic Area, Calif.

[Analyses in parts per million; --, not detected. Semiquantitative emission-spectrographic analyses by J. Harris and B. Spillare using methods of Grimes and Marranzino (1968). Results are reported with a relative standard deviation for each value of plus 50 percent and minus 33 percent. Looked for but not found, at part-per-million detection levels (shown in parantheses); As (150), Au (10), Cd (32), Dy (22), Er (10), Eu (2.2), Gd (15), Ge (1.5), Hf (15), Ho (6.8), In (6.8), Ir (15), Lu (15), Os (22), Pd (1), P (68), Pt (4.6), Re (10), Rh (2.2), Ru (2.2), Sb (32), Sm (10), Ta (460), Tb (32), Tm (4.6), U (320), W (10). Partial chemical analyses by E. Campbell and D. Kobilis using standard methods of Shapiro (1975)]

Analysis No.	Sample 81TT	Ag	B	Ba	Be	Ce	Co	Cr	Cu	Ga	La	Li	Mn	Mo	Nb	Nd	Ni	Pb	Sc	Sn	Sr	
Semiquantitative emission-spectrographic analyses																						
1	40	--	--	860	--	--	--	--	19	10	--	--	33	13	--	--	--	6.9	1.7	--	310	
2	41	--	9.6	320	2	--	--	--	32	13	24	75	95	84	7.5	--	--	--	4.6	4.5	410	
3	42	0.096	--	1,000	3	--	--	--	70	25	25	--	130	190	4.9	--	--	24	4.1	8.3	340	
4	43	1.3	--	600	--	--	--	--	8.6	29	29	--	77	4.3	--	41	--	9	3.1	3.1	300	
5	44	--	5.7	320	2.3	--	--	--	32	10	10	--	110	1.2	10	--	--	18	4.4	--	300	
6	45B	0.38	--	540	--	--	--	--	7.6	18	18	--	65	50	--	--	--	9.3	1.9	--	260	
7	46	1.4	31	440	--	--	--	--	73	22	22	--	50	82	6.9	--	--	16	2.4	1.6	200	
8	47	0.18	24	870	1.5	--	--	--	32	49	49	--	66	81	--	52	--	15	3	2.4	350	
9	48	--	--	600	--	--	--	--	190	19	19	--	60	5.1	4.2	--	--	7.7	2.8	3.1	210	
10	49	--	--	1,000	2.3	--	--	--	32	27	27	--	75	7	4.8	--	--	13	3.3	4.4	390	
11	50	--	--	570	1.7	--	--	--	17	21	21	--	140	7.5	3.3	--	--	--	3.1	1.9	250	
12	51	--	--	640	1.2	--	--	--	32	20	20	--	78	81	3.3	--	--	--	3.2	2.4	250	
13	52	--	--	620	1.8	--	--	1.3	570	31	31	73	90	260	4.2	--	--	9.1	5.5	3	250	
14	53	--	49	1,000	3.2	--	1.5	--	2,400	29	29	89	43	14	5.7	46	--	22	3.4	2.8	580	
15	54	--	--	830	2.4	--	--	1.4	230	21	21	--	67	--	4.7	40	--	12	3.1	3.3	450	
16	55	--	--	730	2.3	--	1.4	--	220	29	29	--	97	--	6.4	53	--	12	4	3.1	460	
17	56	--	--	740	2.4	--	1.7	--	44	12	26	--	99	--	44	40	1.5	13	2.7	3.2	490	
18	57	--	--	720	2.3	--	1.2	--	48	15	22	--	81	--	4.2	--	--	18	2.5	5.5	510	
19	58	0.17	7.7	480	4.3	56	2	--	210	18	40	--	160	9.6	7.2	50	--	26	4.1	3.4	200	
20	59	4.6	--	120	1.3	--	--	--	43	12	--	--	110	460	--	--	2.1	170	2.6	3.1	34	
21	60	0.33	9.7	820	2.7	--	--	--	41	21	16	--	74	87	4.2	32	--	9.6	4	4	300	
22	61	--	--	360	--	--	1.3	--	42	15	15	--	110	--	4.9	--	--	32	2.4	2.7	260	
23	62	--	--	720	1.8	--	1.1	--	70	18	17	--	110	--	6	--	--	25	3	2.5	400	
24	63	--	--	300	--	--	--	--	9.5	6.7	--	--	29	21	6.7	--	1.8	7.6	1.7	4.1	150	
25	64	0.15	38	420	3.6	--	--	--	60	13	28	84	81	86	6	36	--	11	3.9	2.6	290	
26	65	--	5.3	580	3	--	1.6	--	4,000	19	25	--	210	2.3	6.2	--	--	17	3.8	4	280	
27	73	--	41.0	310	2.5	--	--	--	41	21	25	--	94	150	4.3	44	--	28	3.3	2.4	730	
28	76	0.66	--	1,100	5.1	110	--	--	140	25	54	--	260	--	6.1	83	2	7.9	5.4	3	440	
29	77	--	--	560	1.7	--	1.1	2.2	21	20	20	--	110	--	6.1	32	2.1	31	4	1.7	390	
30	78	0.9	--	700	4.8	--	--	--	1.6	99	23	19	--	280	--	8	--	1.6	12	4.8	3.9	270
31	79	--	--	910	37	--	--	1.8	7	22	22	--	220	--	7.2	--	--	25	5	3.8	640	
32	80	0.16	20	1,000	2.4	--	2.3	1.3	67	19	33	--	78	--	5.6	55	1.8	14	4.8	3.3	490	
33	70	--	32	200	200	--	--	--	22	24	14	14	14	4.5	23	--	1.6	24	4.9	5.4	560	
34	71	--	6.6	1,100	1,100	--	2.1	--	13	19	38	38	38	21	5.6	56	--	16	4.7	3.7	540	
35	72	--	--	210	210	--	--	--	32	17	--	--	--	--	7.5	--	--	28	3.2	--	80	
36	81	--	6.0	190	190	--	--	--	32	26	--	--	--	--	30	--	2	12	4.6	1.8	210	
1-4	Variably quartz veined gneissic Mid Hills adamellite of Beckerman and others (1982).										27-31	Variably altered, very weakly quartz veined, gneissic Mid Hills adamellite.										
5	Rhyodacite dike.										32	Surface grab sample; quartz veined, gneissic Mid Hills adamellite.										
6-19	Variably quartz veined gneissic Mid Hills adamellite.										33	Drill core. Sericitically altered, porphyritic rhyodacite.										
20-21	Variably quartz veined gneissic Mid Hills adamellite.										34	DDH York-5-110 ft. Potassic- and sericitically-altered Mid Hills adamellite.										
22	Teutonia adamellite of Beckerman and others (1982).										35	DDH York-5-1,364 ft. Argillic-altered Mid Hills adamellite.										
23-36	Variably quartz veined gneissic Mid Hills adamellite.										36	Surface grab sample; gneissic Mid Hills adamellite.										

**Table 19.** Analyses of rocks in the general area of the Big Hunch stockwork-molybdenum system, New York Mountains, East Mojave National Scenic Area, Calif.—Continued.

Analysis No.	Sample 81TT	V	Y	Yb	Zn	Zr	Cl	F	W
Semiquantitative emission-spectrographic analyses						Chemical analyses			
1	40	5.7	3	0.32	--	41	22	700	2.7
2	41	14	6.8	0.5	23	88	13	2,500	7
3	42	20	4.3	0.54	--	71	13	2,200	7.9
4	43	12	4.6	0.51	18	34	13	1,000	4.6
5	44	5.9	7.9	0.92	--	23	17	1,000	2.8
6	45B	6.5	2.2	--	--	31	16	800	2.5
7	46	5.1	8.3	0.87	--	34	--	1,400	4.1
8	47	12	5.5	0.36	15	39	--	1,100	3.1
9	48	9.6	4.9	0.5	2	42	--	1,200	3.3
10	49	19	7.8	0.68	18	82	--	1,300	3.7
11	50	21	3.7	0.5	19	59	13	1,400	5.2
12	51	14	7.2	0.77	17	44	24	900	4.1
13	52	22	14	1.1	--	73	--	1,800	3
14	53	13	5.9	0.86	32	110	--	1,200	3.9
15	54	11	5.5	0.53	27	73	18	1,200	1.1
16	55	14	8.5	0.78	39	49	24	1,400	1.8
17	56	12	3.1	12	25	54	31	900	0.56
18	57	12	3.9	19	23	68	16	1,100	0.5
19	58	19	7.9	18	24	96	15	880	8.8
20	59	18	2.1	29	17	12	--	1,000	3.5
21	60	29	5.9	4.8	--	100	17	2,100	3.9
22	61	4.8	10	0.25	17	36	19	400	0.26
23	62	8.5	7.6	8.5	45	64	26	1,000	0.96
24	63	3.9	4.1	3.9	17	15	14	500	1.3
25	64	6.8	17	6.8	26	74	16	1,400	3.8
26	65	7.5	15	7.5	56	98	67	1,000	1.7
27	73	15	6.8	15	23	59	--	2,100	4
28	76	23	5.4	0.23	--	130	--	5,800	7.9
29	77	20	4.8	20	56	65	18	900	2.2
30	78	27	2.3	0.27	--	74	--	2,500	12
31	79	20	3	0.38	--	65	--	2,500	57
32	80	13	7.5	0.82	--	93	19	1,800	4
33	70	3.7	12	1.2	17	17	20	1,300	2.3
34	71	16	9.4	1	--	--	25	2,000	3.6
35	72	4.7	6.9	0.64	19	19	--	25	0.5
36	81	2.5	9.2	1.1	18	18	18	1,000	2.2

**Table 20.** Chemical analyses of 97 rocks from 47 mineralized sites designated as gold-silver quartz-pyrite veins in East Mojave National Scenic Area, Calif.

[All concentrations in parts per million except Au, which is in parts per billion; --, not applicable; STD, standard deviation; MIN, minimum; MAX, maximum. Data from U.S Bureau of Mines, 1990a]

Sample No.	Au (ppb)	Ag	Au/Ag Ratio	As	Ba	Cd	Ce	Co	Cr	Cs	La	Lu	Mo	Ni	Sb	Sc	Sm	Ta	Th	U	W	Zn
CDC-10	701	1	0.701	2	190	2.5	56	7	300	1	23	0.4	0.5	5	0.2	2	3.4	0.7	14	2.4	1	100
CDC-11	483	37	0.013	14	130	2.5	47	6	210	4	20	0.6	12	5	25.4	5.2	4.4	0.25	3.6	5.2	13	480
CDC-12	5	1	0.005	2	460	2.5	120	2.5	190	5	54	0.9	0.5	5	0.4	11	10.2	1.1	13	2	3	140
CDC-148	3	1	0.003	7	560	2.5	53	8	340	3	25	0.1	1	5	2.4	2.4	3.8	0.25	11	3.1	6	130
CDC-159	11100	5	2.220	14	460	11	29	16	340	2	12	0.1	27	29	1.2	10	3.5	0.5	3.5	5.4	15	1500
CDC-160	635	5	0.127	4	120	2.5	6	15	390	0.5	5	0.1	7	13	0.4	1.1	0.8	0.25	1.9	2	4	50
CDC-166	298	1	0.298	3	140	2.5	68	2.5	300	2	22	1.4	5	5	0.3	3.4	6.8	2.2	31.3	2.9	3	50
CDC-167	794	2	0.397	3	100	2.5	45	13	250	2	17	1	5	5	0.4	3.1	5.4	1.9	12	2.7	4	50
CDC-168	12	1	0.012	1	110	2.5	91	2.5	340	3	26	1.3	0.5	5	0.4	4.1	8.6	2.4	58.8	3.4	3	50
CDC-169	1160	3	0.387	6	430	2.5	59	15	310	2	23	1.1	3	5	0.3	3	5.5	0.7	21.5	10	3	50
CDC-170	261	1	0.261	5	280	2.5	21	21	300	1	7	0.3	1	15	0.3	4.7	2.6	0.25	4.4	4.3	10	50
CEM-24	47	4	0.012	8	25	2.5	31	2.5	180	0.5	13	0.1	18	5	1.2	3.4	1.7	0.25	3.6	2.4	2	50
CEM-28	15	1	0.015	41	57	2.5	2.5	14	300	0.5	3	0.1	21	15	1	1	0.5	0.25	1.7	11	1	50
CJO-04	4350	5	0.870	7	160	2.5	11	14	490	0.5	5	0.2	2	5	1.7	1.1	0.8	0.25	1.2	2.6	0.5	50
CJO-05	885	4	0.221	25	52	2.5	10	5	450	0.5	6	0.8	16	5	4.7	0.4	1	0.25	1.8	6.8	0.5	50
CJO-06	6540	13	0.503	7	25	2.5	2.5	2.5	450	0.5	1	0.2	53	5	0.6	0.2	0.3	0.25	0.8	3.8	0.5	50
CJO-09	20300	288	0.070	17	330	2.5	2.5	2.5	240	2	7	0.1	15	5	0.6	0.1	0.9	0.25	2.6	13	3	280
CJO-11	1270	3	0.423	35	400	2.5	32	12	310	2	15	0.6	17	5	3.8	2	2.9	0.25	5.4	5.3	12	50
CJO-15	72	2	0.036	5	610	2.5	10	6	330	2	6	0.3	183	11	1.1	1.4	1	0.25	8.9	4.3	4	380
CJO-16	5	1	0.005	7	340	2.5	110	7	310	3	44	0.8	3	33	3.7	6.2	7.3	0.25	31.7	4.7	4	120
CJO-17	150	40	0.004	3	340	2.5	2.5	7	420	0.5	3	0.2	41	5	0.8	0.9	0.4	0.25	2	3.1	7	120
CJO-23	581	1	0.581	1	180	2.5	14	9	410	1	7	0.1	0.5	17	0.2	2	1.5	0.25	2.8	0.5	4	110
CJO-30	43	1	0.043	12	320	2.5	37	8	250	2	11	0.1	47	5	56.9	3.8	1	0.25	2.8	8.2	2	50
CJO-33	58	1	0.058	0.5	25	2.5	2.5	2.5	420	0.5	1	0.1	0.5	5	0.9	0.1	0.2	0.25	0.1	0.1	0.5	50
CMM-11-36	3	1	0.003	2	1300	2.5	94	2.5	200	0.5	42	0.05	0.5	12	0.2	3.8	6.2	1	19	1.6	4	50
CMM-11-44	1	1	0.001	1	130	2.5	20	2.5	240	0.5	8	0.1	0.5	5	0.05	0.7	1.3	0.25	3.6	0.2	3	50
CRM-07	1	1	0.001	5	110	2.5	2.5	2.5	280	0.5	1	0.2	5	5	0.3	0.3	0.2	0.25	1.5	4.9	2	50
CRM-14	3	1	0.003	6	250	2.5	16	2.5	350	0.5	8	0.1	0.5	5	0.5	1.1	1	0.6	8.7	1.9	0.5	50
CRM-18	8	1	0.008	23	1900	2.5	70	2.5	300	2	36	0.3	101	5	0.3	2.1	3.7	0.9	17	5.4	2	110
CRM-22	4	1	0.004	9	260	2.5	76	21	230	0.5	27	1.4	1	36	2.7	23.3	5.5	0.5	10	2.2	0.5	150
CRM-25	4	4	0.001	9	470	2.5	26	2.5	200	2	10	0.1	33	5	6.2	2.1	1.4	0.8	3.3	1.1	5	50
CRM-27	8	38	0.000	120	130	2.5	2.5	5	390	0.5	1	0.1	5	5	20.1	1.3	0.3	0.25	0.1	0.7	185	50
CRM-35	1	1	0.001	4	25	2.5	2.5	2.5	340	0.5	1	0.1	217	5	8.3	0.1	0.2	0.25	0.4	0.4	1	50
CRM-40	8	1	0.008	22	870	2.5	44	2.5	150	2	22	0.1	0.5	5	1.3	1.1	2.9	0.25	14	0.4	0.5	50
CRM-54	1	1	0.001	1	25	2.5	2.5	2.5	350	0.5	1	0.1	156	5	1.3	0.5	0.2	0.25	0.5	0.2	2	50
CRR-11	200	1	0.200	5	980	2.5	34	12	390	3	15	0.1	17	5	2.6	1.9	3.3	0.25	1.9	2.8	6	50
CRR-111	6090	1	6.090	3	120	2.5	2.5	2.5	580	0.5	4	0.1	4	5	0.3	0.6	0.5	0.25	3.1	0.7	2	50
CRR-112	674	1	0.674	16	1200	2.5	95	2.5	230	3	41	0.3	3	5	0.4	13	4.9	1.3	20.2	4.8	17	50
CRR-113	9540	1	9.540	8	25	2.5	2.5	2.5	400	0.5	1	0.1	2	5	0.4	0.2	0.05	0.25	0.5	4.4	2	50
CRR-114	1030	1	1.030	2	190	2.5	8	2.5	3250	0.5	8	0.1	1	5	0.4	0.6	0.6	0.25	2.9	0.7	17	50
CRR-115	549	1	0.549	6	120	2.5	8	2.5	360	0.5	4	0.1	3	5	0.6	0.7	0.6	0.25	2.3	0.3	2	50
CRR-116	13	1	0.013	4	250	2.5	13	2.5	320	0.5	6	0.1	3	5	0.4	1.2	1	0.25	5.1	1.6	1	50
CRR-12	9	1	0.009	7	440	2.5	54	6	430	0.5	22	0.1	15	5	3.2	1.2	4.6	0.25	1.1	3	1	50
CRR-13	27	1	0.027	4	300	2.5	48	8	250	1	21	0.1	14	5	2.4	4.6	3.7	0.25	5.5	5.6	4	50
CRR-14	9	1	0.009	8	200	2.5	120	10	330	1	54	0.1	12	5	1.5	5.8	4.2	0.25	4.5	3.8	6	50
CRR-41	804	1	0.804	211	25	2.5	2.5	2.5	240	0.5	3	0.1	46	5	3.7	2.2	0.05	1.4	13	16	11	260
CRR-55	89	1	0.089	5	180	2.5	13	2.5	380	0.5	7	0.1	0.5	5	0.2	0.9	1.3	0.25	4.7	1.4	2	50
CRR-57	224	1	0.224	96	620	2.5	110	36	61	9	37	0.3	3	26	1.3	20	11.3	0.25	8.2	16	8	140
CRR-58	2970	1	2.970	84	680	2.5	77	42	140	3	27	0.3	15	29	0.7	15	9.4	0.5	7.4	9.5	4	110
CRR-59	130	1	0.130	4	120	2.5	16	2.5	420	0.5	9	0.1	3	5	0.3	1	0.7	0.25	6.9	0.8	0.5	50
CRR-60	10	1	0.010	19	1400	2.5	240	2.5	140	2	110	0.1	0.5	5	0.4	6	12.5	1	328	7.7	2	50
CRR-61	516	1	0.516	2	25	2.5	5	2.5	430	0.5	3	0.1	1	5	0.2	0.6	0.4	0.25	2.7	0.8	0.5	50
CRR-62	13	3	0.004	16	380	2.5	60	2.5	310	1	36	0.5	6	12	1	13	3.8	1.2	36.3	4.8	0.5	50
CRR-63	991	4	0.248	74	120	2.5	2.5	63	270	0.5	3	0.1	29	5	1	1.7	0.8	0.25	1.8	14	4	410
CRR-64	84	1	0.084	2	55	2.5	7	15	250	0.5	4	0.1	9	5	0.1	0.5	0.7	0.25	1.3	0.8	3	50
CRR-65	3	1	0.003	7	340	2.5	2.5	2.5	140	2	3	0.1	0.5	5	0.4	15	0.6	2	8.5	5.3	0.5	50
CRR-66	7	1	0.007	2	1200	2.5	88	25	150	2	37	0.4	0.5	44	0.5	19	8.7	1.2	10	2.3	2	150
CRR-67	11200	3	3.733	12	230	2.5	18	13	410	0.5	8	0.1	7	5	0.5	1.5	1.1	0.25	6	1.7	4	50
CRR-68	256	2	0.128	86	25	2.5	9	2.5	200	1	7	0.1	49	5	1.6	1.6	1.2	0.25	2.4	11	10	430
CRR-69	9210	3	3.070	8	89	2.5	2.5	7	350	0.5	3	0.1	8	5	0.3	0.8	0.4	0.25	1.6	3	2	50
CRR-70	12100	4	3.025	31	120	2.5	2.5	5	360	0.5	4	0.1	16	5	0.3	1	0.5	0.25	3.4	1	5	50

**Table 20.** Chemical analyses of 97 rocks from 47 mineralized sites designated as gold-silver quartz-pyrite veins in East Mojave National Scenic Area, Calif.—Continued

Sample No.	Au (ppb)	Ag	Au/Ag Ratio	As	Ba	Cd	Ce	Co	Cr	Cs	La	Lu	Mo	Ni	Sb	Sc	Sm	Ta	Th	U	W	Zn
CRR-75	522	1	0.522	8	620	2.5	110	8	340	1	47	0.3	0.5	21	0.7	10	7.1	1	20	4.7	10	50
CRR-76	496	1	0.496	7	300	2.5	21	10	320	0.5	13	0.1	17	15	0.2	2.2	1.7	0.25	5.6	2.7	4	50
CRR-77	1390	1	1.390	2	380	2.5	25	7	400	0.5	14	0.1	2	5	0.1	1	2	0.25	8.4	1.2	3	50
CRR-78	1250	1	1.250	7	410	2.5	52	2.5	360	0.5	25	0.1	33	12	0.2	1.9	3.3	0.25	10	1.2	2	50
CRR-79	6900	1	6.900	8	180	2.5	25	2.5	370	0.5	15	0.1	7	5	0.2	1	2.2	0.25	6.9	2.6	1	50
CRR-80	7530	1	7.530	3	310	2.5	21	10	290	0.5	7	0.1	2	5	0.1	0.5	1.4	0.25	3.4	1	3	50
CRR-81	4270	1	4.270	3	460	2.5	19	2.5	270	1	14	0.1	1	5	0.2	1.2	2.6	0.25	8	1.2	4	50
CRR-82	45	1	0.045	0.5	210	2.5	15	2.5	270	0.5	8	0.1	1	5	0.05	1	1.4	0.25	10	1.1	3	50
CRR-84	1450	6	0.242	95	25	2.5	6	8	290	0.5	4	0.1	13	5	3.4	1.5	0.8	0.25	2.7	2.1	6	50
CRR-85	17400	6	2.900	103	180	2.5	2.5	32	220	0.5	6	0.1	23	5	3.3	4.5	1.3	0.25	1.1	11	12	50
CRR-86	899	1	0.899	6	82	2.5	7	11	330	0.5	3	0.1	4	11	0.5	0.3	0.6	0.25	2.6	0.7	0.5	50
CRR-87	1390	2	0.695	20	120	2.5	2.5	14	410	0.5	1	0.1	8	5	0.6	0.3	0.3	0.25	1	0.6	1	50
CRR-88	20	1	0.020	5	960	2.5	77	6	190	3	34	0.4	5	20	0.4	11	5.6	1.8	15	4.4	3	50
CRR-89	1	1	0.001	12	25	2.5	2.5	19	61	0.5	3	0.1	0.5	5	0.05	1.4	2.3	0.25	0.7	2.6	28	50
CRR-90	98	1	0.098	9	82	2.5	32	460	250	5	20	0.1	23	57	0.3	1.9	3.1	0.25	5.3	15	22	50
CRR-91	333	1	0.333	5	140	2.5	7	13	300	0.5	4	0.1	48	5	0.2	1.3	0.7	0.25	3.4	1.1	3	50
CRR-92	28	1	0.028	16	320	2.5	67	6	150	0.5	22	0.1	15	23	0.9	17	5.7	0.8	6.9	28.9	6	50
CRR-93	85	1	0.085	2	130	2.5	2.5	2.5	340	0.5	1	0.1	3	12	0.1	0.8	0.2	0.25	1	0.6	0.5	50
CRR-94	7140	1	7.140	4	25	2.5	2.5	2.5	450	0.5	1	0.1	3	5	0.2	0.4	0.2	0.25	0.1	0.8	1	50
CRR-97	268	8	0.034	4	110	2.5	20	2.5	310	0.5	11	0.1	2	5	1.7	1.5	1.5	0.25	18	1.6	3	50
CRR-98	5	1	0.005	17	98	2.5	18	799	350	0.5	13	0.1	5	49	0.2	0.8	0.9	0.25	1.1	5.2	2	50
CTN-54	1	1	0.001	11	180	2.5	2.5	2.5	280	0.5	2	0.1	116	5	1.6	0.1	0.3	0.25	0.5	8.1	0.5	50
CTN-55	8	6	0.001	20	25	2.5	2.5	2.5	310	0.5	1	0.1	10	5	0.05	0.2	0.1	0.25	0.9	5.6	1	50
CTP-031	352	12	0.029	25	1000	2.5	43	6	330	3	22	0.5	32	5	24.6	3.7	3	0.7	17	4.1	4	330
CTP-033	1110	7	0.159	13	590	2.5	28	2.5	250	3	14	0.3	9	5	11.4	1.9	2	1.1	20.5	3.2	2	50
CTP-118	1	1	0.001	2	530	2.5	62	7	170	2	34	0.1	0.5	5	0.1	3.7	2.7	1.6	37.8	6.4	0.5	50
CTP-119	1	1	0.001	2	79	2.5	5	2.5	440	0.5	2	0.1	0.5	5	0.4	0.5	0.4	0.25	2.6	0.4	0.5	50
CTP-120	693	86	0.008	4	370	2.5	57	51	280	3	25	0.1	21	5	0.4	7	4.4	1	9.3	14	21	50
CTP-121	2010	12	0.168	11	130	2.5	32	2.5	170	2	18	0.1	0.5	11	7.8	2.2	1.9	0.25	12	4.6	3	50
CTP-122	263	89	0.033	7	170	2.5	9	2.5	170	0.5	3	0.1	1	5	33.3	0.4	0.4	0.25	1.7	0.9	0.5	50
CWC-28	822	1	0.822	25	82	2.5	2.5	2.5	390	0.5	5	0.3	0.5	22	1.2	5.4	1.1	0.25	1.3	0.6	6	50
CWC-42	82	1	0.082	33	25	2.5	14	9	280	0.5	7	0.1	2	5	1.2	2.8	1.1	0.25	0.8	2.4	2	50
CWC-45	13	1	0.013	10	65	2.5	18	92	290	2	11	0.1	3	5	0.6	3.7	1.3	0.25	1.9	1.7	4	50
CWC-47	36	4	0.009	5	750	2.5	230	2.5	210	1	100	0.5	0.5	5	1.4	4.1	15.6	0.6	89	5.1	0.5	50
CWC-48	7	1	0.007	1	320	2.5	33	2.5	240	0.5	15	0.3	1	5	0.2	0.4	2.5	0.25	11	3	0.5	50
CWC-51	12400	6	2.067	26	370	2.5	62	2.5	250	2	28	0.3	9	11	9	1.2	4	0.25	19	1.9	4	50
AVERAGE:	1813.16	7.21		17.37	315.47	2.59	34.99	22.03	329.71	1.30	15.91	0.24	17.42	9.44	2.90	3.48	2.68	0.49	12.00	4.17	6.15	96.39
STD:	3836.02	30.59		30.87	343.28	0.86	43.01	92.39	312.58	1.32	18.31	0.29	35.69	9.91	7.68	4.74	2.98	0.48	34.60	4.53	18.93	166.92
MIN:	1	1		0.5	25	2.5	2.5	2.5	61	0.5	1	0.1	0.5	5	0.05	0.1	0.05	0.25	0.1	0.1	0.5	50
MAX:	20300	288		211	1900	11	240	799	3250	9	110	1.4	217	57	56.9	23.3	15.6	2.4	328	28.9	185	1500